Tuomo Kainulainen

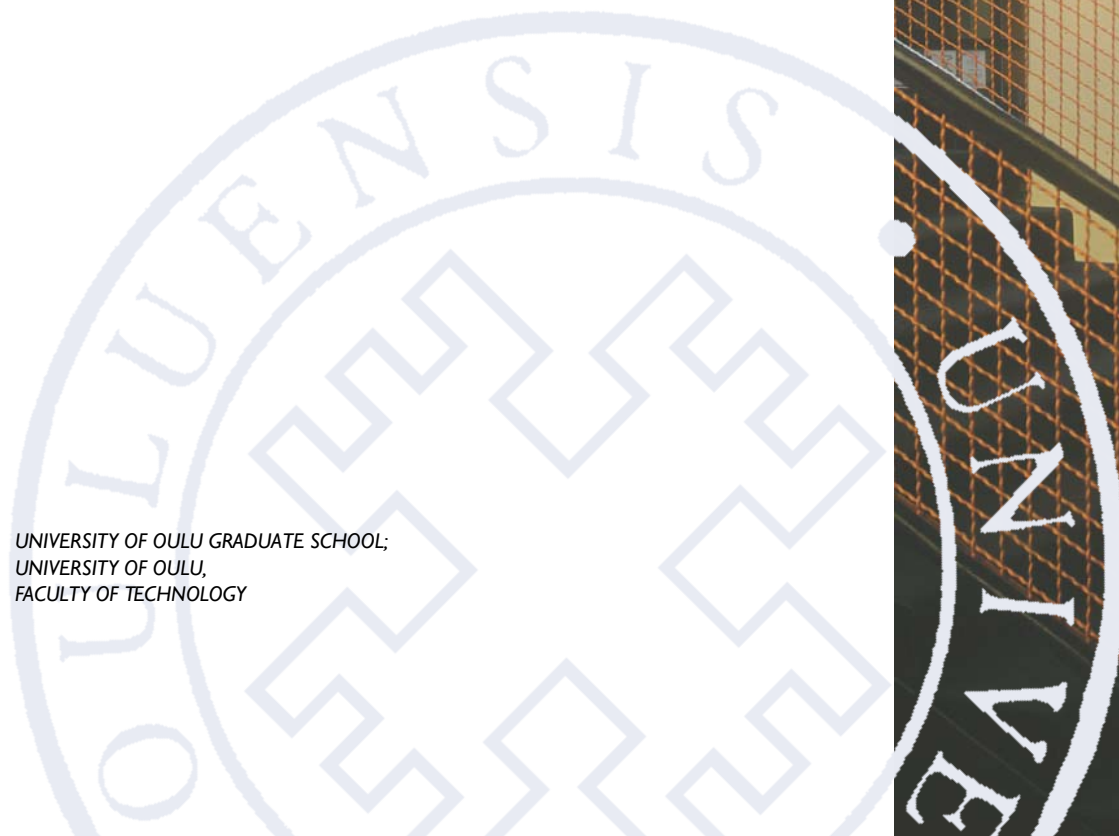# FURFURAL-BASED 2,2'-BIFURANS

SYNTHESIS AND APPLICATIONS IN POLYMERS

UNIVERSITY OF OULU GRADUATE SCHOOL;
UNIVERSITY OF OULU,
FACULTY OF TECHNOLOGY

TUOMO KAINULAINEN

FURFURAL-BASED 2,2'-BIFURANS
Synthesis and applications in polymers

Academic dissertation to be presented, with the assent of the Doctoral Training Committee of Technology and Natural Sciences of the University of Oulu, for public defence in the Oulun Puhelin auditorium (L5), Linnanmaa, on 27 November 2020, at 12 noon

Abstract

Furans are an interesting class of sustainable chemicals derived from biomass. They are prepared from carbohydrate sources and are, therefore, potential platform chemicals and precursors for novel biobased materials. Within the last 20 years, research has elevated 2,5-furandicarboxylic acid (FDCA) into being one of the most important biochemicals, because of its applicability for the preparation of novel polymers. For this reason, its precursor 5-hydroxymethylfurfural has risen to a similar prominence as furfural, despite it not being produced on the same scale currently.

In this work, furfural-based 2,2'-bifuran compounds were studied, with the goal of utilizing them as monomers for novel materials. Novel bifuran-based polyesters were made using dimethyl 2,2'-bifuran-5,5'-dicarboxylate as a monomer, which was prepared using the developed palladium-catalyzed direct coupling method. A traditional melt polycondensation reaction with either ethylene glycol or 1,4-butanediol was used to prepare the bifuran polyesters and FDCA-containing copolyesters. For novel cross-linkable epoxy methacrylates, or so-called vinyl esters, the starting compound was 2,2'-bifuran-5,5'-dicarboxylic acid (BFDCA), and the prepared unsaturated monomers were cross-linked by employing radical polymerization. The materials and monomers were characterized using several techniques (NMR, IR, DSC, TGA, DMA, UV-Vis), which allowed the effects of the bifuran units to be elucidated.

Based on the results obtained, 2,2'-bifuran–based polyesters and copolyesters are a very promising class of materials. Based on measurements, their glass transition temperatures are noticeably higher than those of the corresponding polyesters derived from either terephthalic acid or FDCA. Additionally, their UV and oxygen barrier properties were excellent, and for the latter, close to FDCA-based polyesters, which are considered to be some of the best oxygen-barrier polyesters. Based on tests done on the vinyl esters prepared from FDCA and BFDCA, they are possible replacements for bisphenol A -derived vinyl esters. They can be used to prepare thermosets with high glass transition temperatures.

Keywords: biomass, coupling reaction, dicarboxylic acid, furans, furfural, oxygen barrier, polyester

Kainulainen, Tuomo, Furfuraaliin pohjautuvat 2,2'-bifuraanit. Synteesi ja soveltaminen polymeereissä
Oulun yliopiston tutkijakoulu; Oulun yliopisto, Teknillinen tiedekunta
Acta Univ. Oul. A 749, 2020
Oulun yliopisto, PL 8000, 90014 Oulun yliopisto

Tiivistelmä

Furaanit ovat kestävän kemian näkökulmasta mielenkiintoinen yhdisteryhmä. Niiden läheinen yhteys biomassojen hiilihydraatteihin mahdollistaa niiden käytön uusiutuvina platform-kemikaaleina ja sitä kautta lähtöaineina biomassapohjaisille materiaaleille. Erityisesti viimeisten 20 vuoden aikana tehdyt tutkimukset ovat hiljalleen nostaneet 2,5-furaanidirkarboksyylihapon (FDCA) yhdeksi potentiaalisesti tärkeimmäksi biokemikaaliksi johtuen sen soveltuvuudesta uudenlaisten polymeerien monomeeriksi. Tämän vuoksi sen lähtöaine, 5-hydroksimetyylifurfuraali, on noussut furfuraalin rinnalle toiseksi merkittäväksi furaaniyhdisteeksi, vaikka sen tuotantomäärät ovat vielä vaatimattomia.

Tässä työssä tutkittiin nimenomaan furfuraalipohjaisiksi luokiteltavia 2,2'-bifuraaniyhdisteitä ja niiden käyttöä uudenlaisten polymeerien lähtöaineina. Uudenlaisten bifuraani-polyestereiden monomeerina käytettiin dimetyyli-2,2'-bifuraani-5,5'-dikarboksylaattia, jonka valmistamiseksi kehitettiin palladiumkatalysoitu suorakytkentämenetelmä. Polyestereiden ja FDCA-pitoisten kopolyestereiden valmistukseen käytettiin perinteistä polykondensaatioreaktiota joko etyleeniglykolin tai 1,4-butaanidiolin kanssa. Sen sijaan ristisilloitettavien epoksimetakrylaattien, eli niin kutsuttujen vinyyliestereiden, lähtöaineena käytettiin 2,2'-bifuraani-5,5'-dikarboksyylihappoa (BFDCA), ja saadut tyydyttymättömät monomeerit kovetettiin radikaalipolymeraatiolla. Materiaaleja ja lähtöaineita karakterisoitiin useilla tekniikoilla (NMR, IR, DSC, TGA, DMA, UV-Vis), joiden pohjalta bifuraanirakenteiden vaikutuksia kartoitettiin.

Saatujen tulosten perusteella 2,2'-bifuraani-pohjaiset polyesterit ja kopolyesterit ovat erittäin lupaava materiaaliryhmä. Mittausten perusteella niiden lasisiirtymälämpötilat ovat selvästi korkeammat kuin tereftaalihappoon tai FDCA:han pohjautuvilla vastaavilla polyestereillä. Lisäksi niiden UV:n esto- ja happibarriääriominaisuudet osoittautuivat erinomaisiksi, ja jälkimmäisen osalta mitatut arvot olivat lähellä tässä suhteessa parhaimmistoa edustavia FDCA-pohjaisia polyestereitä. FDCA- ja BFDCA-pohjaisille vinyyliestereille tehtyjen kokeiden perusteella ne ovat puolestaan mahdollisia korvikkeita bisfenoli-A-pohjaisille vinyyliestereille, ja niitä käyttäen on mahdollista valmistaa kertamuoveja, joilla on korkeat lasisiirtymälämpötilat.

Asiasanat: biomassa, dikarboksyylihappo, furaanit, furfuraali, happibarriääri, kytkentäreaktio, polyesteri

Acknowledgments

Abbreviations

BFDCA	2,2'-Bifuran-5,5'-dicarboxylic acid
Cy	Cyclohexyl
DEG	Diethylene glycol
DG-Bf	Diglycidyl 2,2'-bifuran-5,5'-dicarboxylate
DG-F	Diglycidyl 2,5-furandicarboxylate
DM-Bf	Dimethyl 2,2'-bifuran-5,5'-dicarboxylate
DM-F	Dimethyl 2,5-furandicarboxylate
DMA	Dynamic mechanical analysis
DMAc	*N,N*-dimethylacetamide
DMSO	Dimethyl sulfoxide
DSC	Differential scanning calorimetry
FDCA	2,5-Furandicarboxylic acid
HMF	5-(Hydroxymethyl)-2-furancarboxaldehyde, 5-hydroxymethylfurfural
HRMS	High-resolution mass spectrometry
IR	Infrared radiation
m-CPBA	*meta*-Chloroperoxybenzoic acid
ME	Methacrylated eugenol
NMP	*N*-Methyl-2-pyrrolidone
NMR	Nuclear magnetic resonance
PBBf	Poly(butylene bifuranoate)
PBF	Poly(butylene furanoate)
PBT	Poly(butylene terephthalate)
PEBf	Poly(ethylene bifuranoate)
PEF	Poly(ethylene furanoate)
PET	Poly(ethylene terephthalate)
PivOH	Pivalic acid (trimethylacetic acid)
PTF	Poly(trimethylene furanoate)
PTFE	Poly(tetrafluoroethene)
PTT	Poly(trimethylene terephthalate)
RH	Relative humidity
TBAB	Tetrabutylammonium bromide
TBT	Tetrabutyl titanate
TFA	Trifluoroacetic acid
T_g	Glass transition temperature

TGA	Thermogravimetric analysis
T_m	Melting temperature
UV-Vis	Ultraviolet-visible (light)–spectroscopy

Original publications

List of original publications included in this thesis:

I   Kainulainen, T. P. & Heiskanen, J. P. (2016). Palladium catalyzed direct coupling of 5-bromo-2-furaldehyde with furfural and thiophene derivatives. *Tetrahedron Letters*, *57*(45), 5012–5016. doi.org/10.1016/j.tetlet.2016.09.097

II   Kainulainen, T. P., Sirviö, J. A., Sethi, J., Hukka, T. I., & Heiskanen, J. P. (2018). UV-Blocking Synthetic Biopolymer from Biomass-Based Bifuran Diester and Ethylene Glycol. *Macromolecules*, *51*(5), 1822–1829. doi.org/10.1021/acs.macromol.7b02457

III Kainulainen, T. P., Hukka, T. I., Özeren, H. D., Sirviö, J. A., Hedenqvist, M. S., & Heiskanen, J. P. (2020). Utilizing Furfural-Based Bifuran Diester as Monomer and Comonomer for High-Performance Bioplastics: Properties of Poly(butylene furanoate), Poly(butylene bifuranoate), and Their Copolyesters. *Biomacromolecules*, *21*(2), 743–752. doi.org/10.1021/acs.biomac.9b01447

IV Kainulainen, T. P., Erkkilä, P., Hukka, T. I., Sirviö, J. A., & Heiskanen, J. P. (2020). Application of Furan-Based Dicarboxylic Acids in Bio-Derived Dimethacrylate Resins. *ACS Applied Polymer Materials*, *2*(8), 3215–3225. doi.org/10.1021/acsapm.0c00367

The first drafts for Papers I–IV were written by the author of this thesis as the primary author, and the coauthors provided additional writing contributions. The primary author carried out the syntheses, material preparations, and the related experimental design. The author of this thesis also participated in analyzing the compounds and materials, and the related experimental design. The publications are referenced in the text as Papers I–IV.

Table of contents

1   Introduction

1.1   Background

1.1.1 Current use and origin of plastics

Over the last few decades, the negative environmental impacts related to the growing production and use of synthetic organic polymers (plastics or resins) have gained wider attention. Two concerning issues are evident: 1) plastics are mostly derived from fossil resources 2) most plastics have little to no appreciable biodegradability, compounding the environmental contamination because of improper handling (Chamas et al., 2020; Geyer, Jambeck, & Law, 2017). The issues have become more pressing because the production rate of plastics has increased massively since the 1950s. Around half of the plastics ever produced were made in the 21st century: The total production of plastics from 1950 to 2017 has been estimated at 7800 million tons, with 3900 million tons produced in the 13 years leading up to 2017 (Geyer et al., 2017). While fossil resources in the form of crude oil, coal, and natural gas contribute heavily to the production of fuels and generation of electricity, the modern manufacture of organic compounds has also become heavily dependent on fossil hydrocarbons (Okkerse & van Bekkum, 1999). In the inevitable future, these non-renewable resources will deplete, while in the meantime, their use continues to release carbon dioxide into the atmosphere. For these reasons, the production of bulk organic compounds will have to transition over from utilizing fossil hydrocarbons to relying on renewable biomass sources, most notably carbohydrates (Lichtenthaler & Peters, 2004; Werpy & Petersen, 2004).

The recycling of plastics can alleviate some of their negative environmental impacts, but many challenges are still associated with trying to form a closed-loop system (Hahladakis & Iacovidou, 2019). Polymeric materials may be crudely divided into thermoplastics and thermosets, which differ in key characteristics (Crawford, 1998). Thermoplastics typically soften and melt at elevated temperatures since they consist of long, mostly linear macromolecules ("chains"). Thus, by weakening the intermolecular interactions through heating, the manufacture of shaped articles is possible from a flowing polymer melt. Thermoplastics can in principle be reshaped and, thus, recycled as many times as

necessary, but in practice, their properties usually degrade measurably after each processing cycle because of several factors.

For this reason, thermoplastics are typically recycled into lower grade products, e.g., a bottle made from poly(ethylene terephthalate) (PET) is preferably recycled as polyester fibers or as products other than new bottles for beverages because of possible contamination, degradation etc. during recycling operations (Iacovidou, Velenturf, & Purnell, 2019; Raheem et al., 2019). On the other hand, thermosets consist of complex three-dimensional networks held together by several covalent bonds between the monomers. Because of this cross-linking, they cannot be reshaped in the same way that thermoplastics can be since they will not melt or dissolve without an undesirable breakdown of the polymer. As such, they typically cannot be recycled. As the covalent cross-links provide a unique set of properties, thermosets have numerous applications that depend on these specific characteristics, such as high-performance composites. However, some materials incorporate certain characteristics of both thermoplastics and thermosets. So-called covalent adaptable networks or vitrimers are, in simple terms, cross-linked polymers that can be reshaped through dynamic reorganization of covalent bonds when a certain external stimulus (e.g., heat) is applied to the material (Fortman et al., 2018; Kloxin, Scott, Adzima, & Bowman, 2010). The development of these unique, novel materials demonstrates that solutions to issues such as sustainability can be brought about by the understanding and careful design of monomers and polymer networks.
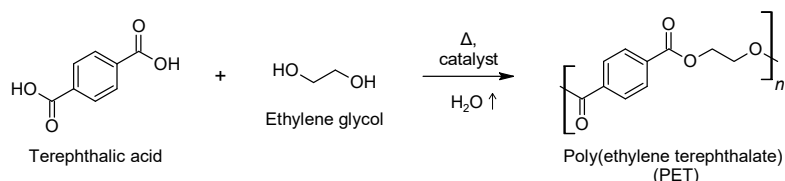
Fig. 1. Synthesis and structure of PET, common polyester used in plastic packaging and synthetic fibers.

Currently, the manufacture of packaging materials represents the largest application of plastics, and packaging is responsible for around half of the plastic waste generated annually (Geyer et al., 2017). Currently, the thermoplastics polyethylene (PE), polypropylene (PP), and poly(ethylene terephthalate) are the most common packaging materials in terms of production tonnage. As a polyester, PET is

synthesized in a polycondensation reaction (Fig. 1), which separates it from the other commodity plastics. It is among the most common thermoplastics because of its prevalent use in water and soft-drink bottles and packaging films, where its high-performance characteristics are important (McKeen, 2012). Overall, PET is a material with excellent properties compared to other common plastics: It has excellent mechanical and gas-barrier properties, along with high melting (T_m) and glass transition (T_g) temperatures. It is also useful in demanding applications and can be made into highly transparent products. Because of its value as a material, it is collected and recycled extensively in some parts of the world. Since polyesters such as PET may be obtained through polycondensation reactions between dicarboxylic acids and diols (or hydroxycarboxylic acids), biomass-based chemicals should be an ideal feedstock for renewable polyesters. Afterall, biomasses tend to contain many reactive functional groups available for modification, especially those containing oxygen atoms (e.g., -OH, -COOH) (Vassilev, Baxter, Andersen, & Vassileva, 2010).

1.1.2 The movement to renewable polymers

The conveniences provided by the low density, high specific strength, and ease of processing for many applications have made organic polymer materials indispensable for today's societies. For this reason, reduced usage and increased recycling must be supported by the utilization of sustainable chemical feedstocks (Belgacem & Gandini, 2008). Certainly, the global availability of biomass suggests that it would be possible to satisfy the demand of chemicals by replacing the current petrochemical feedstocks with biobased feedstocks. For traditional polymers such as PET, this fact offers mainly two possibilities (Fig. 2):

1) The current fossil-based raw materials can be simply derived from a renewable feedstock using a new chemical route, meaning there is no change from the perspective of the final product.

2) Using novel renewable building blocks to develop new materials to replace the old ones. The possible advantage of the latter is that unique materials with improved properties, e.g., better biodegradability or reduced oxygen permeability, could be discovered and developed. The advantage of the former, of course, is that the product (e.g., a plastic bottle) does not differ in its chemical makeup, and a proper drop-in replacement is always achieved.

For some of the current commodity plastics, renewable routes have been developed (Gandini & Lacerda, 2015; Siracusa & Blanco, 2020). For example, PE

may be produced from renewable ethylene, which is derived from bioethanol. On the other hand, the availability of renewable ethylene glycol has meant that (partially) biobased PET can now be manufactured, though routes to renewably sourced terephthalic acid are also being investigated (Pang et al., 2016; Tachibana, Kimura, & Kasuya, 2015). Biobased ethylene glycol is made from glycerol, which allows this by-product of the biodiesel industry to be utilized (Kandasamy, Samudrala, & Bhattacharya, 2019). Limonene, furfural, and 5-hydroxymethylfurfural (HMF) have all been suggested as possible feedstocks for terephthalic acid (Fig. 2). However, there is no apparent source of renewable terephthalic acid. In the most favorable case, the route should naturally utilize existing wastes from other processes (e.g., limonene from orange peels) to decrease environmental impact as much as possible. However, the suggested routes for renewable terephthalic acid can be lengthy, and their ability to compete with "fossil-PET" appears unclear. Again, the main advantage is that there is no question whether "bio-PET" will perform in applications since it is chemically identical to currently available PET.
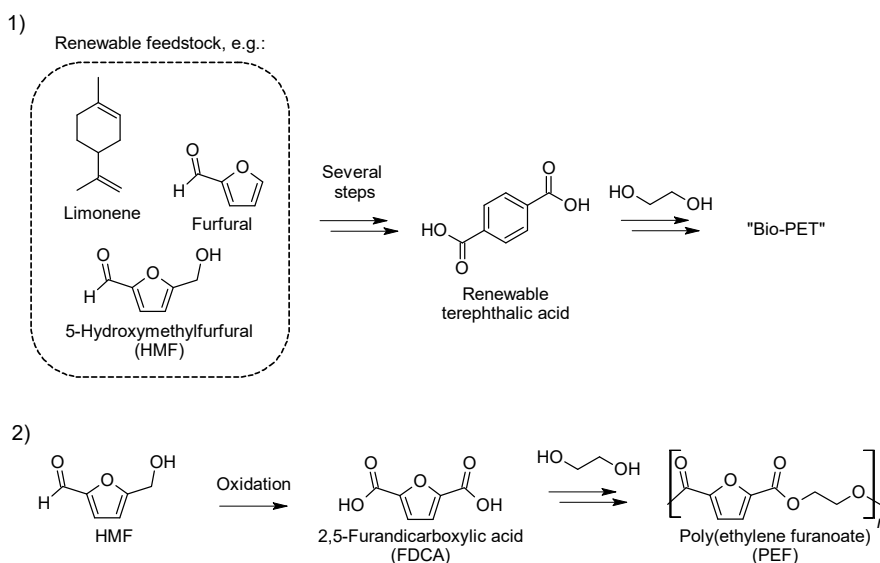

Fig. 2. Replacement of fossil PET by renewable alternatives.

There is currently considerable interest in developing novel materials such as polyesters from uniquely renewable compounds. A good demonstration of the

18

possible merits of novel biobased materials is poly(ethylene furanoate) (PEF) (Fig. 2). It has an obvious structural resemblance to PET, which has placed it into a prime position to replace PET (Fei, Wang, Zhu, Wang, & Liu 2020). While there exists a certain structural similarity, the two are not strictly interchangeable. Fortuitously, the furan units lead to several property enhancements that allow PEF to outperform PET, particularly as a gas barrier material. The renewability of PEF comes from its key monomer, 2,5-furandicarboxylic acid, which can be obtained from suitable C6 carbohydrates (e.g., fructose) through dehydration and oxidation. Furans are, in general, recognized as well-established biochemicals, which polymer chemists have long been interested in (Gandini & Belgacem, 1997). Furan-based materials such as PEF will undoubtedly be deployed as useful renewable alternatives to plastics currently in the commercial market, considering the multifaceted chemistry of furans. Accordingly, this work focused on the development and characterization of novel materials derived from furfural-based monomers. Furfural is one of the simplest furans and among the oldest synthetic biochemicals produced at a large commercial scale (Zeitsch, 2000).

1.2   Research aims

In broad terms, the objective of the research was to study the preparation and properties of novel biomass-based materials. Specifically, this research focused on utilizing furfural or furfural derivatives as precursors for 2,2'-bifuran–based monomers and applying them in the synthesis of new materials. This research included the investigation of synthetic methods for the preparation of 2,2'-bifuran–based precursors and various analyses that were carried out on the materials. The thesis aimed to investigate the three formulated hypotheses:

i.   Pd-catalyzed coupling of furfural, or a derivative thereof, is a feasible strategy to produce the proposed bifuran structure efficiently.
ii. Utilizing 2,2'-bifuran-5,5'-dicarboxylic acid or its derivatives, renewable alternatives to traditional oil-based monomers and polymers can be prepared.
iii. Improved properties can be achieved by replacing the traditional monomers with the proposed 2,2'-bifuran monomer(s).

1.3 Thesis outline

This work is based on four publications (Papers I–IV): In Paper I, the coupling chemistry of furfural was explored to develop a new Pd-catalyzed route to 2,2'-bifurans. In Paper II, the work was continued, and an efficient Pd-catalyzed direct coupling reaction was developed successfully and applied in gram-scale monomer syntheses. The synthesis and properties of a novel 2,2'-bifuran–based polyester were also reported. In Paper III, the study of polyesters was expanded to copolyesters of furan and 2,2'-bifuran-derived dicarboxylic acids, which were shown to retain excellent barrier characteristics of their parent homopolyesters. In Paper IV, the uses of the same furan and 2,2'-bifuran-derived dicarboxylic acids were expanded to novel dimethacrylate monomers used to prepare biobased polymer networks.

Following the background provided by this introductory chapter (Chapter 1), Chapter 2 will provide a short review of the literature related to the utilization of furans in polymers to familiarize the reader with the subject. Chapter 3 includes the descriptions of the relevant experimental and analytical procedures used to obtain the results presented in this thesis. Chapter 4 presents and discusses the key results obtained in this work. As a closing summary, Chapter 5 provides a brief description of the most notable parts of the work.

2 Literature review

2.1 Production and use of furfural and 5-hydroxymethylfurfural

Furfural and 5-hydroxymethylfurfural are simple furans derived from biomass, and as aromatic heterocycles, they have many potential applications in polymers (Gandini, Lacerda, Carvalho, & Trovatti, 2016). In addition, the versatile chemistry of furans allows them to be utilized as furan-derivatives or as a platform for non-furan compounds. Furfural (C5 platform) and 5-hydroxymethylfurfural (C6 platform) are obtained directly in a facile manner from abundant pentoses and hexoses, respectively (Istasse & Richel, 2020). Furfural has already been utilized as a renewable chemical for almost a century. In the past, it provided a way to valorize the side-streams generated by the cereal industry (Zeitsch, 2000). HMF on the other hand has garnered much attention, mostly during the last few decades as another, highly versatile biochemical (van Putten et al., 2013). The reactions leading from a sugar to furfural or HMF are very similar, usually involving sequential dehydrations in the presence of acid catalysts. Despite the simple nature of the transformation, the dehydration steps are mechanistically contested and quite intricate.

2.1.1 Feedstocks

Plants mainly consist of three organic polymers suitable as chemical feedstocks: cellulose, hemicellulose, and lignin (Belgacem & Gandini, 2008; Zhou, Xia, Lin, Tong, & Beltramini 2011). The ratio of the three varies to some extent, according to the plant, but cellulose is the most abundant natural polymer. Combined, they form lignocellulose, a kind of natural composite material. In trees, the matrix of hemicellulose and lignin is reinforced by oriented and highly crystalline cellulose fibers that combine to form structural support. Obviously, the native forms of these polymers are widely used as materials (e.g., wood). On the other hand, some chemically modified forms, most notably, cellulose acetates and cellulose nitrates, were among the first synthetic plastics to be produced. In the future, however, lignocellulosic biomasses can act as the source of (organic) chemicals. With the development of numerous conversion strategies, simple platform chemicals can be further converted into the myriad of organic compounds necessary for modern industrial products. Furfural and HMF thus become important as initial "frontline"

platform chemicals because they are directly derived from the abundant carbohydrate fractions of biomasses (Corma, Iborra, & Velty, 2007; Mika, Cséfalvay, & Németh, 2018).

Naturally, the utilization of cellulose, hemicellulose, and lignin as chemical feedstocks requires depolymerization and efficient conversion into the desired target compounds. As polyacetals, cellulose and hemicellulose are both degraded by the usual chemical methods, e.g., hydrolysis in the presence of an aqueous acid. The structural regularity of cellulose makes it highly crystalline, which, together with the high number of repeating units (from hundreds to several thousand glucose molecules), makes it resistant to depolymerization. Since cellulose is made up of linear chains of glucose linked in (1,4)-manner (Fig. 3a), its depolymerization yields hexoses (i.e., glucose), which can be dehydrated into HMF. By comparison, the heterogeneity of hemicelluloses makes them much more amorphous and easily degradable, which is further helped by their usually much lower molar masses. Therefore, it is unsurprising that the commercial production of furfural, derived from hemicellulose, has been going on since the early 20th century (Zeitsch, 2000).
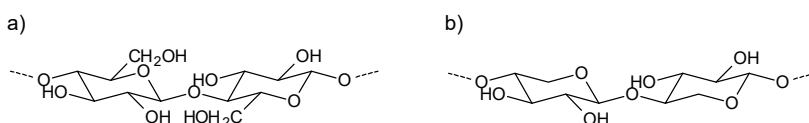
Fig. 3. *β*-(1,4)-glycosidic linkages between units of glucose in cellulose (a) and xylose units in hemicellulose (b).

2.1.2 5-Hydroxymethylfurfural

HMF is primarily obtained from the dehydration of fructose, from which three water molecules are eliminated (Fig. 4). The isomerization of glucose into fructose is possible, e.g. through a 1,2-enediol intermediate, enabling the cheaper glucose to be a possible feedstock for HMF (Fig. 4). As glucose can be obtained from cellulose, the potential amount of feedstock for HMF is immense, as is the number of further derivatives down the line (Caes, Teixeira, Knapp, & Raines, 2015; van Putten et al., 2013). Furthermore, several available cellulosic biomass sources are considered inedible (e.g., sawdust), which would reduce the potential for conflict with food production. However, compared to highly purified fructose, the direct

22

conversion of lignocelluloses or glucose into HMF does not necessarily provide yields as high because of the necessary extra steps.
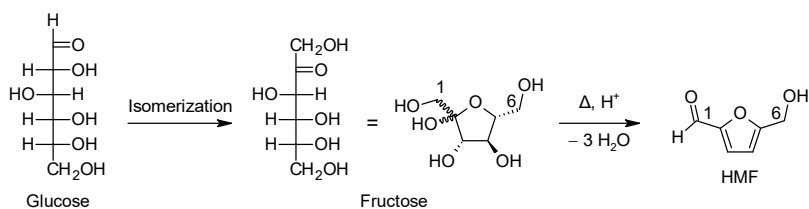
Fig. 4. The general route for conversion of glucose or fructose into HMF.

There has been some uncertainty around the exact mechanisms of the dehydration steps that finally yield HMF. For the dehydration of fructose into HMF, different intermediates and pathways were suggested (Antal, Mok, & Richards, 1990; Moreau et al., 1996): The acyclic pathway from the open-chain forms, and a cyclic pathway, where the fructofuranose ring stays intact during the dehydration. Certain aspects of the dehydration of fructose were studied by Zhang & Weitz (2012), who used fructose labeled with ^{13}C at carbons 1 or 6 (Fig. 4). In that study, the generated HMF was shown to have the ^{13}C label at the corresponding positions, which they considered consistent with previous mechanisms involving cyclic intermediates. However, the course of the reaction and the products formed may be altered depending on the catalysts and solvents, which they also showed by comparing the dehydrations taking place in either DMSO or water.

Because of the process by which it forms, 5-hydroxymethylfurfural is usually present in small quantities in many types of foods and beverages, particularly when processed using high temperatures, as discussed by van Putten et al. (2013). In terms of its properties, HMF is a low melting crystalline solid (melting point ca. 30 ºC), with a high boiling point (ca. 115 ºC at 1 mbar). However, it is a relatively sensitive compound, particularly towards strong aqueous acids, because of its two highly reactive functional groups (Gandini & Belgacem, 1997). Therefore, various side-processes are to be expected during the dehydration of sugars into HMF. Common byproducts include levulinic and formic acids and humins, generally poorly soluble solids (Cheng et al., 2018). Humins are quite complex polymers or oligomers that contain furans and various other dehydrated, sugar-derived structures. Levulinic acid, on the other hand, is formed by the rehydration reaction of HMF, which also eliminates the carbonyl group as formic acid (Zhang & Weitz, 2012). Preventing HMF from reacting to these byproducts plays a key part in

improving yields. Many organic solvents as reaction media or as cosolvents in water have proven helpful at reducing unwanted reactions from happening at high conversions (Kuster & van der Steen, 1977).

Besides the different sugar precursors, HMF differs from furfural in the potential uses that the compound may have because of its additional carbon atom. It can allow other chemical platforms to be accessed, e.g., levulinic acid or HMF may be used to manufacture other important furans such as 2,5-dimethylfuran and 2,5-furandicarboxylic acid, among others (Mika et al., 2018; Román-Leshkov, Barrett, Liu, & Dumesic, 2007). From the perspective of polymer chemistry, FDCA can be identified clearly as its most important "descendant." FDCA is a simple oxidized derivative of HMF. Like other dicarboxylic acids, it can be used as a versatile monomer in renewable polymers, particularly as a replacement for terephthalic acid. For this reason, FDCA-derived polymers should be seen as important drivers for the demand and commercialization of HMF. At the same time, there has also been interest in using HMF as a platform for currently oil-based monomers such as terephthalic acid (Pacheco & Davis, 2014). As an example, the Diels-Alder reactivity of furans has been exploited to prepare renewable terephthalic acid, according to Figure 5. The Diels-Alder reaction takes place between an appropriate HMF-derivative and ethene. The intermediate (not shown) then undergoes a dehydrating aromatization step. After oxidation, terephthalic acid can be obtained. The ability of HMF to act as a precursor for either FDCA or terephthalic acid is a fitting demonstration of its flexibility as a feedstock for polymers.
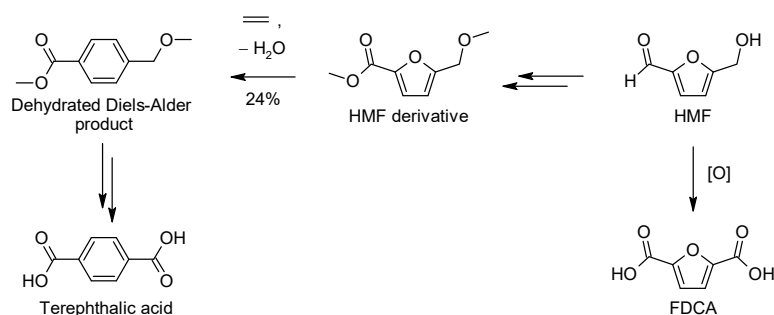
Fig. 5. HMF as a precursor for terephthalic acid and its renewable alternative, FDCA.

24

2,5-Furandicarboxylic acid

2,5-Furandicarboxylic acid is an intensely studied monomer that may challenge terephthalic acid as the chief aromatic dicarboxylic acid used in thermoplastic polyesters. While FDCA is obtained via the oxidation of HMF, terephthalic acid is traditionally obtained through the oxidation of *p*-xylene (Tomás, Bordado, & Gomes, 2013). A well-known industrial method used for this transformation is the so-called Amoco process, which is used to produce terephthalic acid in high yield by employing cobalt and manganese catalysts. The process is aerobic, meaning (pressurized) air is used as the oxidant. Similar catalyst systems have been evaluated for the production of FDCA from HMF (Partenheimer & Grushin, 2001). However, the production of FDCA from HMF has also been studied using a wider variety of oxidants and catalysts, and these methods have been reviewed recently (Wojcieszak & Itabaiana, 2020; Zhang & Huber, 2018). In addition to stoichiometric oxidants or catalytic systems, biocatalytic routes are being developed, but the well-known toxicity of HMF and similar furans on microorganisms are a hurdle (Yuan et al., 2020).
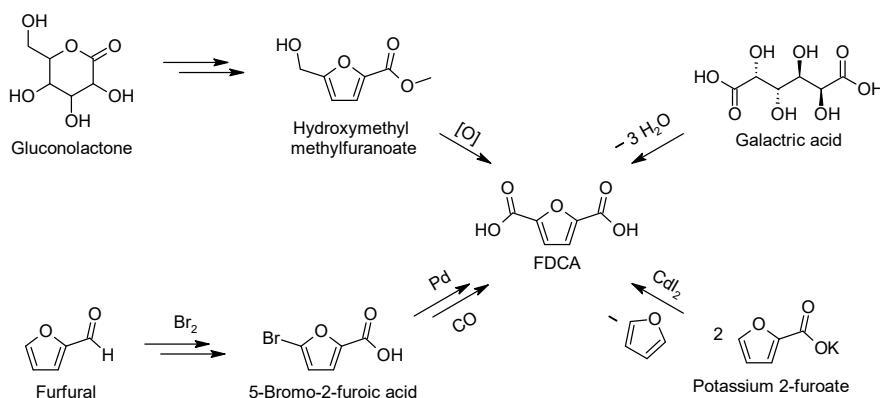
Fig. 6. Examples of HMF-avoiding routes to FDCA.

It is interesting to consider the different ways that 2,5-FDCA has been prepared while avoiding HMF (Fig. 6): Using carboxylic acids derived from glucose is relatively straightforward, and patents that describe the use of different sugar acids such as galactric acid in various processes that yield FDCA or its derivatives can be found (Zhang & Huber, 2018; international patent application WO2016166421A1, 2016; US patent US9701652B2, 2017). As another alternative,

gluconolactone has been demonstrated as a precursor for HMF-derivatives, which can be converted into FDCA (M. J. Pedersen, Jurys, & C. M. Pedersen, 2020). The supposed advantage of these intermediates is their improved stability compared to HMF. Unsurprisingly, furfural has also been investigated as a possible feedstock for FDCA. Specifically, 2-furoic acid, the oxidized derivative of furfural, has been used as the starting compound. The Pd-catalyzed carbonylation reactions require the use of brominated intermediates, with carbon monoxide providing the additional carbon atom (Shen et al., 2019; Zhang, Lan, Chen, Yin, & Li 2017). The Henkel reaction, on the other hand, can be used to transform 2-furoic acid into FDCA via potassium 2-furoate, with one equivalent of the starting material acting as the carbon atom source (Thiyagarajan, Pukin, van Haveren, Lutz, & van Es 2013). 2-Furoic acid can also be directly carboxylated using alkali metal carbonates and a CO_2 atmosphere (not shown), avoiding the brominated derivatives (Dick, Frankhouser, Banerjee, & Kanan, 2017). In the Henkel reaction, 2-furoic acid undergoes a disproportionation, and therefore furan is produced along with FDCA. However, the reaction can be a source for varying amounts of 2,4- and 3,4-furandicarboxylic acids. These FDCA isomers have been evaluated as polyester precursors as well, and they have shown deviate from FDCA-based polyesters in some interesting, and potentially useful ways (Thiyagarajan et al., 2014).

While FDCA can be considered one of the primary renewable alternatives to terephthalic acid, the non-drop-in nature between these two dicarboxylic acids affects the properties of the resulting polymers. More problematically, the costs associated with FDCA are currently too high to allow it to be used as a synthetic commodity, like terephthalic acid. It is commonly thought that the price of FDCA should be in the order of 1000 dollars per ton, which is significantly below the current estimate (Zhang & Huber, 2018). Commercially viable industrial-scale processes towards HMF, FDCA, and PEF are being developed to meet this goal, notably by Avantium (https://www.avantium.com/) in the Netherlands. Their estimates suggest that the commercialization of FDCA is anticipated within the next few years, which would suggest that the commercialization of poly(ethylene furanoate) is still several years away, even in the most optimistic views.

2.1.3 Furfural

Furfural is a high-boiling, somewhat reactive heteroaromatic aldehyde with a long history of commercial significance. Samples typically have a yellow to very dark brown appearance, though when freshly distilled it is an entirely colorless liquid.

In keeping with HMF, furfural has a characteristic aroma that contributes to the flavor of many foods and drinks, and it may be formed whenever carbohydrates are exposed to high temperatures. In a sense, furfural is a prototypical renewable platform chemical, with the initiation of its industrial production dating back to the 1920s, now almost a century ago, when the Quaker Oats Company (in Iowa, US) begun production. Nowadays, the industrial production (ca. 200 000 tons annually) of furfural appears to be mostly concentrated in China, which is likely because of the availability of feedstock (Mamman et al., 2008; Zeitsch, 2000).

The synthesis of furfural from a feedstock containing pentoses, primarily xylose, generally involves the use of elevated temperatures and the presence of a strong Brønsted acid (Fig. 7) (Zeitsch, 2000). Pentosans, i.e., hemicelluloses rich in pentoses, may be found, for example, in corncobs and sugar-cane bagasse. The feedstock is usually treated with a dilute acid solution and then heated using steam injected into the lined steel reactor. After rapid acid-catalyzed depolymerization of pentosan, the released pentoses are dehydrated into furfural. Furfural is then distilled off together with water, and the furfural is separated from the mixture. The rapid removal of furfural is necessary to prevent degradation, as the reaction conditions are usually harsh. As with HMF, byproducts such as humin-type condensation products can be formed from furfural, carbohydrates, and intermediates of the dehydration, reducing yields far below the ideal (Zeitsch, 2000). Despite the low yields of around 50% and the general crudeness of typical industrial processes, furfural does appear to be a relatively affordable chemical. While its price is hardly constant, it appears to be comparable to oil-based aromatics such as benzene, toluene, and the xylenes (Mika et al., 2018; Straathof & Bampouli, 2017).
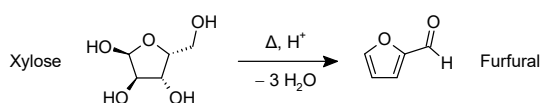
Fig. 7. Representative acid-catalyzed dehydration of pentose sugars into furfural.

As mentioned in Chapter 1, furfural and other furans have a long-recognized place as raw materials in polymer chemistry: Historically, furfural was mostly reduced catalytically into furfuryl alcohol: Furfuryl alcohol is a useful precursor for cross-linked thermoset resins and binders (Gandini & Belgacem, 1997; Zeitsch, 2000). By itself, furfural can also be used in some special applications: It has been used as a solvent in the liquid-liquid extraction of unsaturated compounds from oils and as

an active ingredient for soil sterilization or elimination of plant parasites in agriculture. While furfural is still important as the raw material for furfuryl alcohol, the current interest in furfural is driven by the search for potential biochemicals (Li, Jia, & Wang, 2016). Besides other furans, furfural could also be used as a feedstock for several important and promising non-furan chemicals, such as succinic acid and 1,5-pentanediol (Choudhary, Nishimura, & Ebitani, 2013; Liu, Amada, Tamura, Nakagawa, & Tomishige 2014).

The preparation of furfural is associated with certain challenges, such as the dubious "greenness" of the production methods currently in use (Zeitsch, 2000). Despite this, furfural continues to be produced commercially at a modest scale, although only a limited market. However, the seemingly established position of furfural as a commercial, heteroaromatic biochemical should be strengthened through further development and diversification of how furfural is utilized. In this work, the less studied strategy of applying furfural in aromatic coupling products, 2,2'-bifurans, was investigated as an approach towards novel polymers.

2,2'-Bifurans

As discussed in previous sections, FDCA has been firmly established as one of the most promising renewable dicarboxylic acids (or furans for that matter). It provides direct access to important materials such as polyesters. The goal of this work was to prepare analogous materials by utilizing furfural. As demonstrated earlier in this chapter, furfural could simply be converted into FDCA by introducing an additional carbon atom. However, the dimerization (joining together) of two molecules of furfural, or its derivative, can be fathomed as a conceptually similar, yet simple solution to the problem (Fig. 8): The products (2,2'-bifurans) have appropriate functional groups at each end of the molecule providing reactive sites for polymerization, and the rigid two-ring structure should be conducive to mechanically and thermally robust materials.
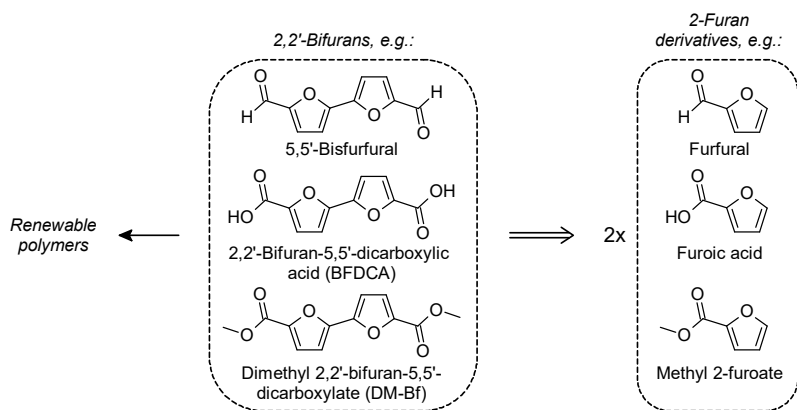
Fig. 8. Using biomass-derived 2-substituted furans as polymer precursors.

2,2'-Bifurans (as shown in Fig. 8) are not entirely novel compounds: Previously, the synthesis of 2,2'-bifurans from furan derivatives has mainly been achieved using transition metals as catalysts. Some of the earliest work on this transformation was reported in the 1960s by Grigg, Knight, & Sargent (1966). Despite this long history, the furfural-derived 2,2'-bifuran monomers depicted in Figure 8 are uncommon, largely ignored in polymer chemistry. However, similar rigid monomers composed of two linked (or fused) aromatic rings find use in high-performance polymers (Asrar, 1999). For example, 4,4'-biphenyldicarboxylic acid (4,4'-BDA) may be used to improve the properties of polyester materials (international patent applications WO2017112031A1, 2017; WO1993002122A1, 1993). However, unlike 4,4'-BDA and many similar dicarboxylic acids, the 2,2'-bifuran monomers are biobased with all carbon atoms derived from biomass. Therefore, they offer the potential for novel biobased, high-performance plastics.

It is important to note that the 2,2'-bifuran moiety may be found as a conjugating part in polymers and small molecules such as α-oligofurans, which are used as semiconducting materials (Gidron & Bendikov, 2014). A notable feature of these 2,2'-bifuran moieties is their preference for planar conformations, which are favored by increased conjugation between the two furan rings (Gidron, Varsano, Shimon, Leitus, & Bendikov 2013a). The resultant properties can enhance certain characteristics important in organic electronics, so the moiety is not uncommon in the field (Gidron et al., 2013b; Mulay, Bogoslavky, Galanti, Galun, & Gidron 2018). Based on simulations, simple 2,2'-bifurans are also expected to prefer a planar conformation, with the torsion angle between the furan rings at 180º (i.e., the

oxygen atoms are *anti*) (Bloom & Wheeler, 2014). Accordingly, carbonyl groups at positions 5 and 5' should prefer coplanar conformations with the 2,2'-bifuran unit (Tachibana, Hayashi, & Kasuya, 2018). Previously, the related 2,2'-bithiophenes have been experimentally shown to have similar conformational preferences, with carbonyl groups at positions 5 and 5' preferring coplanarity with the 2,2'-bithiophene unit (Wang & Brisse, 1998).

In light of the previous considerations, the three bifuran monomers shown in Figure 8, therefore, have potentially promising properties: 5,5'-Bisfurfural has a high melting point of more than 260 ℃ (Taljaard & Burger, 2002a), 2,2'-bifuran-5,5'-dicarboxylic acid decomposes at 315 ℃ without melting, and its dimethyl ester melts at 234 ℃ (Cresp & Sargent, 1973). Such properties entail polymers with high glass transition and melting temperatures. In addition, the highly conjugated 2,2'-bifuran monomers display red-shifted absorbance of light compared to similar "monofurans." Furfural and 2,5-diformylfuran are colorless compounds, while 5,5'-bisfurfural is a yellow solid with absorption maxima (λ_{max}) at 347 and 365 nm in dichloromethane (Tachibana et al., 2018). DM-Bf, on the other hand, has two maxima at 325 and 342 nm in chloroform (Paper II), i.e., the oxidation of the aldehyde moieties lowers the wavelengths considerably. Thus, dimethyl 2,2'-bifuran-5,5'-dicarboxylate (DM-Bf) has a colorless appearance, though it can absorb UV light at higher wavelengths than the dimethyl ester of FDCA (λ_{max} = 265 nm). Therefore, materials containing 2,2'-bifuran moieties should potentially provide transparency to visible light and a degree of protection from UV light.

Synthesis of 2,2'-bifurans

Despite their relative rarity, several reported methods for the coupling of furans into 2,2'-bifurans exist (Fig. 9). Since furfural has long been a cheap and easily available furan, it is not surprising that 5,5'-bisfurfural is one of the most common 2,2'-bifurans. The earliest report by Grigg et al. (1966) describes the synthesis of 5,5'-bisfurfural along with other 2,2'-bifuran derivatives. They utilized Ullman-type couplings with stoichiometric copper-bronze powder to dimerize various halogenated furans: 5,5'-Bisfurfural was prepared via the homocoupling of 5-iodo-furfural in 50% yield, whereas DM-Bf was afforded in 68% yield from methyl 5-bromo-2-furoate using similar conditions. Many other synthetic methods have been used since then to afford 2,2'-bifurans from furan derivatives: A high yield of 5,5'-bisfurfural may be obtained using a Cu(II)-catalyzed homocoupling of 5-formyl-2-furanboronic acid (Cao et al., 2017). A palladium-catalyzed direct coupling reaction

between furfural and 5-bromofurfural may also be used, with this method giving 5,5'-bisfurfural in reported 64% yield (McClure et al., 2001). To varying degrees, these methods have the potential drawback of requiring (halogen or boron) derivates to drive the reactions, introducing additional costs and lowering atom economy.
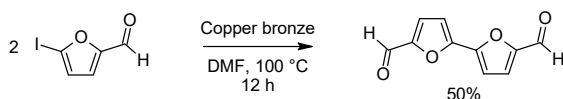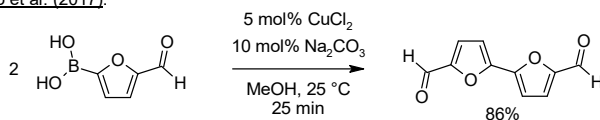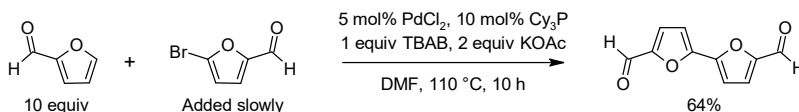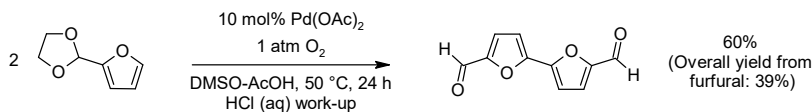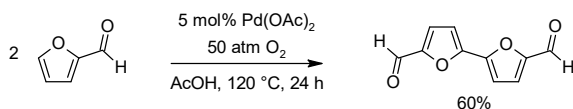
Fig. 9. Examples of 2,2'-bifuran syntheses via metal-catalyzed couplings.

To mitigate the issues, several works have examined the oxidative homocoupling of furans, including furfural, into 2,2'-bifurans. In such a reaction, H_2 is formally released when the two furans are joined together. However, the reaction requires a

terminal oxidant to "absorb" the hydrogen atoms. O_2 and even air have been appropriate oxidants in some cases. For example, the Pd-catalyzed oxidative homocoupling of electron-rich alkyl furans and thiophenes can take place at ambient temperatures to afford high yields of 2,2'-bifurans and 2,2'-bithiophenes (Li et al., 2014). While an O_2 atmosphere at ambient pressure was able to act as the terminal oxidant, the reaction could evidently be run under air but with reduced yield. The major limitation of the method is that electron-poor furans (e.g., furfural) are unsuitable substrates. In the case of furfural, the problem is obviated by converting the aldehyde into a cyclic acetal using ethylene glycol (Tachibana et al., 2018). In this way, the electron-withdrawing character of the carbonyl moiety is "neutralized" temporarily so that the coupling may take place. This route has been used to prepare 5,5'-bisfurfural in an overall yield of 39% (starting from furfural).

The Pd-catalyzed aerobic oxidative homocoupling of furfural has been previously reported in the literature (Taljaard & Burger, 2002b). It may be considered to be inherently the most attractive method in terms of "greenness." However, to achieve reasonable yields, the method reported by Taljaard & Burger (2002b) required extreme partial pressures of O_2 to make the reaction run catalytically (30–50 atm). Nonetheless, 5,5'-bisfurfural may be obtained in 60% yield using these rather forcing conditions. In a complete departure from the previous methods, Taljaard & Burger (2002a) have also reported a photochemical radical coupling of furfural into 5,5'-bisfurfural (see also: International patent application WO2000015623A1, 2000). According to them, the reaction is initiated by a small amount of 5-bromofurfural and proceeds under appropriate UV irradiation. The interesting aspect of the reaction is its reported ability to sustain itself once the bromide has been consumed. According to the more detailed description in the book by Zeitsch (2000), furfural may simply be replenished as it is consumed to continue the reaction. 5,5'-Bisfurfural, which has low solubility in the reaction solvent (acetonitrile), is filtered out and collected. Sadly, few attempts to replicate or utilize this reaction can be found (Comer, Aurand, & Jessop, 2007).

During the current thesis work, the coupling chemistry of furans was also explored (Papers I and II). Eventually, a straightforward palladium-catalyzed reaction was developed to prepare DM-Bf as a monomer for polyester synthesis. However, there continues to be a need for a reliable, atom efficient (or "green"), and highly economical synthesis of 2,2'-bifurans starting from affordable furans. The aerobic oxidative coupling might best meet these requirements; however, electron-withdrawing substituents make furfural and furoic acid esters challenging substrates, at least based on current literature. Additionally, the new methods should

instead employ low catalyst loadings (e.g., < 5 mol%) with expensive metals such as palladium (preferably recyclable). Of course, there is limited interest in such transformations because of the currently incredibly limited applications of 2,2'-bifurans.

2.2   Furan-based polymers

Polymers with a furan ring as either a chain-forming part or as a simple pendant group in the repeating unit are quite numerous in the literature.They encompass most types of polymers, e.g., polyesters (Sousa et al., 2015), polyamides (Cureton, Napadensky, Annunziato, & La Scala, 2017), polyacrylates (Davidenko, Zaldívar, Peniche, Sastre, & San Román 1996), polyurethanes (Laita, Boufi, & Gandini, 1997), and epoxy resins (Cho et al., 2013). However, the scope of the short review here will be limited to examples of FDCA as a monomer in polyesters or as a precursor for cross-linkable derivatives. Because of the general scarcity of literature on 2,2'-bifuran -derived monomers and their polymerization, however, they will be discussed in wider scope barring semiconducting polymers, which will not be included.

2.2.1 FDCA-based polyesters

At present, furan-based thermoplastics are yet to be commercialized on a large scale. However, the furan-based thermoplastics have a significant presence within the research and patent literature, which is made clear by any cursory search using the term 'FDCA.' Furan polyesters are therefore poised to be the first thermoplastics derived from FDCA to enter the commercial market, mostly thanks to the interest in PEF (Fei et al., 2020). The prospect is that because of the similarities in applications between FDCA and terephthalic acid, furan-based polyesters may be used in place of current widely used polyesters. However, FDCA-based polyesters and traditional aromatic polyesters differ in numerous ways. Besides differences arising in the materials because of the substitution of terephthalic acid, there are also challenges associated with the use of FDCA, e.g. its stability under high temperatures (Tsanaktsis, Papageorgiou, & Bikiaris, 2015a). Additionally, preparing PEF that is comparable to commercial PET in appearance (i.e., colorless) is still a challenge. It seems to require optimization of catalyst systems and reaction conditions (Banella et al., 2019).

Common commercial homopolyesters based on terephthalic acid include PET, poly(trimethylene terephthalate) (PTT), and poly(butylene terephthalate) (PBT), where the diol components are ethylene glycol, 1,3-propanediol, and 1,4-butanediol, respectively (Fig. 10). With 2,5-furandicarboxylic acid, homopolyesters with diols having up to 12 atom carbon chains have been reported (Jiang, Liu, Zhang, Ye, & Zhou 2012; Papamokos, Dimitriadis, Bikiaris, Papageorgiou, & Floudas 2019). Among them, PEF (Gandini, Silvestre, Neto, Sousa, & Gomes 2009), poly(trimethylene furanoate) (PTF) (Seo et al., 2011), and poly(butylene furanoate) (PBF) (Zhu et al., 2013) are the most interesting because of their similarities with current commodity polyesters (Fig. 10). Compared to traditional polyesters, their properties are also promising (Table 1), e.g., they have relatively high glass transition and melting temperatures and excellent gas barrier characteristics (Guidotti et al., 2020; Knoop, Vogelzang, van Haveren, & van Es, 2013). The glass transition temperatures of PEF, PTF, and PBF are almost the same or slightly higher than their terephthalic acid counterparts. In contrast, the melting temperatures show the opposite tendency of being slightly lower. The lower melting temperatures would suggest that lower processing temperatures are possible. At the same time, the comparable T_g values mean that the materials should retain stiffness at the temperatures necessary in many applications. Additionally, the mechanical properties of PEF, PTF, and PBF are promising.

Poly(ethylene terephthalate)
(PET)

Poly(trimethylene terephthalate)
(PTT)

Poly(butylene terephthalate)
(PBT)

Poly(ethylene furanoate)
(PEF)

Poly(trimethylene furanoate)
(PTF)

Poly(butylene furanoate)
(PBF)
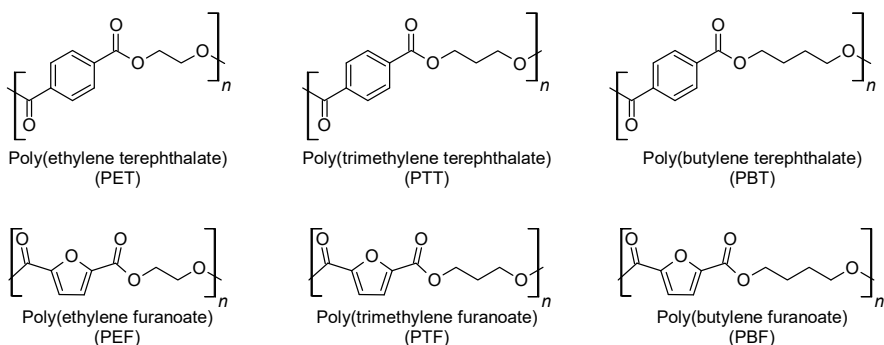
Fig. 10. Structures of common terephthalate polyesters and their furan-based alternatives.

Table 1. Comparison of relevant homopolyesters derived from terephthalic and 2,5-furandicarboxylic acids.[1]

Polyester	T_g	T_m	Oxygen permeability
	(ºC)	(ºC)	(cm^3 mm m^{-2} d^{-1} atm^{-1})
PET	75	260	7.5[2]
			1.5[3], 2.5–3[3]
PEF	77	212	0.7[2]
			0.2–0.7[3]
PTT	46	227	1.6[3]
PTF	51	174	0.5[2]
			<0.05[4]
PBT	40	220	15.2
PBF	34	169	1.2[2]

[1] Data selected from Papamokos et al. (2019); McKeen (2017); Burgess et al. (2014); van Berkel et al. (2018); Vannini et al. (2015); Kim et al. (2018); Guidotti et al. (2018); Wang et al. (2017b). [2] Amorphous samples. [3] Biaxially oriented samples. [4] Annealed, crystalline sample.

The notable property enhancement with FDCA-based polyesters comes from their decreased gas permeabilities (Table 1). Amorphous and semi-crystalline PEF samples have significantly lower oxygen permeabilities than similar PET samples (Burgess, Karvan, Johnson, Kriegel, & Koros 2014a). Furthermore, biaxially oriented PEF shows a similar trend of decreasing O_2 permeability as PET, with further improvements in the gas barrier that correlate with increased crystallinities in the oriented films (van Berkel, Guigo, Kolstad, & Sbirrazzuoli, 2018). PTF has also shown excellent gas barrier properties, exceeding some of the reports for PEF (Vannini, Marchese, Celli, & Lorenzetti, 2015). However, the low oxygen permeability was observed for crystalline samples, prepared by annealing the PTF films at 135 ºC, as PTF crystallizes slowly. Still, the reported oxygen transmission coefficients with or without annealing were lower compared to PTT (Kim et al., 2018). Interestingly, the analogous 2,5-thiophenedicarboxylic acid–based polyester has been reported to have similar gas permeability characteristics as PTF (Guidotti et al., 2018). The trend is continued by PBF (Wang, Liu, Zhu, & Jiang, 2017), which has lower oxygen permeability than PET despite the flexible butylene moieties. FDCA polyesters prepared from even longer and more flexible diols have shown remarkable barrier properties as well. Poly(pentamethylene furanoate) (PPeF) films can achieve some of the lowest oxygen permeabilities reported for polyesters despite the absence of crystallinity and sub-ambient glass transition temperature (Guidotti et al., 2019). The properties have been explained through the existence of

an impermeable mesophase, which in PPeF forms because of the combination of very flexible pentamethylene units and rigid FDCA moieties.

Permeability testing carried out on PEF suggests that the decreased chain mobility within the PEF chains reduces the diffusivities for O_2 (Burgess et al., 2014a) and CO_2 (Burgess, Kriegel, & Koros, 2015) significantly compared to PET. The low chain mobility resulting from the FDCA unit has been explained by its hindered ring-flipping motion and intermolecular hydrogen bonds (Araujo et al., 2018; Burgess et al., 2014b). The non-linear axis of rotation makes the furan ring less free to rotate than the 1,4-phenyl moiety of PET, decreasing the ability of penetrants to move within the bulk material. However, the polarity of the furan ring must also play a role, as the isophthalate unit of poly(ethylene isophthalate) (PEI) has a non-linear axis of rotation as well, yet PEF outperforms PEI as a gas barrier material by a noticeable margin (Burgess et al., 2015). Some results suggest that the polarity results in hydrogen bonding, which takes place between neighboring PEF chains and their FDCA units. These interactions then further restrict the motion of the polymer chains and influence the crystalline structure of PEF (Araujo et al., 2018).

Besides the glass transition and melting temperatures, the thermal decomposition behavior of a polymer is obviously very important. A potential drawback with furan-based polyesters is their slightly lower thermal stability compared to polyesters derived from terephthalic acid, though the choice of diol component may have a role as well (Poulopoulou et al., 2018; Thiyagarajan et al., 2014). This problem may tie into the increased discoloration often encountered when synthesizing polyesters from 2,5-furandicarboxylic acid. However, many factors such as catalysts, monomer purity, etc. are very likely to play a role in this process (Terzopoulou et al., 2017). Typical polyester decomposition mechanisms have been suggested based on TGA and analysis of pyrolysis gases under high temperatures (Tsanaktsis et al., 2015b). One such process is the β-scission, which yields a vinyl end group while cleaving the polyester chain in two at a random location (Fig. 11). The same reaction can result in the release of toxic acetaldehyde when a terminal hydroxyethyl ester group decomposes (Hong, Min, Nam, & Park, 2016).

Interestingly, the two isomers of FDCA, i.e., 2,4-FDCA and 3,4-FDCA, seem to result in polyesters ("2,4-PEF" and "3,4-PEF", respectively) that have increased thermal stabilities: Of the three isomers, 2,4-FDCA gave polyesters with the highest thermal stabilities with various diols (Thiyagarajan et al., 2014). Despite this stability they were still slightly inferior compared to reference PET samples. 2,4-

36

PEF and 3,4-PEF also had much lower glass transition and melting temperatures than PEF, making them perhaps less useful as rigid materials.
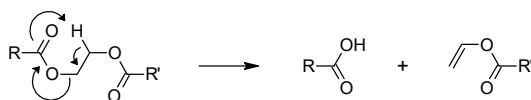
Fig. 11. *β*-Scission of the ethylene unit of a polyester.

Studies characterizing the degree of discoloration under various reaction conditions have been carried out previously (Banella et al., 2019; Gruter, Sipos, & Dam, 2012). They have shown that the color of FDCA-based polyesters can significantly differ depending on the catalyst used. Generally, titanium alkoxides such as tetrabutyl titanate tend to impart significant yellow or brown color to PEF during the synthesis. As such, catalysts with lower propensity for color are more attractive, but they may be less desirable because of suspected toxicity (antimony catalysts) or expenses (e.g., germanium catalysts). Others might have low activity, resulting in low molar mass within reasonable reaction times. One way to address low molar mass is to use solid-state polycondensation, which is performed at lower temperatures and may result in less discoloration (Banella et al., 2019). This process requires an appropriate catalyst and may be very sensitive towards the catalyst choice.

Some issues related to PEF and similar FDCA-derived polyesters can be alleviated by creating copolyesters, where additional diol or diacid components are used to modify the properties. Generally, the mechanical performance of FDCA-based polyesters is excellent but may fall short of current commercial polyesters in some respects (Knoop et al., 2013; Seo et al., 2011; van Berkel et al., 2018; Wang et al., 2017). A comparison between PET and PEF from different reports shows that PEF is always much more brittle. Even though oriented PEF films have shown relatively high ductility, the brittle character of PEF compared to PET remains a challenge (van Berkel et al., 2018). For this reason, FDCA and ethylene glycol have been quite extensively copolymerized with different diols and dicarboxylic acids for increased toughness and improvements on other properties (Hong et al., 2016; Matos et al., 2014; Yu et al., 2013). The observed drawbacks usually include worsened barrier properties, diminished crystallinity, or lower rigidity because of copolymerization with flexible monomers (Wang, Liu, Zhang, Liu, & Zhu 2016; Wang et al., 2017a). Other copolyesters have targeted increased degradation under various environmental conditions to address plastic pollution within the

environment (Hu et al., 2018; Papadopoulos et al., 2018). This effect has been achieved by creating blends of FDCA and known biodegradability-enhancing monomers such as adipic acid.

In this work (Paper III), FDCA and BFDCA were polymerized with 1,4-butanediol to form new copolyesters. The ratio between the two dicarboxylic acids was varied, and the properties of these copolyesters were compared to the homopolyesters of FDCA and BFDCA.

2.2.2 FDCA in thermosets

Unlike furfural, furfuryl alcohol, or HMF that can easily resinify into cross-linkable polymers under suitable conditions, only the derivatives of 2,5-furandicarboxylic acid can generally be used in cross-linking resins. However, the literature concerning such materials appears somewhat limited in scope. As diepoxy compounds such as DGEBA (Fig. 12) are components in commercially relevant high-performance resins, there has been interest in developing FDCA-based diepoxy compounds as novel alternatives (Deng, Liu, Li, Jiang, & Zhu 2015a). The diglycidyl ester of FDCA (DG-F) essentially mimics the function of DGEBA and can be cured using diamino or carboxylic anhydride compounds such as those depicted in Figure 12. DG-F has been prepared through several different routes: The most straightforward way is to react FDCA with epichlorohydrin, which is very similar to the route used to manufacture DGEBA from bisphenol A (Marotta, Ambrogi, Cerrutic, & Mija, 2018). However, in the current literature, DG-F has mostly been synthesized via the diallyl ester of FDCA, which has been oxidized using *m*-CPBA (Meng et al., 2019a; Nameer, Larsen, Duus, Daugaard, & Johansson 2018). DG-F may also be prepared through esterification or transesterification with glycidol (Liu et al., 2020; Marotta et al., 2018). Besides being an ester rather than an ether, DG-F also differs from DGEBA with to its relatively high melting point of ca. 88 ºC (Marotta et al., 2018), whereas (monomeric) DGEBA melts at ca. 42 ºC (Wiesner, 1967). In practice, DGEBA typically contains some oligomers and is thus commercially available as a liquid.
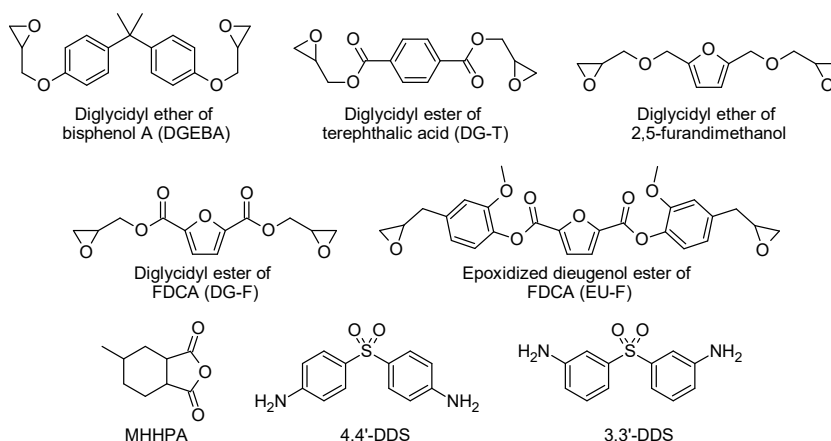
Fig. 12. Chemical structures of DGEBA, DG-T, three furan-based alternatives, and some common high-performance curing agents used in epoxy resins.

Deng et al. (2015a) previously compared the curing and cured properties of DG-F and DG-T–based resins (Fig. 12) that were hardened using either MHHPA or diamine D230 (a short-chain polyether with two terminal amino groups). They found that DG-F led to higher glass transition temperatures when either hardener was used. However, they noted no significant differences between the mechanical properties of DG-T and DG-F resins. Similarly, they discovered that there was little difference in their thermal stabilities based on TGA. The difference in glass transition temperatures was ascribed to a higher degree of hydrogen bonding in the furan-based resins. Later results by Liu et al. (2020) have supported hydrogen bonding as having a major role in improving the stiffness of DG-F epoxy resins. Their study compared DG-F to the isophthalic acid -derived diglycidyl ester rather than DG-T. Using several techniques such as FTIR, they showed that the thermomechanical improvements showed by the DG-F resin were correlated with hydrogen bonding. Again, this property was ascribed to the polarity of the FDCA moiety, which allowed for denser hydrogen bonding in the network. Thus, the biobased furan units can bring additional value to these applications because of their unique structure.

More recently, epoxy resins based on either DG-F or DGEBA were studied by Meng et al. (2019a), who used two different high-performance curing agents, 4,4'-DDS and 3,3'-DDS (Fig. 12). While the DG-F networks showed similar or lower glass transition temperatures than the DGEBA-based networks, at 176–216 ℃ (DSC and DMA), their storage moduli at low to moderate temperatures were

superior, indicating improved rigidity. The results also indicated that the thermal decomposition of DG-F networks takes place at lower temperatures compared to DGEBA-based materials. However, at the same time, the DG-F network had more promising fire-retardant properties. Meng et al. (2019b) and others (Hu, La Scala, Sadler, & Palmese, 2014) have also reported similar epoxy resins prepared from the diglycidyl ether of 2,5-furandimethanol (Fig. 12), which is closely related to DG-F. By substituting the carbonyl groups with the methylene bridges on both sides, significant improvements were observed in flame-retardancy: Resins cured with either 4,4'-DDS or 3,3'-DDS were able to rapidly self-extinguish in the burn test. Accordingly, the 2,5-furandimethanol–based epoxy resins also showed much higher char yields in TGA, and the burned specimens had dense, charred surfaces. However, the flexible methylene bridges resulted in much lower glass transition temperatures, which were 97–114 ºC, i.e., much lower than for similar DGEBA or DG-F resins. Interestingly, the networks still had superior storage moduli at low temperatures when compared to the DGEBA networks.

Besides the diglycidyl derivatives, other diepoxy resins have also been prepared from 2,5-furandicarboxylic acid: Robust DGEBA alternatives were synthesized from FDCA by first preparing a diester with eugenol, a biobased naturally occurring phenolic compound (Miao, Yuan, Guan, Liang, & Gu 2017). The diaryl ester was then oxidized in the usual way, using m-CPBA to yield diepoxy compound EU-F with three aromatic rings (Fig. 12). EU-F cured using MHHPA was then compared against a DGEBA-based sample. The furan-based resin showed higher a T_g, slightly lower thermal stability, and comparable flexural properties. Also, since EU-F is derived from eugenol and FDCA, its biobased carbon content was high at 93%. Some other examples where FDCA has been utilized in cross-linked polymers include hyperbranched epoxy resins (Chen et al., 2020), branched poly(ester amide)s (Wilsens et al., 2015), and coatings derived from epoxidized fatty acid esters (Kovash, Pavlacky, Selvakumar, Sibi, & Webster 2014). The allyl ester of FDCA has also been used as a monomer in thiol-ene thermosets, prepared with multifunctional thiols (Larsen, Sønderbæk-Jørgensen, Duus, & Daugaard, 2018). However, epoxy acrylates or methacrylates derived from DG-F or similar diepoxy compounds have scarcely been reported. In contrast, BisGMA, an epoxy methacrylate prepared from DGEBA (or bisphenol A and glycidyl methacrylate, Fig. 13) is a common unsaturated monomer, which is used e.g., in dental resins (Peutzfeldt, 1997; Van Landuyt et al., 2007).

Novel monomers were prepared from FDCA and BFDCA for study in this thesis (Paper IV) to evaluate the suitability of furan-based epoxy methacrylates as components of unsaturated resins. The properties of the monomers and the cured resins were compared against BisGMA-based resins.
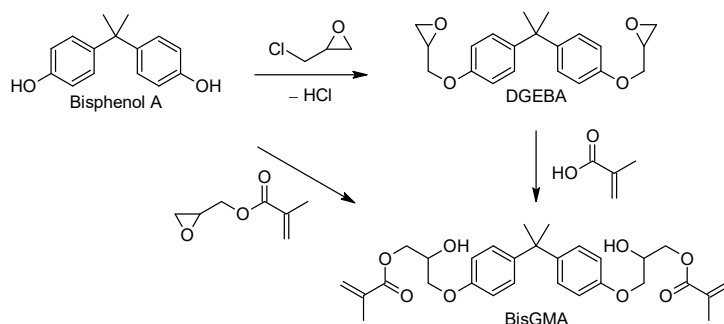
Fig. 13. Two synthesis routes for BisGMA, an aromatic epoxy methacrylate.

2.2.3 2,2'-Bifuran–derived thermoplastics and thermosets

Compared to the abundance of materials prepared from 2,5-furandicarboxylic acid, the literature concerning the use of BFDCA, 5,5'-bisfurfural, or similar 2,2'-bifurans as monomers in polymer synthesis is scant. In this thesis, several BFDCA-derived polymers are reported, including polyesters, copolyesters, and thermosets. In fact, most of the literature consists of almost simultaneous reports from the last few years. The earliest report concerning the use of 5,5'-bisfurfural as a monomer can found as early as 1985 (Goncharov, Grekov, Chumikova, & Rudakov). Poly(acyl hydrazone)s were synthesized from 5,5'-bisfurfural and various dicarboxylic acid dihydrazides (Fig. 14a), producing materials with high melting temperatures of >300 ºC. Later, in the 2000 book, Zeitsch suggested that 5,5'-bisfurfural was investigated as a precursor for thermally stable materials. However, the next time 5,5'-bisfurfural appeared in this role was not until the report by Tachibana et al. in 2018. They reported a series of poly(Schiff base)s that were synthesized from 5,5'-bisfurfural and various aliphatic and aromatic diamines (Fig. 14b). The group was able to prepare free-standing films from the poly(Schiff base)s and obtained Young's modulus values of up to around 1 GPa and tensile strengths of up to 53 MPa from the samples. The thermal stabilities varied with

decomposition onset temperatures ($T_{d5\%}$) between 258 and 339 °C depending on the diamine used.
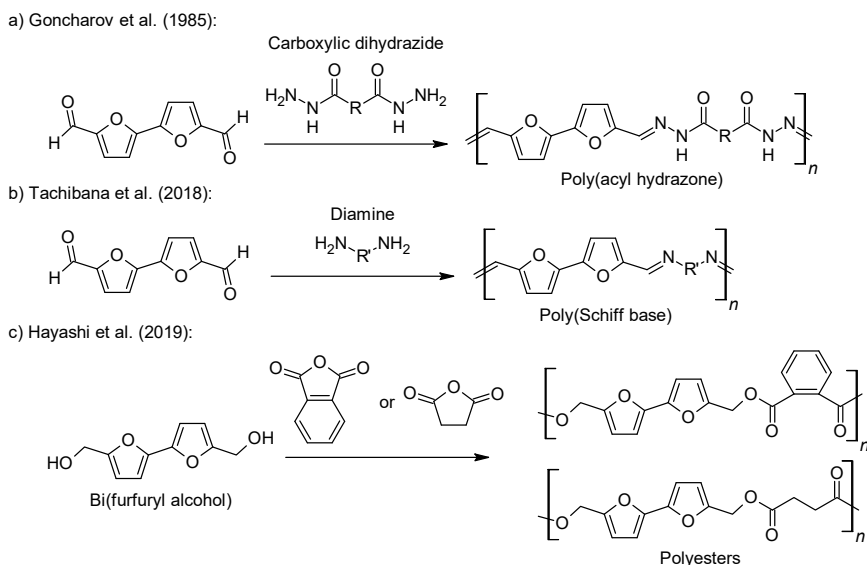
Fig. 14. Previous examples of 2,2'-bifuran–derived polymers.

Even more recently, the potential reduction product of 5,5'-bisfurfural, bi(furfuryl alcohol) (Fig. 14c) was applied by Hayashi, Narita, Wasano, Tachibana, & Kasuya (2019) in their study of novel cross-linkable polyesters. However, they chose instead to synthesize it starting from furfuryl alcohol. Furfuryl alcohol was first protected by converting it into an acetate. A Pd-catalyzed aerobic oxidative coupling reaction was then used to give bi(furfuryl acetate), which upon hydrolysis of the protecting esters, gave bi(furfuryl alcohol). They polymerized the diol with succinic and phthalic anhydrides, forming novel polyesters (Fig. 14c). The cross-linking of the succinate polyester via Diels-Alder reactions was also explored. By cross-linking the bifuran polyester using bismaleimides, they found that the molar mass of the polyester could be roughly doubled: Curiously, they obtained soluble polymers despite successful Diels-Alder reactions, which they attributed to the formation of a ladder-type structure. Using bi(furfuryl acetate) as a model compound, they also noted that both furan rings in the electron-rich 2,2'-bifuran system could form adducts with a strong dienophile such as a maleimide.
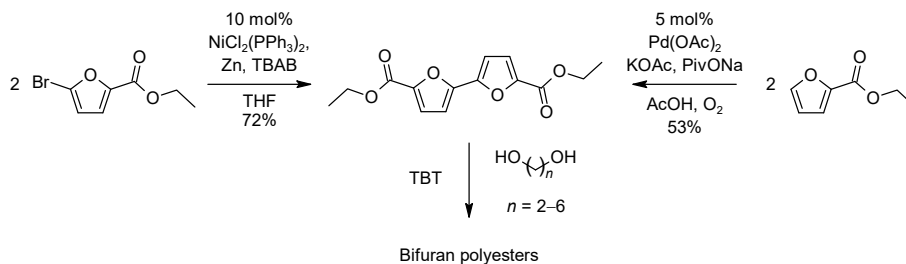
Fig. 15. The strategy used by Miyagawa et al. (2017) towards the synthesis of BFDCA-based polyesters.

2,2'-Bifuran-5,5'-dicarboxylic acid had no reported uses in polymers until the articles (Papers II–IV) in this work and other almost simultaneous reports on their study were published within the time window of 2–3 years. BFDCA was used in 2017 by Huang et al. to prepare novel coordination polymers, which comprised inorganic-organic polymers with Zn^{II}, Cd^{II}, and Co^{II} as metal centers. Technically the first report of BFDCA in polyester synthesis came in the same year from Miyagawa et al. (2017), who used the diethyl ester of BFDCA as a monomer (Fig. 15). Additionally, they addressed the synthesis of the 2,2'-bifuran monomer, for which they elected to use both a nickel-catalyzed homocoupling of ethyl 5-bromo-2-furoate and an aerobic oxidative homocoupling of ethyl 2-furoate (Fig. 15). Using diethyl 2,2'-bifuran-5,5'-dicarboxylate, they prepared a series of polyesters using ethylene glycol, 1,3-propanediol, 1,4-butanediol, 1,5-pentanediol, and 1,6-hexanediol. The polymers were analyzed using the usual techniques: The molar masses between the different polyesters varied according to size-exclusion chromatography and NMR, but thermal decomposition properties (TGA) were observed to be similar between the polyesters. The melting temperatures of BFDCA-derived polyesters expectedly varied depending on the diol, but in each instance, they were higher than for the corresponding FDCA polyester. The possibility of using the bifuran polyesters as UV blocking materials was also discussed. They based this on measured absorbance spectra in chloroform, which they found significantly red-shifted compared to dimethyl 2,5-furandicarboxylate. Sadly, the glass transition temperatures were not reported for any of the polyesters that they had prepared.

In addition to polymerizable monomers, there has been some interest in using esters of BFDCA as plasticizers for other polymers, chiefly PVC (Sanderson, Schneider, & Schreuder, 1995). PVC is commonly plasticized with dialkyl esters

such as dioctyl phthalate. However, their leaching is a concern since many of them may be considered harmful to humans (van Vugt-Lussenburg et al., 2020). A recent patent application also describes the use of 2,2'-bifuran-5,5'-dicarboxylates as plasticizing agents for PVC (Chinese patent application CN110776668A, 2020). The description of the patent claims that the bifuran dioctyl ester is much less prone to leaching than dioctyl phthalate while providing good plasticizing effectiveness. Recently, the biological toxicity of several FDCA-based plasticizers was evaluated (van Vugt-Lussenburg et al., 2020). They were found less harmful than traditional phthalates used for that role, which gives good prospects for furan-based plasticizers to act as renewable replacements.

3 Materials and Methods

3.1 Synthetic methods

Reactions were conducted under an atmosphere of argon, and commercial reagents were used as received unless otherwise indicated. Aluminium backed TLC plates (silica gel 60) were used for monitoring reactions. For column chromatography and filtrations, silica gel 60 was used. Commercial solvents were dried using appropriate (3 or 4 Å) molecular sieves, when necessary.

Pd-catalyzed synthesis of 5,5'-bisfurfural and furfural-substituted thiophenes 1–5

The general procedure is represented by the synthesis of 5,5'-bisfurfural: A deoxygenated solution of 5-bromofurfural (0.15 g, 0.86 mmol) in dry DMAc (1.5 mL) was first prepared and drawn into a glass syringe. Then, to a solution of furfural (2 equiv) in dry DMAc (7.5 mL), Na_2CO_3 (2.5 equiv), pivalic acid (30 mol%), P(*t*-Bu)$_3$HBF$_4$ (10 mol%), and Pd(OAc)$_2$ (5 mol%) were added after the solution was bubbled with argon for 10 min. The 2-necked reaction flask was connected to a reflux condenser and an argon-filled balloon, and the closed system was evacuated and filled with argon five times. The reaction mixture was heated to 110 ºC using an oil bath, and the 5-bromofurfural solution was slowly added into the reaction mixture through a septum at a rate of 75 μL/h using a syringe pump. After the 20 h addition had finished and an additional hour had passed, 5-bromofurfural was no longer found to be present within the reaction mixture (TLC). After dilution with ethyl acetate, the mixture was filtered through a layer of silica gel. After evaporation to dryness under reduced pressure, the crude product was washed by boiling it in toluene (5 mL) for 10 minutes. After the solution had cooled, the product was filtered off and washed with a small amount of toluene and cold methanol, which afforded 5,5'-bisfurfural as a light brown solid (73.1 mg, 45%). ^{1}H NMR (400 MHz, CDCl$_3$, ppm): δ 9.72 (s, 2H), 7.35 (d, 2H, $J = 3.7$ Hz), 7.06 (d, 2H, $J = 3.7$ Hz). ^{1}H NMR (400 MHz, (CD$_3$)$_2$SO, ppm): δ 9.67 (s, 2H), 7.72 (d, 2H, $J = 3.7$ Hz), 7.34 (d, 2H, $J = 3.7$ Hz). HRMS [M + H]$^+$: C$_{10}$H$_7$O$_4$, 191.0344. Found 191.0339.

Compound **1**: Synthesized as above but using 0.26 mmol of 3-hexylthiophene (43.1 mg) and 4 equiv of 5-bromofurfural at 150 ºC. Purification of the crude

product using flash chromatography (ethyl acetate/toluene 1:10) gave an orange solid (23.3 mg, 26%). ^{1}H NMR (400 MHz, CDCl$_3$, ppm): δ 9.66 (s, 1H), 9.64 (s, 1H), 7.40 (s, 1H), 7.34 (d, 1H, J = 3.8 Hz), 7.31 (d, 1H, J = 3.8 Hz), 6.73 (d, 1H, J = 3.8 Hz), 6.69 (d, 1H, J = 3.8 Hz,), 2.88–2.83 (m, 2H), 1.75–1.66 (m, 2H), 1.46–1.39 (m, 2H), 1.36–1.31 (m, 4H), 0.93–0.88 (m, 3H). ^{13}C NMR (100 MHz, CDCl$_3$, ppm): δ 176.9, 153.8, 153.8, 151.8, 151.5, 143.9, 131.5, 129.1, 127.3, 109.6, 108.5, 31.6, 29.9, 29.8, 29.2, 22.6, 14.0. HRMS [M + H]$^+$: C$_{20}$H$_{21}$O$_4$S, 357.1161. Found 357.1157.

Compound **2**: Synthesized following the general procedure but using 0.36 mmol of 3,3'''-dihexyl-2,2':5',2'':5'',2'''-quaterthiophene (177.9 mg) and 1.1 equiv of 5-bromofurfural with a reaction temperature of 150 ºC. The crude product was purified using flash chromatography (ethyl acetate/toluene 1:10), which gave a dark red solid (73.9 mg, 37%). ^{1}H NMR (400 MHz, CDCl$_3$, ppm): δ 9.61 (s, 1H), 7.39 (s, 1H), 7.30 (d, 1H, J = 3.8 Hz), 7.20 (d, 1H, J = 5.0 Hz), 7.17–7.15 (m, 2H), 7.10 (d, 1H, J = 3.8 Hz), 7.04 (d, 1H, J = 3.8 Hz), 6.96 (d, 1H, J = 5.3 Hz), 6.66 (d, 1H, J = 3.8 Hz), 2.83–2.77 (m, 4H), 1.74–1.62 (m, 4H), 1.47–1.29 (m, 12H), 0.93–0.88 (m, 6H). ^{13}C NMR (100 MHz, CDCl$_3$, ppm): δ 176.7, 154.5, 151.5, 140.7, 140.0, 137.7, 136.3, 135.8, 134.1, 133.0, 130.2, 130.1, 129.2, 128.8, 127.1, 126.5, 124.2, 124.0, 124.0, 107.6, 31.7, 31.6, 30.6, 30.3, 29.5, 29.3, 29.2, 29.2, 22.6, 22.6, 14.1. HRMS [M + H]$^+$: C$_{33}$H$_{37}$O$_2$S$_4$, 593.1676. Found 593.1693.

Compound **3**: Synthesized following the general procedure but using 0.25 mmol of 3,3'''-dihexyl-2,2':5',2'':5'',2'''-quaterthiophene (125.7 mg) and 4 equiv of 5-bromofurfural. Purification of the crude product by flash chromatography (ethyl acetate/n-heptane 1:1) gave a dark red solid (35.9 mg, 22%). ^{1}H NMR (400 MHz, CDCl$_3$, ppm): δ 9.61 (s, 2H), 7.39 (s, 2H), 7.29 (d, 2H, J = 3.7 Hz), 7.17 (d, 2H, J = 3.7 Hz), 7.11 (d, 2H, J = 3.9 Hz), 6.66 (d, 2H, J = 3.7 Hz), 2.83–2.77 (m, 4H), 1.74–1.66 (m, 4H), 1.47–1.38 (m, 4H), 1.37–1.31 (m, 8H), 0.95–0.87 (m, 6H). ^{13}C NMR (100 MHz, CDCl$_3$, ppm): δ 176.7, 154.4, 151.5, 140.8, 137.2, 134.5, 132.8, 129.2, 128.9, 127.1, 14.1, 22.6, 124.3, 107.6, 31.6, 30.3, 29.5, 29.2. HRMS [M + H]$^+$: C$_{38}$H$_{39}$O$_4$S$_4$, 687.1731. Found 687.1740.

Compound **4**: Synthesized following the general procedure but using 88.6 μmol of the thiophene derivative (Manninen et al., 2014) (76.0 mg) and 4 equiv of 5-bromofurfural at a temperature of 150 ºC. The crude product was purified by flash chromatography (ethyl acetate/toluene 1:10), which gave a dark green solid (23.2 mg, 28%). ^{1}H NMR (400 MHz, CD$_2$Cl$_2$, ppm): δ 9.58 (s, 1H), 9.01 (d, 1H, J = 4.2 Hz), 9.00 (d, 1H, J = 4.2 Hz), 7.40 (s, 1H), 7.36 (d, 1H, J = 4.2 Hz), 7.31–7.28 (m, 3H), 7.00 (d, 1H, J = 5.1 Hz), 6.72 (d, 1H, J = 3.7 Hz), 4.08–3.97 (m, 4H), 2.88–

2.81 (m, 4H), 1.98–1.88 (m, 2H), 1.77–1.64 (m, 4H), 1.44–1.27 (m, 28H), 0.92–0.85 (m, 18H). ^{13}C NMR (100 MHz, CD$_2$Cl$_2$, ppm): δ 177.1, 162.0, 161.9, 154.4, 152.3, 142.9, 142.8, 142.0, 141.1, 140.3, 139.4, 136.8, 136.5, 132.7, 131.2, 130.7, 130.3, 130.3, 129.9, 129.5, 127.5, 127.0, 125.8, 109.1, 108.7, 46.5, 40.0, 39.9, 32.3, 32.3, 31.1 30.8, 30.5, 30.3, 29.9, 29.0, 29.0, 24.1, 24.1, 23.7, 23.7, 23.2, 23.2, 14.4, 14.4, 10.8, 10.8. HRMS [M + H]$^+$: C$_{55}$H$_{71}$N$_2$O$_4$S$_4$, 951.4297. Found 951.4293.

Compound **5**: From the foregoing reaction and its crude product, compound **5** was separated as a dark green solid (8.6 mg, 9%) during column chromatography. ^{1}H NMR (400 MHz, CDCl$_3$, ppm): δ 9.64 (s, 2H), 9.06 (d, 2H, J = 4.2 Hz), 7.43 (s, 2H), 7.35 (d, 2H, J = 4.2 Hz), 7.31 (d, 2H, J = 3.9 Hz), 6.71 (d, 2H, J = 3.9 Hz), 4.12–4.04 (m, 4H), 2.90–2.82 (m, 4H), 2.00–1.92 (m, 2H), 1.77–1.68 (m, 4H), 1.45–1.27 (m, 28H), 0.96–0.87 (m, 18H). ^{13}C NMR (100 MHz, CDCl$_3$, ppm): δ 176.8, 161.6, 154.0, 151.7, 142.2, 140.9, 139.5, 136.5, 132.0, 130.2, 129.6, 129.4, 127.2, 108.6, 108.2, 46.1, 39.3, 31.7, 30.3, 29.9, 29.3, 28.5, 23.6, 23.2, 22.6, 14.1, 10.5. HRMS [M + H]$^+$: C$_{60}$H$_{73}$N$_2$O$_6$S$_4$, 1045.4351. Found 1045.4351.

Dimethyl 2,2'-bifuran-5,5'-dicarboxylate (DM-Bf)

4.18 g of methyl 5-bromo-2-furoate together with Pd(OAc)$_2$ (1 mol%), pivalic acid (30 mol%), and potassium acetate (2 equiv) were added to 30 mL of distilled methyl 2-furoate. The mixture was agitated at 90–100 ºC for 24 h. The cooled reaction mixture was then diluted with chloroform and poured over a layer of silica gel. The silica layer was rinsed warm chloroform until the crude product had been collected completely. Evaporation of the chloroform under reduced pressure yielded a mixture of the product and methyl 2-furoate, which was distilled under reduced pressure and recycled. Alternatively, the vacuum distillation of methyl 2-furoate could be done directly after the reaction to yield a dry mixture of the product and various salts. The crude product could be then extracted using chloroform. The impurities were separated from the crude product in boiling solvent (20+20 mL of chloroform and ethanol). After briefly cooling to room temperature, the product was filtered off as a white crystalline powder (4.53 g, 91%). ^{1}H NMR (400 MHz, CDCl$_3$, ppm): δ 7.26 (d, 2H, J = 3.7 Hz), 6.90 (d, 2H, J = 3.7 Hz), 3.93 (s, 6H). ^{13}C NMR (100 MHz, CDCl$_3$, ppm): δ 158.8, 148.2, 144.3, 119.7, 109.4, 52.1. HRMS [M + H]$^+$: C$_{12}$H$_{11}$O$_6$, 251.0556. Found 251.0551.

Poly(ethylene bifuranoate) (PEBf)

DM-Bf (4–8 mmol) was added to a mixture of ethylene glycol (5 equiv) and tetrabutyl titanate (1 mol%) in a 50 mL round-bottom flask. The flask was connected to a distillation bridge, which led to vacuum and argon lines. The closed system was purged with argon by five argon-vacuum cycles. The reaction mixture was then magnetically agitated at 180 ºC, which gradually turned the mixture into a homogeneous, clear liquid after 30 min. After a 3 h reaction, the pressure inside the reaction system was slowly lowered over 1 h to 3–4 mbar to remove ethylene glycol from the molten mixture. At this stage, the transesterification was considered complete, and the dimethyl ester could no longer be detected via TLC (eluent: ethyl acetate/*n*-heptane 1:1). The temperature was then increased to 270 ºC for 1.5 h. After cooling back to room temperature, the polymer was dissolved in a mixture of trifluoroacetic acid (TFA) and chloroform (1:1). The polymer was precipitated out by mixing the solution into a 10-fold excess volume of methanol. After filtration, vacuum drying at 120 ºC was continued until the mass of the polymer sample stabilized. The final product was an off-white, fibrous solid (yield: 94%). ^{1}H NMR (400 MHz, CF_3COOD, ppm): δ 7.48 (d, 2H, J = 3.8 Hz), 7.01 (d, 2H, J = 3.8 Hz), 4.87 (s, 4H).

Dimethyl 2,5-furandicarboxylate (DM-F)

4.00 g of 2,5-furandicarboxylic was reacted with 120 mL of refluxing methanol and 2 equiv of 97% sulfuric acid. After 18 h, the mixture was evaporated to half-volume and diluted with cold deionized water. The precipitated product was vacuum filtered onto a paper, and the formed filter cake was then rinsed with deionized water and dried under air. For further purification, the crude product was dissolved in ethyl acetate, and the solution was passed through silica gel. Evaporation of the solvent under reduced pressure gave dimethyl 2,5-furandicarboxylate as a white powder (4.25 g, 93%). ^{1}H NMR (400 MHz, $CDCl_3$, ppm): δ 7.23 (s, 2H), 3.94 (s, 6H).

Poly(butylene furanoate), poly(butylene bifuranoate), and their random copolyesters

Copolyester sample codes are designated according to PBF_XBf_Y, where the molar fractions of DM-F and DM-Bf in the feed were X and Y, respectively. The

preparation of PBF$_{50}$Bf$_{50}$ illustrates the general procedure of the polyester syntheses: 1.00 g of DM-Bf and 0.74 g of DM-F (for a total of 8 mmol) were added into a 50 mL flask with a mixture of distilled and dried 1,4-butanediol (3 equiv) and tetrabutyl titanate (0.03M in toluene, 0.1 mol% Ti relative to DM-Bf and DM-F). The flask was attached to a short-path distillation bridge, which was connected to argon and vacuum lines. After evacuation and filling with argon, the flask was heated to 180 ºC under magnetic stirring. After 3 h, the pressure inside the system was decreased slowly over 1 h. After reaching a pressure of ca. 2 mbar, the temperature of the reaction mixture was increased to 250 ºC to initiate the polycondensation. After 1 h, the reaction was stopped, and the cooled polymer was dissolved in a mixture of TFA and chloroform (1:5). After complete dissolution, the polymer was precipitated in 10-fold excess volume of methanol. The off-white polymer was collected by filtration onto paper, and vacuum dried at 60 ºC until its mass stabilized. The structure was then analyzed using ^{1}H and ^{13}C NMR.

PBF: ^{1}H NMR (400 MHz, CF$_3$COOD, ppm): δ 7.33 (s, 2H), 4.51 (s, 4H), 1.98 (s, 4H).

PBBf: ^{1}H NMR (400 MHz, CF$_3$COOD, ppm): δ 7.34 (d, 2H, $J = 3.7$ Hz), 6.89 (d, 2H, $J = 3.7$ Hz), 4.52 (s, 4H), 2.01 (s, 4H).

PBF$_{90}$Bf$_{10}$: ^{1}H NMR (400 MHz, CF$_3$COOD, ppm): δ 7.35 (d, $J = 3.7$ Hz), 7.32 (s), 6.90 (d, $J = 3.7$ Hz), 4.50 (s), 1.97 (s).

PBF$_{75}$Bf$_{25}$: ^{1}H NMR (400 MHz, CF$_3$COOD, ppm): δ 7.36 (m), 7.33 (s), 6.91 (m), 4.52 (m), 1.98 (s).

PBF$_{50}$Bf$_{50}$: ^{1}H NMR (400 MHz, CF$_3$COOD, ppm): δ 7.36 (m), 7.34 (s), 6.91 (m), 4.53 (m), 2.01 (s).

PBF$_{25}$Bf$_{75}$: ^{1}H NMR (400 MHz, CF$_3$COOD, ppm): δ 7.35 (m), 7.33 (s), 6.90 (m), 4.52 (m), 2.00 (m).

PBF$_{10}$Bf$_{90}$: ^{1}H NMR (400 MHz, CF$_3$COOD, ppm): δ 7.38 (d, $J = 3.7$ Hz), 7.36 (s), 6.93 (m), 4.56 (s), 2.05 (s).

Diglycidyl ester of FDCA (DG-F)

2,5-Furandicarboxylic acid (1.56 g) was reacted with SOCl$_2$ (2.5 equiv) and dimethylformamide (3 drops) in 20 mL of dry dichloromethane. After refluxing for 10 h, a clear solution was obtained. Evaporation of the colorless solution under reduced pressure gave off-white crystals. The crude diacyl chloride and dry, distilled triethylamine (2.25 equiv) were mixed in dry dichloromethane (40 mL) at 0 ºC. Then, distilled glycidol (2.25 equiv) diluted with dichloromethane (1:1 v/v)

was injected into the mixture over 15 min. The mixture was then allowed to warm to 20 °C and stirred for 1 h before being successively washed with deionized water and saturated aqueous NaHCO$_3$. The dichloromethane solution was dried with anhydrous Na$_2$SO$_4$ and filtered through silica. Evaporation of the yellow solution under reduced pressure yielded a viscous oil that rapidly crystallized upon standing. Color and impurities were removed by first dissolving the crude product in 5 mL of warm dichloromethane and then precipitating it by diluting it with diisopropyl ether (40 mL). The precipitate was separated by filtration and washed with diisopropyl ether and small portions of methanol. After vacuum drying, the diglycidyl ester of FDCA was isolated as a white crystalline powder (2.38 g, 89%). T_m: 89 °C (DSC). ^{1}H NMR (400 MHz, CDCl$_3$, ppm): δ 7.28 (s, 2H), 4.66 (dd, 2H, J = 12.2, 3.2 Hz), 4.20 (dd, 2H, J = 12.2, 6.4 Hz), 3.35 (m, 2H), 2.91 (m, 2H), 2.74 (dd, 2H, J = 4.9, 2.5 Hz). ^{13}C NMR (100 MHz, CDCl$_3$, ppm): δ 157.5, 146.5, 119.0, 66.0, 49.1, 44.8.

2,2'-Bifuran-5,5'-dicarboxylic acid (BFDCA)

3.00 g of DM-Bf was reacted with refluxing 10% aqueous NaOH (10 equiv). After 4 h, the insoluble starting material had completely disappeared, and the reaction was stopped. The solution was cooled on ice and adjusted to acidic pH (1–2) using concentrated (37%) hydrochloric acid. The precipitated dicarboxylic acid was separated via vacuum filtration and washed with deionized water and finally with methanol. The product was first allowed to dry in the air, before being ground into a powder and dried under vacuum at 60 °C. BFDCA was collected as an off-white powder (2.30 g, 87%). ^{1}H NMR (400 MHz, (CD$_3$)$_2$SO, ppm): δ 13.38 (br s, 2H), 7.35 (d, 2H, J = 3.4 Hz), 7.08 (d, 2H, J = 3.4 Hz). ^{13}C NMR (100 MHz, (CD$_3$)$_2$SO, ppm): δ 158.8, 146.9, 144.9, 119.3, 109.8.

Diglycidyl ester of BFDCA (DG-Bf)

The procedure largely followed the preparation of DG-F: Briefly, 2.22 g of 2,2'-bifuran-5,5'-dicarboxylic acid together with SOCl$_2$ (2.5 equiv) and 3 drops of dimethylformamide were reacted in dry dichloromethane (20 mL). After refluxing 10–12 h, the solution had turned yellow and had a large amount of crystalline sediment. Evaporation to dryness yielded a crude product, confirmed to be the diacyl chloride (^{1}H NMR). It was directly reacted with glycidol (2.25 equiv) in the presence of dry triethylamine (2.25 equiv) in dry dichloromethane (40 mL)

50

following the procedure described for DG-F. The resulting reaction mixture was diluted with dichloromethane (100 mL) and then treated in the same way as DG-F. Final purification of the crude solid was accomplished by triturating it in warm ethyl acetate-hexane mixture (50 mL, 1:4 v/v). The solid product was filtered off after stirring and rinsed with several small portions of methanol. It was dried in air to yield DG-Bf as a white powder (2.88 g, 86%). T_m: 165 ºC (DSC). ^{1}H NMR (400 MHz, CDCl$_3$, ppm): δ 7.31 (d, 2H, J = 3.7 Hz), 6.93 (d, 2H, J = 3.7 Hz), 4.67 (dd, 2H, J = 12.2, 3.2 Hz), 4.17 (dd, 2H, J = 12.2, 6.4 Hz), 3.35 (m, 2H), 2.92 (dd, 2H, J = 4.9, 4.2 Hz), 2.74 (dd, 2H, J = 4.9, 2.5 Hz). ^{13}C NMR (100 MHz, CDCl$_3$, ppm): δ 157.9, 148.4, 143.9, 120.2, 109.6, 65.6, 49.2, 44.7.

Furan dimethacrylates (F-D and iso-F-D)

DG-F (0.80 g) was mixed with methacrylic acid (3 equiv) and triethylamine (1 equiv) in dry dichloromethane (1.5 mL) inside a small glass tube. The tube was sealed, and after an overnight (20 h) reaction at 70 ºC under air, the reaction was stopped. The reaction mixture was diluted with ethyl acetate and washed with saturated aqueous NaHCO$_3$, deionized water, and brine. The ethyl acetate solution was dried using anhydrous Na$_2$SO$_4$ and filtered through a layer of silica gel. The evaporation of the solvent left a viscous, light-yellow liquid. Methanol (5 mL) was added twice, followed by evaporation under reduced pressure at 50 ºC, to remove any ethyl acetate residue. The product, designated F-D, was a viscous, pale-yellow liquid (1.13 g, 86%). It was analyzed using ^{1}H NMR (Fig. 22).

Alternatively, a base-free procedure using similar techniques was used to prepare iso-F-D: 134.1 mg of DG-F was reacted with methacrylic acid (3 equiv) in 0.5 mL of 1,1,1,3,3,3-hexafluoroisopropanol (HFIP), and after stirring for 50 h at 65 ºC, the product was separated in the same manner as above. After filtration through silica and evaporation to dryness, the product was obtained as a colorless liquid (210.6 mg, 95%). The product developed insoluble precipitates upon standing. The product was analyzed using ^{1}H NMR (Fig. 22), and white flocs were also observed within the NMR sample prepared in CDCl$_3$.

Bifuran dimethacrylates (Bf-D and iso-Bf-D)

The bifuran dimethacrylates Bf-D and iso-Bf-D were prepared using the same synthetic methods as F-D and iso-F-D: Bf-D was obtained from the reaction between DG-Bf (0.67 g) and methacrylic acid (3 equiv) in the presence of

triethylamine (1 equiv), which gave highly viscous pale yellow liquid (0.85 g, 83%). Using the base-free conditions, the reaction between DG-Bf (0.84 g) and methacrylic acid (3 equiv) in HFIP yielded iso-Bf-D, a colorless liquid (1.23 g, 97%). Both products were analyzed by ^{1}H NMR (Fig. 22).

Methacrylated eugenol (ME)

Methacrylated eugenol was synthesized using similar methods used in previous literature (Deng, Yang, Chen, & Liang, 2015b; Rojo et al., 2006; Weber & Brückner, 2015). Methacryloyl chloride was first prepared by mixing methacrylic acid (4.30 mL) with $SOCl_2$ (1.05 equiv) and 2 drops of dimethylformamide at 0 ºC. The mixture was agitated at 50 ºC in a sealed tube until the evolution of gas stopped. The obtained liquid was drawn into a syringe and added slowly into a closed flask containing a mixture of eugenol (0.9 equiv) and triethylamine (0.9 equiv) in dry ethyl acetate at 0 ºC. The mixture was then stirred at 40 ºC for 1 h and filtered and diluted with ethyl acetate before being washed with saturated aqueous $NaHCO_3$, deionized water, and brine. The ethyl acetate solution was dried with Na_2SO_4 and subsequently evaporated to dryness under reduced pressure to give a crude product (10.35 g, 99%). Purification using flash chromatography (ethyl acetate/hexane 1:9) gave ME as a colorless oil (8.03 g, 77%). Monomethyl ether hydroquinone (200 ppm) was added into the product as a stabilizer. ^{1}H NMR (400 MHz, $CDCl_3$, ppm): δ 6.98 (d, 1H, $J = 7.8$ Hz), 6.81 (d, 1H, $J = 2.0$ Hz), 6.79 (dd, 1H, $J = 7.8, 2.0$ Hz), 6.42–6.31 (m, 1H), 5.98 (ddt, 1H, $J = 16.9, 10.1, 6.8$ Hz), 5.78–5.71 (m, 1H), 5.18–5.05 (m, 2H), 3.82 (s, 3H), 3.4 (d, 2H, $J = 6.8$ Hz), 2.13–2.03 (m, 3H).

Resin curing

The dimethacrylates were mixed with *tert*-butyl peroxybenzoate (2 wt%) and optionally with methacrylated eugenol (60 wt% dimethacrylate, 40 wt% ME). A small amount of dichloromethane was added before being subsequently removed under vacuum to homogenize the diluent with the dimethacrylates. The resins were transferred into a stainless-steel mold (pre-heated to 90 ºC if the diluent was not added). The mold with the resin was then degassed under vacuum before being place under an inert atmosphere. The resins were heated in three distinct steps: 90, 150, and 180 ºC for 1 h, 5 h, 2h, respectively. The specimens were punched out after curing and collected for characterization.

3.2   Analytical methods

Additional full-size NMR spectra, FTIR spectra, and other additional characterization data of relevant compounds and materials may be found in Papers I–IV and their supporting information.

NMR spectroscopy

NMR measurements were carried out using Bruker Avance 400 MHz instrument at 23–25 ºC. ^{1}H and ^{13}C NMR chemical shifts are referenced to internal tetramethylsilane standard (0.00 ppm) or the residual solvent signals (^{1}H: CD_2Cl_2, 5.32 ppm; $CDCl_3$, 7.27 ppm; $(CD_3)_2SO$, 2.50 ppm; CF_3COOD, 11.50 ppm. ^{13}C: CD_2Cl_2, 54.0 ppm; $CDCl_3$, 77.0 ppm; $(CD_3)_2SO$, 39.51 ppm; CF_3COOD, 116.6/164.2 ppm).

UV-Vis

Absorption and transmittance values were determined using a spectrophotometer (Shimadzu UV-1800) run using quartz cuvettes. Chloroform stabilized with ethanol (0.6%) was used as the solvent.

ATR FTIR spectroscopy

IR spectra were collected using a Fourier transform infrared spectrometer (Perkin-Elmer Spectrum One FTIR Spectrometer) with an attenuated total reflectance module (ATR). Eight scans were collected between 650 and 4000 cm^{-1} at a resolution of 2 cm^{-1}.

Differential scanning calorimetry

A differential scanning calorimeter (Mettler Toledo DSC821e or DSC1) was used to characterize polymer and monomer samples. Generally, the accurately weighed sample (ca. 5 mg) was placed into a 40 μL Al crucible, sealed using a pierced lid. The samples were then scanned at the appropriate temperature ranges at scan rates between 5 and 15 ºC/min under pure nitrogen flow (50 or 60 mL/min).

Thermogravimetric analysis

TGA was performed using a thermogravimetric analyzer (Mettler-Toledo TGA851e). Accurately weighed samples (ca. 10–13 mg) were placed into 70 μL Al_2O_3 crucibles, covered with a pierced lid. The samples were heated from 25 to 700 or 1000 ºC under nitrogen flow (95 mL/min) with a heating rate of 10 (PBF, PBBf, and their copolyesters) or 20 (PEBf, PET, and methacrylate resins) ºC/min.

Intrinsic viscosity

Dried polyester samples were dissolved in TFA, diluted to known concentration, and the solutions were filtered before the measurements. The flow time measurements were carried out using either an Ostwald (9.0 mL fill) or a micro-Ubbelohde viscometer. The viscometer was submerged into a water bath held at 30.0 ºC. The flow times were measured within 0.01 s using a stopwatch, with 10 repeats used to calculate the average. For PEBf, the flow times of three different concentrations (ca. 0.2, 0.4, and 0.6 g/dL) were determined using an Ostwald viscometer. A three-point determination of intrinsic viscosity [η] was then done using reduced viscosities (η_{red}) calculated from equation 1, where c is the concentration of the solution, and t and t_0 are the flow times for the polymer solution and the pure solvent, respectively. Reduced viscosities were plotted against concentration, and a line was extrapolated to $c = 0$ to give the intrinsic viscosity. For PBBf, PBF, and PBF-co-PBBf copolyesters, a single point measurement at ca. 0.5 g/dL concentration was carried out using a micro-Ubbelohde viscometer. The intrinsic viscosity [η] was determined, according to Billmeyer (1949) (equation 2), where $\eta_{rel} = t/t_0$.

$$\eta_{red} = \frac{(t-t_0)/t_0}{c} \tag{1}$$

$$[\eta] = \frac{1}{4} \times \left(\frac{\eta_{rel} - 1 + 3 \times \ln{(\eta_{rel})}}{c} \right) \tag{2}$$

Dynamic viscosity

Dynamic viscosity was measured using a rheometer (TA Instruments Discovery HR-1) operated with parallel plate geometry (40 mm diameter). Measurements were carried out between shear rates of 1 and 100 s^{-1} under the various temperatures.

Polyester film preparation

The solution cast PEBf films were prepared by dissolving the polyester (800 mg) in a TFA-chloroform mixture (2:1 v/v, 30 mL). The solution was filtered using a fritted glass disc and poured onto a petri dish made from PTFE (diameter 100 mm). The solvent was allowed to evaporate under reduced pressure to give a film, which was finally dried under vacuum for several days at 20 ºC. The films were almost transparent with a yellow hue. The PET film was prepared from commercially available PET pellets (Polysciences Inc.).

Melt-pressed films were made from carefully and freshly dried (vacuum, elevated temperature) polymer samples. For PEBf, PTFE-coated glass-fiber mats were used between the aluminium press plates and the polymer. Thickness was controlled using steel shims of approximately the desired thickness. A pressing force of 200 kN was applied for 1 min after the sample had been held slightly above its melting temperature for 3 minutes. The aluminium press plates were then quickly quench cooled in cold water, and the polymer film was carefully loosened from the PTFE-coated mat.

In the pressing procedure used for PBF, PBBf, and their copolyesters, two aluminium plates coated with a thin polyimide film were used for the pressing, with the appropriate amount of polyester added between the pre-heated plates. The thickness was controlled using layers of glass fiber mat placed around the sample. The polyesters were first allowed to melt inside the press for 5 minutes at temperatures 20–30 ºC above their estimated melting temperatures. 20 kN pressing force was then applied for 1 minute. The samples were cooled inside the press at 30–40 ºC/min with an integrated water-cooling system. After separating the aluminium plates, the films were carefully peeled off to yield flexible, transparent films.

Dynamic mechanical analysis

The thermomechanical properties of the polyester films were measured using a dynamic mechanical analyzer (TA Instruments DMA Q800). Measurements were carried out in multifrequency mode at 1 Hz. Rectangular specimens 5 mm wide were prepared from the polyesters by cutting the films, while cured methacrylate resin specimens were directly obtained from open mold castings. Test specimens were heated at a rate of 5 ºC/min (PEBf and the cross-linked resins) or 3 ºC/min (PBF, PBBf, and their copolyesters) over the appropriate temperature range.

Tensile testing

Tensile tests were done using a tensile tester (Instron 5544). Gage length was set at 30 mm, and a crosshead speed of 5 mm/min was used. Test specimens were cut from the films in rectangles with a width of 5 mm and thicknesses in the order of 100–200 μm. The specimens were generally stored at room temperature for one or more weeks before being stored under stable conditions for 48 h (23 ºC, 50% RH for PET and PEBf, 10% RH for PBF, PBBf, and their copolyesters). Thicknesses were then measured individually for each test specimen at several points just before the measurement (Hanatek FT3, UK). At least 5–10 specimens were evaluated for each reported material.

Permeability analysis

Oxygen transmission rates (OTR) of melt-pressed polyester films were measured using an oxygen permeation analyzer (MOCON OxTran 2/20). Experiments were carried out at 23 ºC at either 0% (PEBf) or 50% relative humidity. One side of the sample film (area: 5 cm^2) was exposed to pure oxygen at atmospheric pressure, with pure nitrogen gas acting as the carrier gas on the opposite side of the film. The oxygen permeability was calculated by multiplying the OTR by the sample thickness and dividing it by the difference in O_2 partial pressure between the two sides of the sample. Water vapor transmission rates (WVTR) of melt-pressed PET and PEBf films (area: 5 cm^2) were measured using a water vapor permeation analyzer (MOCON Permatran-W 3/33). The samples were exposed to humid nitrogen gas (100% relative humidity) on one side, with dry N_2 on the other side. The permeability was calculated by multiplying the WVTR by the thickness of the sample.

XRD

X-ray diffraction measurements (PANalytical X'pert MPD Pro) were carried out using copper radiation ($K_{\alpha 1}$ = 1.5405980 Å).

4　Results and discussion

4.1　Synthesis of furan-based monomers
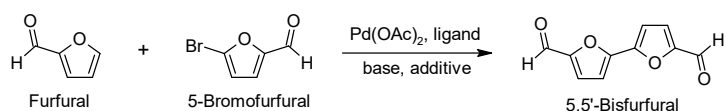
Synthesis of 5,5-bisfurfural

Fig. 16.　**Pd-catalyzed synthesis of 5,5'-bisfurfural. (Paper I)**

Pd-catalyzed coupling reactions have been classically used to prepare various furan aryl or heteroaryl derivatives, and similar methods were used in the current work. The direct coupling reaction between furfural and 5-bromofurfural was the first reaction to be optimized (Fig. 16). The product of this reaction, 5,5'-bisfurfural, was a potential precursor to the bifuran intermediates and polymers employed in this work. The method reported by McClure et al. (2001) was the most efficient direct coupling protocol reported up to that point (64% yield), so it was investigated first. However, a matching yield could not be readily achieved using a stable HBF$_4$-salt as the phosphine ligand source, and 5,5'-bisfurfural was obtained in <10% yield. Attention was then turned to Fagnou-type reaction conditions (Lafrance & Fagnou, 2006), and a maximum isolated yield of 45% could be obtained after several optimizations (Table 2).

　　Using the optimized conditions, 5-bromofurfural was also coupled to some thiophene derivatives found in organic electronic materials to yield compounds **1**–**5** (Fig. 17a). However, these reactions gave low yields compared to the moderate yield of 5,5'-bisfurfural. Another set of optimizations would likely have improved the results in the case of the thiophenes, and the results serve to demonstrate that the reactions conditions most appropriate for electron-poor furans are unlikely to yield good results with other substrates. Also, reactions between furfural and brominated thiophenes were problematic, as the expected products were very difficult to discern from the complex mixtures that were formed (Fig. 17b). A possible explanation for this may be the occurrence of homocoupling reactions between the different thiophene rings. Together, these results indicated that coupling reactions involving furfural or 5-bromofurfural can be challenging to optimize.

Table 2. Optimization of Pd-catalyzed synthesis of 5,5'-bisfurfural. (Paper I)

Entry	Ligand	Base	Additive	Solvent	Yield (%)[1]
1	-	K_2CO_3	PivOH	DMAc	6
2	JohnPhos	K_2CO_3	PivOH	DMAc	23
3	Xantphos	K_2CO_3	PivOH	DMAc	23
4	P(o-tolyl)$_3$	K_2CO_3	PivOH	DMAc	26
5	PCy$_3$HBF$_4$	K_2CO_3	PivOH	DMAc	29
6	P(t-Bu)$_2$MeHBF$_4$	K_2CO_3	PivOH	DMAc	36
7	P(t-Bu)$_3$HBF$_4$	K_2CO_3	PivOH	DMAc	40
8	P(t-Bu)$_3$HBF$_4$	K_2CO_3	PivOH (20 mol%)	DMAc	34
9	P(t-Bu)$_3$HBF$_4$	K_2CO_3	PivOH (40 mol%)	DMAc	39
10	P(t-Bu)$_3$HBF$_4$	K_2CO_3	TFA	DMAc	20
11	P(t-Bu)$_2$(neopentyl)HBF$_4$	K_2CO_3	PivOH	DMAc	20
12[2]	P(t-Bu)$_3$HBF$_4$	Li_2CO_3	PivOH	DMAc	Trace[4]
13[2,3]	P(t-Bu)$_3$HBF$_4$	Li_2CO_3	PivOH	DMAc	29
14	P(t-Bu)$_3$HBF$_4$	Na_2CO_3	PivOH	DMAc	45
15	P(t-Bu)$_3$HBF$_4$	Na_2CO_3	Propanoic acid	DMAc	21
16	P(t-Bu)$_3$HBF$_4$	Na_2CO_3	Hexanoic acid	DMAc	26
17	P(t-Bu)$_3$HBF$_4$	Na_2CO_3	Octanoic acid	DMAc	20
18	P(t-Bu)$_3$HBF$_4$	Cs_2CO_3	PivOH	DMAc	Trace[5]
19	P(t-Bu)$_3$HBF$_4$	KOAc	PivOH	DMAc	33
20	P(t-Bu)$_3$HBF$_4$	K_3PO_4	PivOH	DMAc	Trace[5]
21	P(t-Bu)$_3$HBF$_4$	t-BuOK	PivOH	DMAc	Trace[5]
22	P(t-Bu)$_3$HBF$_4$	Na_2CO_3	PivOH	NMP	38
23	P(t-Bu)$_3$HBF$_4$	Na_2CO_3	PivOH	DMF	21
24	P(t-Bu)$_3$HBF$_4$	Na_2CO_3	PivOH	1,4-dioxane	14[4]
25[6]	P(t-Bu)$_3$HBF$_4$	Na_2CO_3	PivOH	DMAc	10[4]

Reaction conditions: Furfural (2 equiv), Pd(OAc)$_2$ (5 mol%), ligand (10 mol%), base (2.5 equiv), additive (30 mol%), 110 ºC, 20–24 h, initial solvent volume 7.5 mL, additional solvent (1.5 mL) containing 5-bromofurfural (0.15 g) injected using a syringe pump (75 μL/h). Reactions were monitored by TLC.
[1] Isolated yield of 5,5'-bisfurfural. [2] Reaction temperature 150 ºC. [3] 5-Bromofurfural was added before the reaction. [4] 5-Bromofurfural was not consumed fully. [5] Furfural underwent a condensation reaction with DMAc. [6] Reaction was performed without furfural.
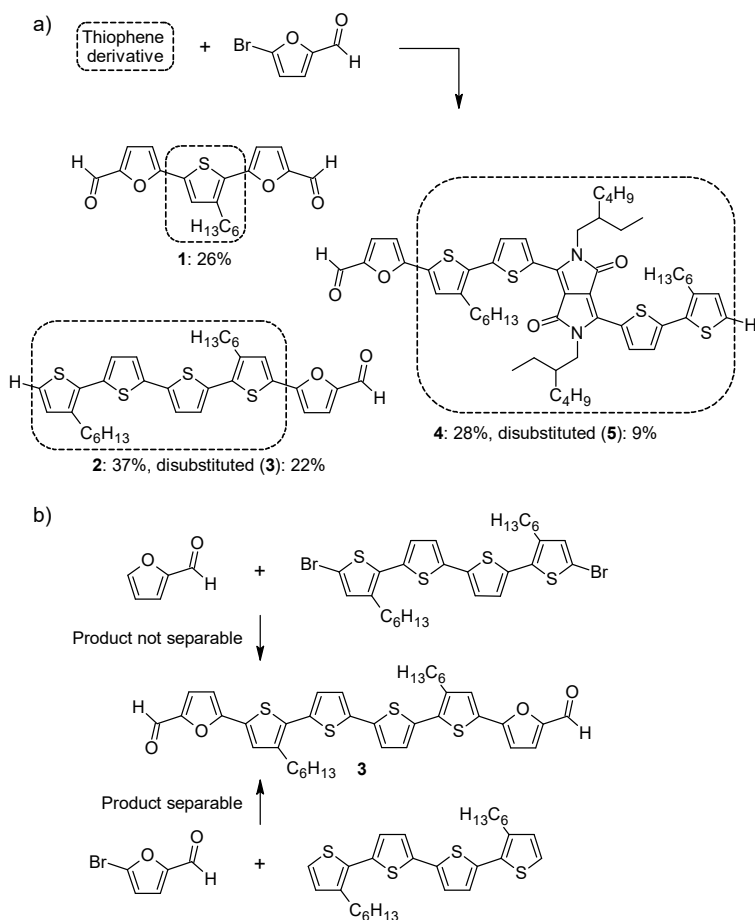
Fig. 17. Direct coupling of 5-bromofurfural with thiophene derivatives (a). Two possible routes for functionalized quaterthiophene derivative (b). (Paper I)

Ligand and solvent-free synthesis of DM-Bf monomer

The oxidization of 5,5'-bisfurfural into 2,2'-bifuran-5,5'-dicarboxylic acid is a scarcely reported reaction, and only a single report exists to date (Osipov, Metlova, Baranova, & Rudakov, 1978). Following the general procedure of the report, KMnO$_4$ in aqueous NaOH was used in an attempt to oxidize the prepared 5,5'-bisfurfural into BFDCA. The oxidation was found to provide a small amount of mixture, which contained some 2,2'-bifuran-5,5'-dicarboxylic acid based on ^{1}H

NMR. Another method tested was a mild $(NH_4)_2Ce(NO_3)_6$ -catalyzed oxidation using 70% *t*-BuOOH in water (Gowda & Chakraborty, 2011), which failed to provide the desired product. In both cases, 5,5'-bisfurfural was completely consumed to yield unknown byproducts mostly. Because of the combination of the unimpressive yield of the coupling reaction and the complexity of the oxidation products, a more easily accessible route to BFDCA was pursued. By using the already oxidized derivatives of furfural in the coupling (protected as esters), the desired monomer, dimethyl 2,2'-bifuran-5,5'-dicarboxylate (DM-Bf), could be obtained directly (Fig. 18). Additionally, both required furans, the methyl esters of 2-furoic and 5-bromo-2-furoic acids, are commercially available and relatively affordable compounds.

Unfortunately, poor results were obtained by utilizing the previously optimized conditions in Table 2 (Fig. 18). As before, the heavily optimized reaction system failed to provide good yield even with these relatively similar substrates, and dimethyl 2,2'-bifuran-5,5'-dicarboxylate was afforded in low yield of 27%. Additionally, the reaction was slower as the bromide was not consumed within the typical 24 h. Instead of reoptimizing the previous method with its complex set-up, another approach was considered. Among the many previously reported coupling methods for similar esters, the procedure developed by Fu, Zhao, Bruneau, & Doucet (2012) stood out: Amidst the other substrates, methyl 5-bromo-2-furoate and ethyl 2-furoate had been coupled under ligand-free conditions to yield the respective bifuran in 71% yield. When their conditions were utilized with methyl 5-bromo-2-furoate and methyl 2-furoate (Entry 1, Table 3), DM-Bf was isolated in a 45% yield. Because of this promising result, a set of experiments was carried out to optimize the method (Table 3).
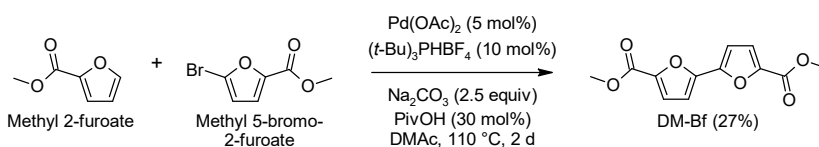

Fig. 18. Pd-catalyzed synthesis of DM-Bf.

Table 3. Optimization of DM-Bf synthesis. (Paper II)

Entry	Equiv of methyl 2-furoate	Base (2 equiv.)	Temperature (ºC)	Time (h)	Yield (%)
1[1]	2	KOAc	120	4	45
2	2	KOAc	120	2	50
3	2	KOAc	100	4	53
4	2	KOAc	80	24[2]	24
5	2	K_2CO_3	100	4	52
6	2	Na_2CO_3	100	24[2]	24
7	2	Cs_2CO_3	100	24[2]	-
8	3	KOAc	100	4	61
9	4	KOAc	100	4	68
10	5	KOAc	100	4	70
11[3]	14	KOAc	100	4[2]	40
12[3]	14	KOAc	100	24	88
13[1,3]	14	KOAc	100	24[2]	50[4]
14[3]	14	KOAc	100	24	87[5]

Reaction conditions: 0.2 g methyl 5-bromo-2-furoate, $Pd(OAc)_2$ (1 mol%), dry DMAc (4 mL), argon atmosphere. [1] No PivOH added. [2] Methyl 5-bromo-2-furoate not fully consumed. [3] No DMAc.
[4] Crude yield after silica gel filtration. [5] The average yield of 10 reactions done with 1.6 g methyl 5-bromo-2-furoate.

After some optimization of the ligand-free coupling method, a simple "solvent-free" procedure was developed (Entry 12, Table 3). In this protocol, methyl 2-furoate is not only a reactant but also a solvent instead of DMAc. The excess methyl 2-furoate is recovered by vacuum distillation after the reaction to reduce waste. The coupling reaction gives DM-Bf in separated yields of up to ca. 90% and does appear to be mostly unaffected by the reaction scale (1–24 mmol). It should be noted that both potassium carbonate and potassium acetate were found to provide practically the same result. As the latter is protonated into acetic acid during the reaction, the recovery of methyl 2-furoate by distillation may be more convenient when potassium carbonate is used as the base. Additionally, pivalic acid is an important additive, as it accelerated the coupling (Entries 12 and 13). It is possible that potassium pivalate (formed *in situ*) simply acts as a more soluble proton "shuttle" between the mostly insoluble base (KOAc or K_2CO_3) and the homogeneous liquid phase.

Using the new approach, DM-Bf or BFDCA could be obtained quite easily and reliably using gram-scale reactions. Conveniently, the product was directly suitable for polyester synthesis. In general, DM-Bf was found to be easier to handle than 5,5'-bisfurfural. However, both compounds still share the high melting point and relatively low solubility in most organic solvents at room temperature, reflecting their strong intermolecular interactions. The conjugation between the furan rings of DM-Bf is easily observable from its UV-light absorbance, which differs dramatically compared to the dimethyl ester of FDCA (DM-F) (Fig. 19). Notably, DM-Bf absorbs UV-light more strongly and at longer wavelengths, which is promising for UV-protective materials.
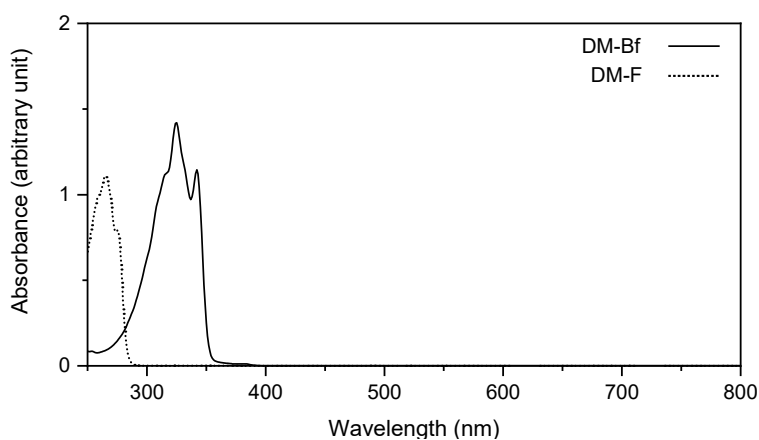
Fig. 19. UV-Vis spectra of DM-Bf and DM-F in chloroform (10 mg/L). (Paper III)

The new coupling method was also tested using furfural and 5-bromofurfural as the substrates. Surprisingly, high separated yields of 5,5'-bisfurfural could be obtained as well using this simple protocol (Fig. 20). However, the method gives three-compound mixtures when the starting furans are not symmetric, as shown by preliminary experiments (Fig. 20). This change will not only lower the yields of the desired bifurans but will also make for a laborious purification. Still, even in these cases, the bifuran conversions remained high, i.e., for 1 mmol of bromide, ca. 0.8 mmol of bifurans could be isolated. It appears that electron-rich furans may not be suitable substrates: 2-Methylfuran did not couple with methyl 5-bromo-2-furoate, even under elevated pressure and microwave irradiation (MW), where the low boiling point of 2-methylfuran should not limit the temperature (Fig. 20).

Altogether these additional results suggest that symmetrical bifurans with electron-withdrawing substituents are most efficiently prepared using this method. These features appear quite different from the original protocol reported by Fu et al. (2012).

i: Methyl 5-bromo-2-furoate or 5-bromofurfural (1 equiv), methyl 2-furoate or furfural (15 equiv), Pd(OAc)$_2$ (1 mol%), PivOH (30 mol%), KOAc (2 equiv), 90–100 ºC, 24 h. Product ratios reflect approximate molar ratios of products in crude mixtures as obtained via ^{1}H NMR analyses.
ii: Methyl 5-bromo-2-furoate (1 equiv), 2-methylfuran (15 equiv), Pd(OAc)$_2$ (1 mol%), PivOH (30 mol%), KOAc (2 equiv), MW 90 ºC, 5 h.
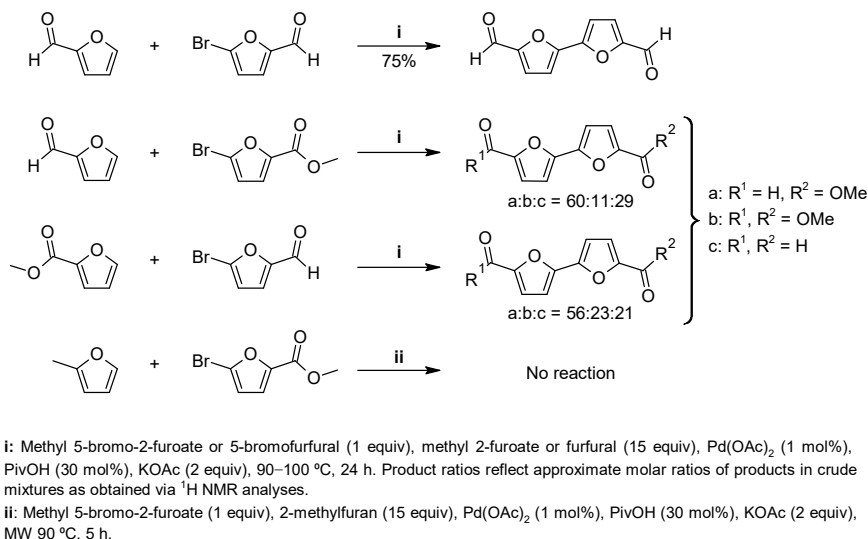
Fig. 20. Other attempted direct coupling reactions using the optimized conditions.

Furan-based dimethacrylate monomers

A two-step route was used to investigate 2,5-furandicarboxylic and 2,2'-bifuran-5,5'-dicarboxylic acids as precursors for novel epoxy methacrylates (Fig. 21). Neither final compound had been previously reported in the literature, though F-D is presented in a Chinese patent application (CN107840923A, 2018). According to the two-step route, the dicarboxylic acids were first converted into diglycidyl esters DG-F and DG-Bf. This reaction was followed by a reaction with methacrylic acid to give the furan dimethacrylate (F-D) and the bifuran dimethacrylate (Bf-D). As an alternative, the reaction between dicarboxylic acids and glycidyl methacrylate can be used to furnish similar epoxy methacrylates (Davy, Kalachandra, Pandain, & Braden, 1998). However, the current two-step route allowed the isolation of DG-

Bf, which had not been previously reported. Additionally, it ensured that oligomers were not formed or were easily removed during purification.
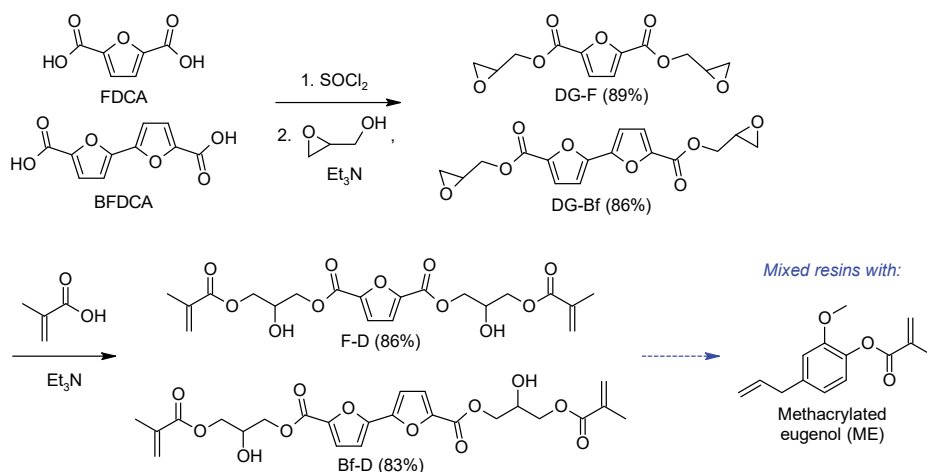

Fig. 21. Synthesis route for F-D and Bf-D, and the structure of the reactive diluent used to prepare mixed methacrylate resins. (Paper IV)

To synthesize DG-F and DG-Bf, FDCA and BFDCA were reacted with thionyl chloride to prepare the corresponding diacid chlorides. Without special purification, they were directly reacted with glycidol in the presence of triethylamine at 0–25 ºC, which gave high yields of the desired diglycidyl esters (87–89%). Glycidol is quite prone to polymerization and purification before use is recommended based on observations: Commercial glycidol stored for a year at 4 ºC gave noticeably lower yields (<75%), and the resulting products sometimes required a second purification because of impurities. Both situations appeared to be linked to polymerized impurities in the glycidol. In many previous reports, DG-F has been synthesized via its diallyl ester, which was then oxidized into DG-F using *m*-CPBA (Deng et al., 2015a; Nameer et al., 2018). Compared to those reactions, the esterification is faster and provides a higher final yield (Liu et al., 2020). Moreover, several experiments that were carried out using the diallyl ester of BFDCA showed that its oxidation with *m*-CPBA was even more sluggish. Even with several days of reaction time and excess *m*-CPBA, full conversion of the diallyl ester was not observed. This result was likely caused by the relatively poor solubility of the diallyl ester and the developing slurry of *m*-chlorobenzoic acid, which hindered the reaction.

Few comments should be made concerning DG-Bf: It has relatively low solubility in common organic solvents such as dichloromethane and acetone because of the 2,2'-bifuran unit. In contrast, DG-F is highly soluble in the same organic solvents. In addition, the 2,2'-bifuran unit increases the melting point considerably: Compared to DG-F (T_m = 89 ºC), DG-Bf has a much higher melting point of 165 ºC. This result surpasses even diglycidyl 2,6-naphthalene dicarboxylate (T_m = 143–144 ºC (Nishiyama, Takata, & Endo, 1996)), which has a very stiff and planar naphthalene unit. Unfortunately, these characteristics made DG-Bf difficult to formulate into an easily processed epoxy resin for study. It certainly seems that liquid epoxy resins containing DG-Bf cannot be made using conventional methods.

As the next step in the route, purified DG-F and DG-Bf were reacted with methacrylic acid to form the corresponding epoxy methacrylates (Fig. 21). The reactions were catalyzed by triethylamine, and in both cases, high yields of epoxy methacrylates were obtained. However, the reaction is not as straightforward as Figure 21 suggests, and the presented chemical structures for F-D and Bf-D do not fully describe them. Rather, F-D and Bf-D are mixtures of isomers, apparent from their NMR spectra (Fig. 22). Three possible configurations for the methacrylate end group was discerned from NMR (Fig. 22). The expected addition at the least hindered carbon atom was favored (end group A), but the two other end groups were formed in noticeable quantities (B and C). From the elucidated structure of end group C, it can be surmised that intramolecular transesterification has taken place during the addition (Jeong et al., 2013). Note that in BisGMA, only end groups analogous to A and B may be observed (Fujisawa, 1994).

The reaction between methacrylic acid and DG-F and DG-Bf was also done using base-free conditions to control the end group ratios. To facilitate the reaction, HFIP was used as the solvent: HFIP is fluorinated alcohol capable of supporting various reactions because of its peculiar hydrogen bonding, including reactions involving epoxy rings (Das, Crousse, Kesavan, Bonnet-Delpon, & Bégué 2000). Surprisingly, HFIP appeared to be one of the few solvents capable of easily dissolving DG-Bf at room temperature. Adding methacrylic acid to a 20% solution of DG-Bf in HFIP and stirring the mixture at 65 ºC for 50 h resulted in the complete conversion of DG-Bf. ^{1}H NMR analysis of the product (iso-Bf-D) showed an unexpected change in the ratios of the methacrylate end groups (Fig. 22). Most notably, the distribution between end groups A and C was inverted when compared to Bf-D. Repeating the same reaction using DG-F as the substrate resulted in an incomplete conversion, as seen from the residual epoxy groups (**x**) in iso-F-D (Fig.

22). In addition, the end group ratios between iso-F-D and iso-Bf-D differed very noticeably. The results suggest that the HFIP-mediated ring-opening of glycidyl esters is sensitive to the electronic properties of the ester group.
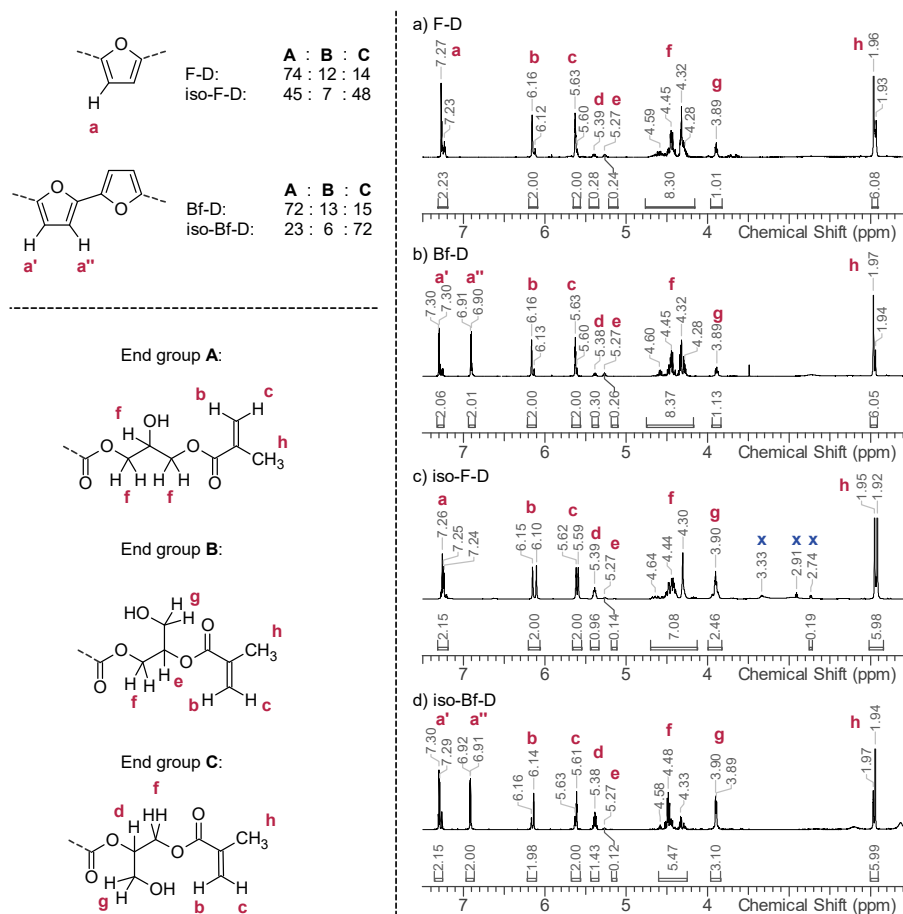
Fig. 22. ¹H NMR spectra and assignation for the synthesized dimethacrylates. x = Residual epoxy signals. (Paper IV)

Further experimentation with DG-Bf revealed that 2-propanol could not be used as a substitute for HFIP, since no reaction took place. Additionally, heating Bf-D and 1 equivalent of methacrylic acid in HFIP did not yield iso-Bf-D: This result rules out simple intramolecular transesterification as the mechanism. The course of the

reaction was not elucidated any further. However, the structure of the major end group (C) is consistent with a cyclic transition state (Stamatov & Stawinski, 2005) (Fig. 23): In the hypothetical transition state, the attack of methacrylic acid should preferentially occur at the less hindered secondary carbon atom (*), resulting in ring-opening of the 5-membered ring. Thus, the ester group will be restored with a tertiary carbon center next to it.
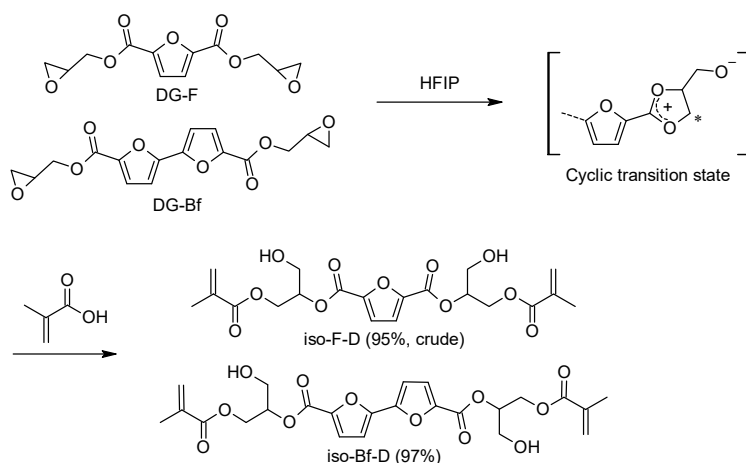
Fig. 23. Possible transition state to epoxy methacrylates mediated by HFIP.

For viscosity characterization, dimethacrylates F-D, Bf-D, and iso-Bf-D were chosen, with iso-F-D excluded from any further experiments because of incomplete conversions and impurities. The dynamic viscosities for the tested systems at different temperatures are presented in Fig. 24. Compared to BisGMA (25 ºC: 593 Pa·s (Zhang et al., 2018)), the new furan-based dimethacrylates had noticeably lower viscosities, which is a benefit from a processing point of view. However, the furan-based units seemed to increase viscosities compared to simple phenyl-derived epoxy methacrylates: Analogous epoxy methacrylates of isophthalic and phthalic acids have viscosities of only 7.7 and 5.8 Pa·s, respectively, at 20 ºC (Davy et al., 1998). Despite the furan-based resins having lower viscosity than BisGMA, the neat resins are still too viscous for easy processing, which would require a viscosity of a few Pa·s.

Fig. 24. Dynamic viscosities of FDCA and BFDCA epoxy methacrylates and their mixtures. (Paper IV)

To help with handling and processing, dilution with methacrylated eugenol (ME) (Fig. 21), a biobased methacrylate, was used to lower the viscosities. ME has previously been used as a diluent for BisGMA, where it allowed the important ther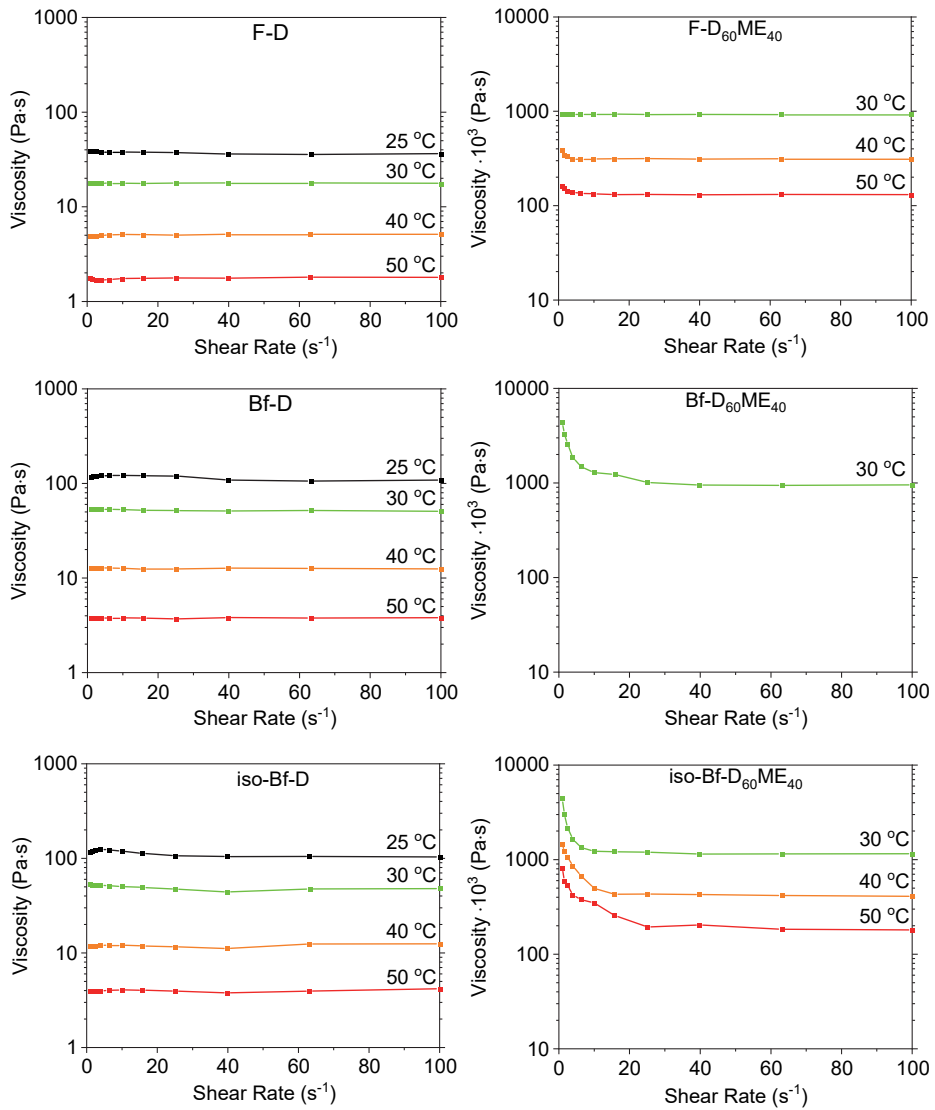momechanical characteristics of BisGMA to be mostly preserved despite the diluent (Zhang et al., 2018). The viscosities were lowered by more than a magnitude using a very typical 40 wt% diluent content (Fig. 24). At 30 ºC, this allowed the biobased dimethacrylate resins to attain viscosities in the range of 1–2 Pa·s, which is typically considered the desirable upper limit in applications.

An incompatibility was noted between the components of Bf-D$_{60}$ME$_{40}$, which began to partially crystallize upon standing for a few days under dry conditions at room temperature. The same process was also noticed during the viscosity measurement, which meant that the measurement was only carried out at the starting temperature when the resin was still homogeneous (Fig. 24). While no significant difference in viscosity was observed between Bf-D and iso-Bf-D, the latter was not prone to partial crystallization. Similarly, iso-Bf-D$_{60}$ME$_{40}$ showed no signs of separation or crystallization during the viscosity measurement and remained homogeneous. Considering the differences in end group ratios between the two, it may be concluded that the distribution affects the behavior of the resins. Because of this result, iso-Bf-D can be considered to be more practical because of its stable physical state. Conversely, it appears that the major components in Bf-D may be crystalline solids, which can separate from the homogeneous mixture under certain conditions. Considering these aspects and the viscosity, F-D is the most promising monomer of the three.

Finally, the curing of the epoxy methacrylates was investigated using DSC. For this purpose, *tert*-butyl peroxybenzoate was added into each resin composition (2 wt%) before a DSC run from 25 to 250 ºC at 10 ºC/min (Fig. 25). The curing activities of the FDCA-based resins appeared the highest, which was likely because of the high density of reactive double bonds in F-D (relative to molar mass). The heat released in the reaction showed a correlation to the relative amount of reactive double bonds by weight (Table 4). Correspondingly, ME presented the highest curing enthalpy, while Bf-D and iso-Bf-D with the highest molar masses had similar, low reaction enthalpies. Curiously, the shapes of the DSC traces for Bf-D and iso-Bf-D were quite different (Fig. 25a), but little difference was observed between Bf-D$_{60}$ME$_{40}$ and iso-Bf-D$_{60}$ME$_{40}$ (Fig. 25b).
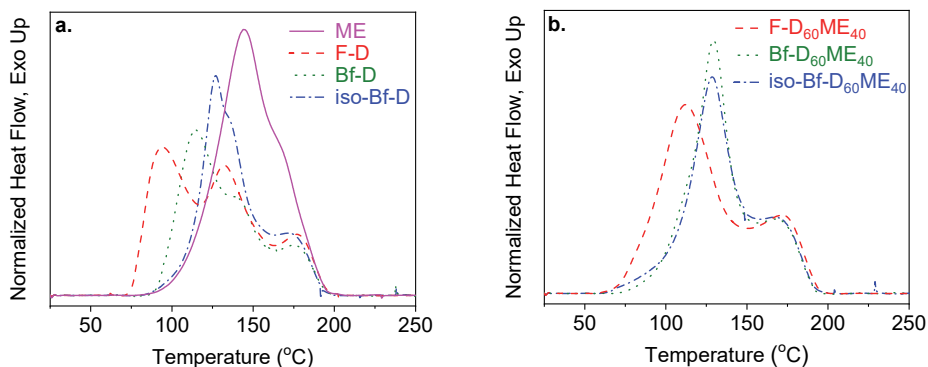
Fig. 25. DSC traces for *tert*-butyl peroxybenzoate–initiated curing of methacrylate resins. (Paper IV)

Table 4. Curing enthalpies and exotherm peak temperatures from DSC. (Paper IV)

Monomer/monomer mixture	ΔH (J g^{-1})	Exotherm peak temperature(s) (ºC)
ME	340	144
F-D	265	95, 132, 177
F-D$_{60}$ME$_{40}$	304	112, 172
Bf-D	230	115, 175
Bf-D$_{60}$ME$_{40}$	273	129, 167
iso-Bf-D	234	127, 172
iso-Bf-D$_{60}$ME$_{40}$	269	129, 167

Scanned 25–250 ºC at 10 ºC/min, N$_2$ atmosphere. 2 wt% *tert*-butyl peroxybenzoate added as an initiator.

4.2 Polymer synthesis and analysis

4.2.1 Poly(ethylene bifuranoate)
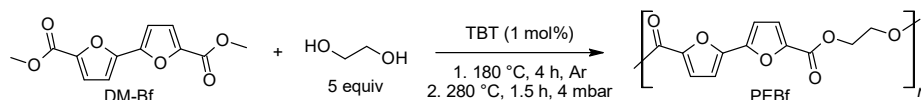
Fig. 26. Synthesis of PEBf using a two-stage reaction. (Paper II)

PEBf was synthesized through a two-step reaction (Fig. 26), where tetrabutyl titanate acted as the catalyst. First, DM-Bf was reacted with excess ethylene glycol at 180 ºC, during which methanol continued to distill off until it was completely displaced from the diester by ethylene glycol. In the second step, the polycondensation reaction was initiated by increasing the temperature to 280 ºC while simultaneously lowering the pressure to remove excess ethylene glycol. During this stage, the polyester melt gradually turned from colorless or pale yellow to a darker brown color. The polyester was then dissolved in trifluoroacetic acid and chloroform at room temperature to form a solution. Introducing the solution slowly into an excess of methanol precipitated the polyester, which was collected after filtration. After drying the collected polyester under vacuum, it was characterized and further processed into melt-pressed or solvent-cast films. The intrinsic viscosity of the synthesized PEBf was determined to be 0.85 dL/g in trifluoroacetic acid at 30 ºC, indicating a successful polycondensation.

While titanium alkoxides are known as highly active and relatively non-toxic transesterification catalysts, they may also cause unwanted side reactions. Notably, they may result in coloring impurities, and titanium catalysts are not preferred for PET synthesis because of this (Shah, Bhatty, Gamlen, & Dollimore, 1984). The dark appearance of PEBf formed chiefly during the high-temperature polycondensation and may have been because of byproducts formed because of titanium. Despite the strong color of the polymer, its ^{1}H NMR analysis did not reveal noticeable by-products. In results published since, Edling et al. (2020) elucidated the origin of the coloration in their synthesized PEBf. Notably, they found that the oxidation of the BFDCA unit is easier relative to the FDCA unit, which may make the bifuran unit more sensitive to oxygen under high temperatures. Additionally, it should be expected that reactions involving conjugated bifuran

moieties can give more highly conjugated degradation products, which in turn will be able to absorb visible light.

The detailed ^{1}H NMR analysis of PEBf revealed small signals attributed to diethylene glycol (DEG). The etherification of ethylene glycol forms it, and thus it can be commonly observed in the NMR spectra of melt-processed ethylene glycol–based polyesters such as PET (Martínez de Ilarduya & Muñoz-Guerra, 2014). It is difficult to avoid, and because of its high boiling point, it stays in the reaction mixture. As a diol, DEG is naturally then able to participate in the polycondensation allowing it to become incorporated into the polyester. Tracking its content is important because it has been shown to influence the properties of PET. Notably, the DEG units can cause worse thermal properties and can act as thermally labile groups in the polyester (Holland & Hay, 2002). In the synthesized PEBf, the concentration of diethylene glycol was evaluated to be quite low despite the high titanium catalyst loading; Based on the ^{1}H NMR spectrum integrals, the estimated content was just under 1% by weight.

The thermal properties of PEBf were analyzed from the as-received, oven-dried precipitate using DSC and TGA (Fig. 27). Based on DSC, PEBf is a semi–crystalline polymer with a glass transition temperature of ca. 107 ºC and a melting temperature of ca. 240 ºC. It also was observed to undergo some cold crystallization at 169 ºC. The observed melting temperature is quite close to that of PET ($T_m \approx 251$ ºC) but higher than that of PEF ($T_m \approx 214$ ºC). However, the T_g of PEBf is much higher than that of either PET or PEF (ca. 75 ºC and 77 ºC, respectively). Thermogravimetric analysis showed that PEBf undergoes a major one-step degradation at 429 ºC under N_2, whereas PET showed a similar degradation step at 458 ºC under the same conditions (Fig. 27b). The furan-based PEF has shown a similar tendency versus PET (Thiyagarajan et al., 2014), and thus furan acid–based polyesters appear to be slightly less thermally stable than those derived from terephthalic acid.
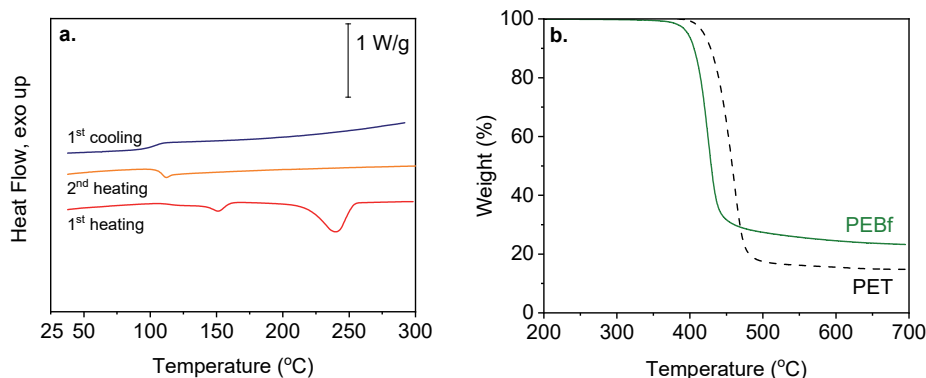
Fig. 27. Thermal analysis of PEBf: DSC (a, 10 ºC/min) and TGA (b, 20 ºC/min). (Paper II)

For tensile testing, dynamic mechanical analysis, and gas permeability determination, free-standing films were prepared from PEBf and commercial PET. PEBf is practically insoluble in most organic solvents, which limited the choice of solvent to a mixture of trifluoroacetic acid and chloroform. The obtained solvent-cast films were surprisingly good quality, with little change to the original color of the polymer (Fig. 28). However, other melt-pressed films were made using a heated press, where the polymer samples were first melted and then compressed into films using a hydraulic press. Sheets of PTFE-coated glass-fiber mats were used to prevent the samples from sticking to the press plates. The melt pressed PEBf usually appeared darker after the pressing, whereas the commercial PET remained colorless.

Dynamic mechanical analysis of the melt pressed PEBf sample did not reveal any particular quirks. It mainly confirmed the high T_g, as can be noted from the peaks of both loss modulus E'' and tan δ, which are located at around 100 ºC (Fig. 29). Additionally, the semi-crystalline character of the polyester (and low crystallinity of the sample) could also be observed as the increasing storage modulus after 150 ºC, which is caused by cold crystallization during the measurement. Tensile testing (Table 5) showed that the prepared PEBf was quite brittle and low tensile strength compared to the PET reference, perhaps indicating inadequate molar mass. The melt-pressed sample, in particular, was very brittle, and this may have been caused by additional degradation or hydrolysis by surrounding air during the pressing procedure.
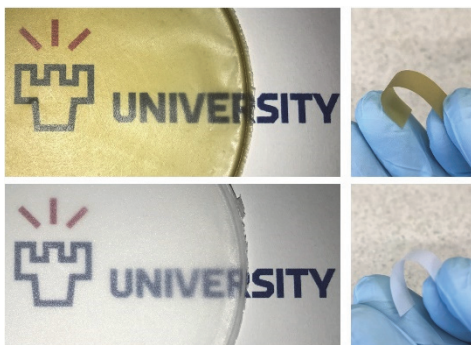
Fig. 28. Digital images demonstrating the appearances of solvent cast PEBf (top) and PET (bottom) films. (Reprinted from Paper II under CC-BY 4.0 license)
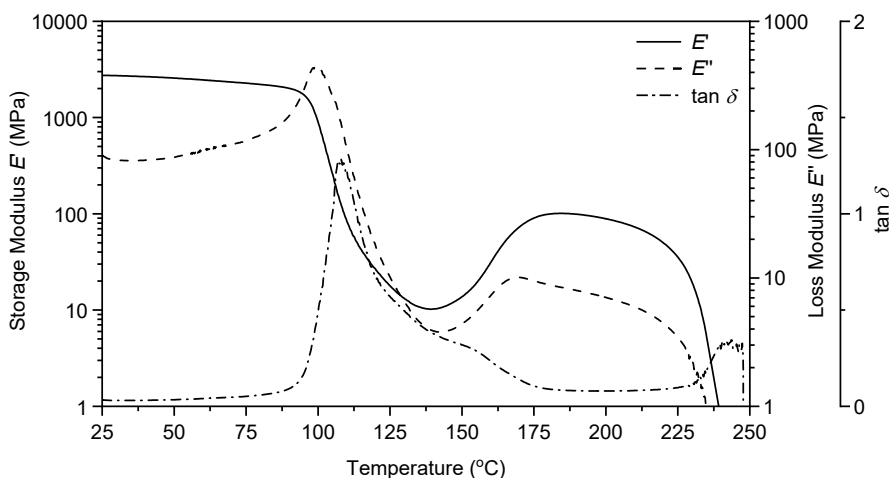
Fig. 29. DMA trace for melt pressed PEBf film sample. (Paper II)

Table 5. Tensile testing results for solvent-cast and melt-pressed PET and PEBf films. (Paper II)

Sample	E_t (MPa)	σ_m (MPa)	ε_b (%)
PEBf (solvent-cast)	1182 ± 149	23 ± 3	4.50 ± 0.97
PET (solvent-cast)	948 ± 60	16 ± 2	3.74 ± 0.37
PEBf (melt pressed)	2453 ± 140	12 ± 1	0.50 ± 0.05
PET (melt pressed)	1622 ± 51	35 ± 6	20.05 ± 7.04

E_t: Tensile modulus. σ_m: Ultimate tensile strength. ε_b: Elongation at break.

As discussed previously, a notable property of current commercial aromatic polyesters such as PET is their relatively good impermeability towards various gases. It was expected that BFDCA-based PEBf would similarly act as a barrier polyester considering the excellent record of FDCA-based polyesters as barrier materials. The hypothesis was investigated using the melt pressed PEBf film, with the PET films acting as reference samples. Despite the poor mechanical properties of the prepared PEBf film, it indeed showed lower permeability towards oxygen (0.041 barrer) and water vapor (346.5 g μm m^{-2} d^{-1}) than the PET reference (0.099 barrer and 616.7 g μm m^{-2} d^{-1}, respectively). Thus, PEBf achieved 2.4× and 1.8× reductions in oxygen and water vapor permeability, respectively, compared to PET. Based on these results, PEBf can be placed between PET and PEF in terms of oxygen permeability, superior to the former, but inferior to the latter. It should also be noted that a later characterization of PEBf by Edling et al. (2020) using material obtained from an optimized polymerization procedure showed a similar trend. However, they reported a lower oxygen permeability value (0.017 barrer).
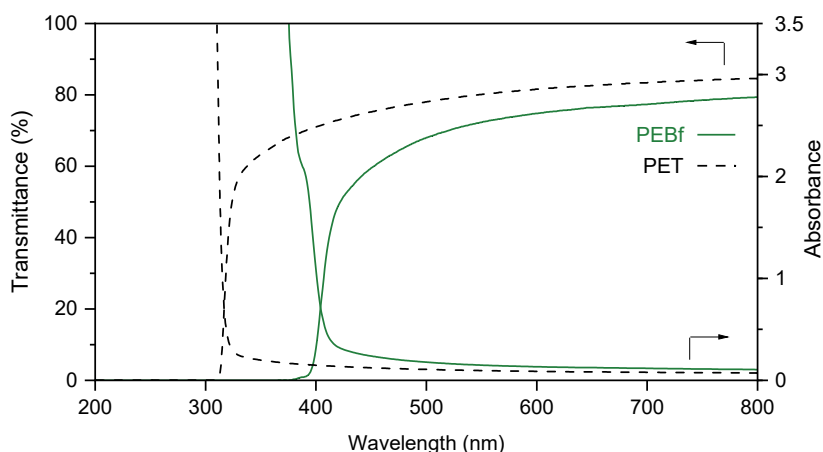
Fig. 30. UV and visible light transmittance and absorbance of PET and PEBf films. (Paper II)

Finally, the UV-Vis properties of PET and PEBF films were compared (Fig. 30). Since PEBf has a high concentration of bifuran units, which are able to absorb UV light at wavelengths >300 nm, PEBf films showed very low light transmittances at wavelengths below 400 nm. Simultaneously, the yellowish color of the PEBf films is made apparent by the increased absorption at visible wavelengths (>400 nm). As

previously shown, in a dilute chloroform solution, the DM-Bf monomer has a relatively sharp absorption peak at ca. 325 nm (Fig. 19). In the solid state, this peak is expected to broaden and red-shift because of intermolecular interactions (Sippola et al., 2018), which may further enhance UV-absorbance. The result indicates that BFDCA-based polymers could be quite effective at filtering out most UV-light. In contrast, PET (and PEF) lacks a suitable chromophore and does not have significant absorbance at longer UV wavelengths of >300 nm.

4.2.2 Poly(butylene furanoate-co-bifuranoate)
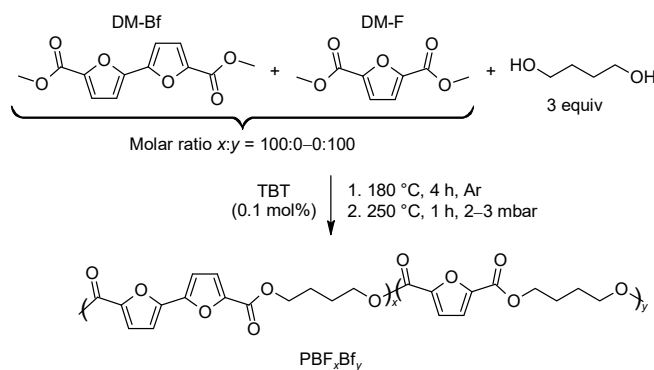
Fig. 31. Synthesis of PBF, PBBf, and random PBF-*co*-PBBf polyesters. (Paper III)

The furan-bifuran copolyesters based on 1,4-butanediol were synthesized similarly as PEBf, except the feed ratio of the two ester monomers DM-F and DM-Bf was varied to synthesize either pure homopolyesters or their random copolyesters (Fig. 31). Additional adjustments were made to the amount of the catalyst and the reaction temperature to account for the differences arising from the new diol. The resulting polymers obtained from the two-step process were colorless to light yellow in appearance. After dissolution and precipitation, they were collected in the form of white, fibrous materials. As the reaction conditions were fixed for all samples, differences in molar masses could be surmised based on the intrinsic viscosities (Table 6). Notably, the solution viscosities were lowest for the polyesters with a high content of the stiffer bifuran units.

^{1}H NMR analysis of the synthesized polyesters showed that the ratio of furan and bifuran units in the feed and the final polymer had very little difference (Table 6). Also, since 1,4-butanediol is unlikely to dimerize, the NMR spectra lacked signals arising from the ether side-products. Some etherification may still have

occurred, as 1,4-butanediol can dehydrate into highly volatile tetrahydrofuran (which simply escapes the reaction). However, with the employed excess of 1,4-butanediol this was hardly a concern. Because of the closeness of the chemical shifts for signals arising from the different structures in the copolyesters, ^{13}C NMR analysis (Witt, Müller, & Deckwer, 1996) had to be carried out to provide a quantitative assessment of the chain randomness.

Table 6. Characterization of synthesized polyesters. (Paper III)

Sample	Furan:Bifuran mol%-ratio		Yield (%)	Intrinsic viscosity[2] (dL/g)	Number-average sequence length[3]		R_i[4]
	Feed	Product[1]			L_{FF}	L_{BB}	
PBF	100:0	100:0	93	0.77	-	0	0
PBF$_{90}$Bf$_{10}$	90:10	90:10	93	0.95	8.84	1.16	0.98
PBF$_{75}$Bf$_{25}$	75:25	76:24	95	0.90	3.65	1.38	1.00
PBF$_{50}$Bf$_{50}$	50:50	51:49	98	0.87	2.08	1.89	1.01
PBF$_{25}$Bf$_{75}$	25:75	26:74	90	0.67	1.27	4.13	1.03
PBF$_{10}$Bf$_{90}$	10:90	10:90	91	0.70	1.12	6.94	1.04
PBBf	0:100	0:100	97	0.72	0	-	0

[1] Determined from the integrals of ^{1}H NMR spectra. [2] Determined in TFA (0.5 g/dL) at 30 °C, according to Billmeyer (1949). [3] Determined using equations 3 and 4. [4] Randomness index.

The sequence lengths and the randomness index could be calculated based on the peak areas under the signal(s) evolving from one of the carbon atoms on the tetramethylene unit (Fig. 32) using equations 3–5. A_{FF} represents the area under the peak at 68.97 ppm, A_{BB} the area under the peak at 68.64 ppm, and A_{FB} represents the area under the two peaks at 69.06 and 68.54 ppm. Calculations from equations 3–5 indicated that these copolyesters had highly random distributions of furan and bifuran units, i.e., the copolyesters showed no signs of block ($R_i < 1$) or alternating ($R_i = 2$) chain structures (Table 6).

$$L_{FF} = \frac{A_{FF}}{^1/_2(A_{FB})} + 1 \tag{3}$$

$$L_{BB} = \frac{A_{BB}}{^1/_2(A_{FB})} + 1 \tag{4}$$

$$R_i = \frac{1}{L_{FF}} + \frac{1}{L_{BB}} \tag{5}$$
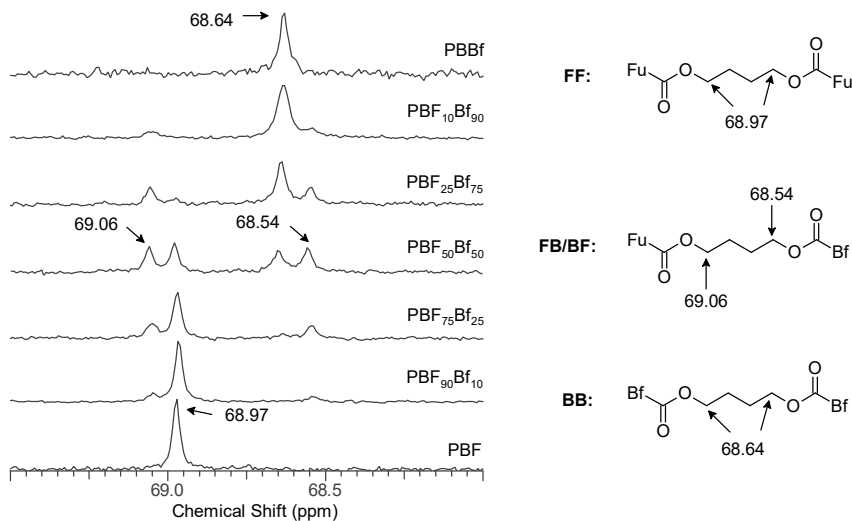
Fig. 32. ^{13}C NMR analysis of the sequence sensitive carbon atom of the butylene moiety in PBF, PBBf, and their random copolyesters. (Paper III)

Key thermal properties were analyzed via DSC and TGA (Table 7). Single glass transition was observed in the case of each polymer, and the glass transition temperatures of the copolyesters varied monotonously depending on the ratio of the furan and bifuran units, with the two extremes represented by PBF ($T_g = 39$ ℃) and PBBf ($T_g = 62$ ℃). In contrast, the melting temperatures appeared to follow the expected eutectic pattern for two incompatible units. However, melting temperatures for PBF$_{75}$Bf$_{25}$, PBF$_{50}$Bf$_{50}$, and PBF$_{25}$Bf$_{75}$ were not observed apart from the as-received, solvent precipitated samples. Copolyesters in this range appear to crystallize very slowly and should also be expected to achieve only low crystallinities compared to the other polyesters prepared. The thermogravimetric analyses (at 20 ℃/min under N_2) revealed that the furan-bifuran ratio only had a small effect on apparent decomposition, resulting in slightly higher decomposition temperatures for the bifuran rich polyesters. All polyesters in the series were relatively stable and comparable to other FDCA-based polyesters, suggesting no ill effect from the random copolymerization of furan and bifuran dicarboxylic acids.

Table 7. Thermal properties of PBF, PBBf, and random PBF-*co*-PBBf copolyesters. (Paper III)

Sample	T_g[1]	T_m[2] (ºC)		T_{CC}[3]	$T_{d5\%}$[4]	T_d[5]
	(ºC)	1st Heating	2nd Heating	(ºC)	(ºC)	(ºC)
PBF	39	173	172	109	366	391
PBF$_{90}$Bf$_{10}$	43	81, 157	156 (158*)	nd (119*)	365	391
PBF$_{75}$Bf$_{25}$	49	82, 130	nd	nd	364	392
PBF$_{50}$Bf$_{50}$	53	97, 145	nd	nd	365	393
PBF$_{25}$Bf$_{75}$	58	89, 188	nd	nd	367	398
PBF$_{10}$Bf$_{90}$	60	202	202 (184*, 202*)	144 (134*)	364	397
PBBf	62	217	215	122	370	402

[1] Obtained from the 2nd heating. [2] Melting temperature from heating at 10 ºC/min (*: 5 ºC/min) [3] Peak of cold crystallization from 2nd heating at 10 ºC/min (*: 5 ºC/min). [4] Temperature at 5% sample mass-loss. [5] Temperature at peak mass-loss rate. nd: Not determined.

To evaluate once again the mechanical properties and gas barrier characteristics, melt-pressed films with thicknesses between 0.1 and 0.2 mm were made. This time the films retained the original appearance through the pressing, ranging from yellowish for PBBf to mostly colorless for PBF (Fig. 33). Strips cut from the films were analyzed using DMA, and the tan δ peaks were in good agreement with the T_g values determined from DSC (Fig. 34). However, PBF differed from the others by having a low-intensity peak. This difference probably arose because of the higher crystallinity of the film, as polarizing optical microscopy revealed small crystalline structures. However, XRD only revealed amorphous halos for all samples.

During the tensile testing, the performance of the films remained very similar irrespective of the comonomer ratio (Table 8). The films had high tensile strengths and elastic moduli, though their elongation values were lower than expected. Some previously reported values for PBF go up to 300% elongation at break (Wu et al., 2014). This result may be because of different molar masses, which may have limited the ductility in the prepared films. Nevertheless, it appears that PBBf and PBF both have similar mechanical properties, which their random copolyesters reflect by having very similar properties.
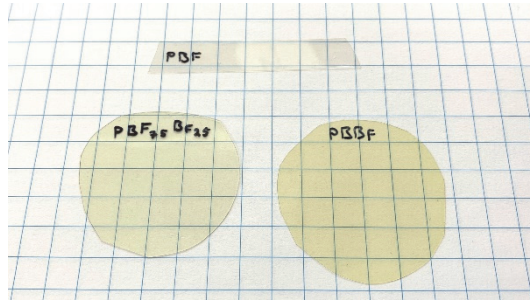
Fig. 33. Digital images taken of pieces cut from the melt-pressed films. PBF (top), PBBf (right), and PBF$_{75}$Bf$_{25}$ (left).
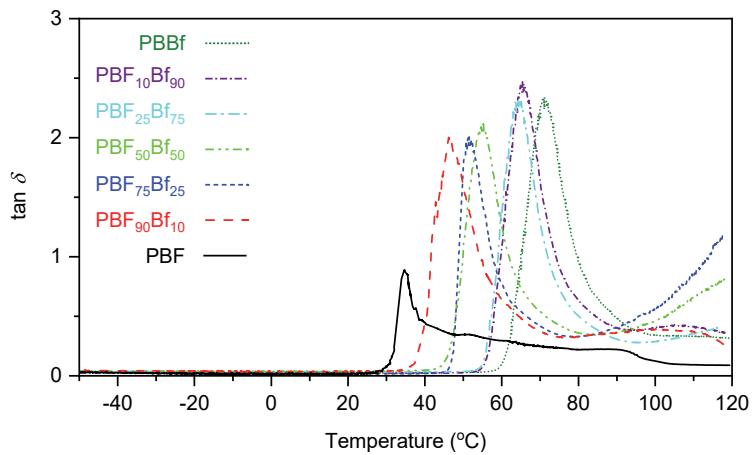
Fig. 34. tan δ traces for the polyester series. (Paper III)

Table 8. Tensile testing results of the homopolyesters and copolyesters. (Paper III)

Sample	E_t (GPa)	σ_m (MPa)	ε_b (%)
PBF	2.0 ± 0.1	58.9 ± 2.2	4.0 ± 0.3
PBF$_{90}$Bf$_{10}$	2.1 ± 0.02	65.1 ± 2.5	4.2 ± 0.2
PBF$_{75}$Bf$_{25}$	2.0 ± 0.1	66.6 ± 3.1	5.0 ± 0.2
PBF$_{50}$Bf$_{50}$	2.2 ± 0.1	66.0 ± 1.3	4.3 ± 0.4
PBF$_{25}$Bf$_{75}$	2.0 ± 0.1	65.8 ± 4.2	5.0 ± 0.2
PBF$_{10}$Bf$_{90}$	2.1 ± 0.04	65.5 ± 2.7	5.0 ± 0.4
PBBf	2.0 ± 0.1	66.0 ± 3.0	5.4 ± 0.2

E_t: Tensile modulus. σ_m: Ultimate tensile strength. ε_b: Elongation at break.

Next, the melt-pressed films were tested against the permeation of oxygen, an important gas penetrant. Much like the similar furan and bifuran polyesters, PBBf, and random PBBf-*co*-PBF polyesters were excellent barriers against oxygen (Table 9). Despite the low crystallinity of the sample films, their O_2 permeabilities were low compared to even crystalline aromatic polyesters, such as oriented PBT. It is also interesting that PBF and PBBf are quite similar in performance. This result suggests that the diol plays an important part in determining the relative performance difference between furan and bifuran polyesters. PEF and PEBf, for example, have a much larger disparity between in their O_2 permeability (Edling et al., 2020).

Table 9. O_2 barrier performance of various polyesters versus the synthesized polyesters and copolyesters. (Paper III)

Entry	Sample	Permeability coefficient (barrer)	BIF vs. PET	Conditions
1	PBF	0.0246 ± 0.0002	2.4–4	
2	PBF[90]Bf[10]	0.0225 ± 0.0004	2.7–4.4	25 °C at 50% RH
3	PBF[75]Bf[25]	0.0217 ± 0.0015	2.8–4.6	
4	PBBf	0.0285 ± 0.0021	2.1–3.5	
5	PET[1]	0.099	1	23 °C, 0% RH
6	PEBf[1]	0.041	2.4	23 °C, 0% RH
7	PET[2]	0.060	1[2]	30 °C, 50% RH
8	PBF[2]	0.018	3.3[2]	30 °C, 50% RH
9	PBT[3]	0.231	-	23 °C, 50% RH
10	PBT[3,4]	0.0456	-	25 °C, 0% RH
11	PBT[3,5]	0.0258	-	25 °C, 0% RH
12	PEN[6]	0.008	-	23 °C, 50% RH

[1] Paper II. [2] From Wang et al., 2017b. [3] From McKeen, 2017. [4] Unoriented films. [5] Biaxially oriented film. [6] From Lange & Wyser, 2003. 1 barrer ≈ 65.66 cm^3 mm m^{-2} d^{-1} atm^{-1}.

As with PEBf, another barrier property to consider with these polyesters is their UV-light transmittance. Since the bifuran unit is much more conjugated than the furan unit, an apparent decrease in the UV-transmittance could be observed when the bifuran unit was introduced into PBF (Fig. 35). Lacking a suitable chromophore, PBF does little to hinder the transmission of longer UV wavelengths (300–400 nm), having a cutoff-wavelength of ca. 300 nm. At a similar thickness of ca. 0.15 mm, there is a noticeable effect on the UV-transmittance even at 1 mol% bifuran content (Fig. 35, PBF[99]Bf[1]). Further increasing the bifuran loading decreased the amount of UV-light transmitted, though, at the tested film thickness of around 0.15 mm,

PBF$_{90}$Bf$_{10}$ provided most of the same UV blocking effect as PBBf, which was the least permeable to UV light.
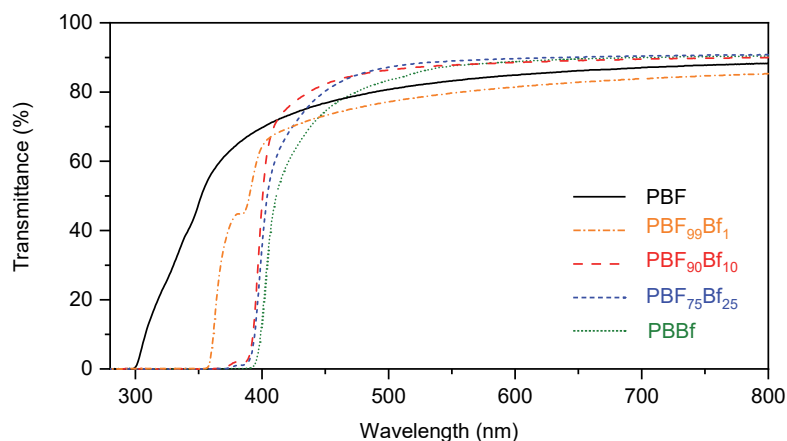

Fig. 35. The light transmittance of the selected polyester films. (Paper III)

4.2.3 Cross-linked furan ester–based dimethacrylate networks

Using dimethacrylate monomers F-D, Bf-D, and iso-Bf-D, neat and ME-diluted (40 wt% ME) resins were cured using via thermally initiated radical polymerization. As with the DSC curing runs, 2 wt% of *tert*-butyl peroxybenzoate was added into each resin to act as the radical initiator. Additionally, ME, BisGMA, and BisGMA$_{60}$ME$_{40}$ mixture were also prepared and cured as reference samples. The thermal curing was accomplished using open steel molds, where the liquid resins were transferred before being degassed using a vacuum and placed under argon. Samples were then heated at 90, 150, and 180 ºC for 1, 5, and 2 hours, respectively. Complete or near-complete curing was evidently achieved under these conditions. Solid resin pieces heated using a DSC showed absent or negligible exothermic events between 25 and 250 ºC at a 10 ºC/min scanning rate.

Next, the thermal stability of the resins was evaluated. Based on TGA, the dilution with methacrylated eugenol significantly influenced the degradation (Table 10): The furan-based resins had early onsets of decomposition ($T_{d5\%}$) below 330 ºC, with main decomposition happening at 410–420 ºC. By comparison, the ME-diluted resins began decomposing at ca. >359 ºC, with higher main decomposition steps (>430 ºC). For BisGMA, dilution with ME had little effect on decomposition

82

temperatures. Furthermore, the BisGMA resins were obviously much more stable towards thermal degradation, possibly because of the more stable aryl ether linkages.

Table 10. Thermogravimetric analysis of cured resin networks. (Paper IV)

Sample	$T_{d5\%}$ (ºC)	$T_{d50\%}$ (ºC)	R_{800} (ºC)
ME	379	453	9.9
BisGMA	372	436	10.1
BisGMA$_{60}$ME$_{40}$	384	437	9.9
F-D	327	415	4.0
F-D$_{60}$ME$_{40}$	372	431	10.5
Bf-D	289	421	9.5
Bf-D$_{60}$ME$_{40}$	375	433	13.2
iso-Bf-D	258	418	9.1
iso-Bf-D$_{60}$ME$_{40}$	359	432	12.7

$T_{d5\%}$: 5% mass-loss temperature. $T_{d50\%}$: 50% mass-loss temperature. R_{800}: Residue at 800 ºC.

The thermomechanical properties of the cured resins were next investigated using DMA. Results are collected in Table 11, while the DMA traces are presented in Figures 36 and 37. Compared to ME, the three furan-based epoxy methacrylates lead to higher stiffness (high E') and increased glass transition temperature (Table 11). On the other hand, BisGMA clearly resulted in a material with the highest glass transition temperature. However, the difference mostly disappeared between the ME-diluted furan and BisGMA resins, which showed glass transition temperatures of ca. 200 ºC. Both results are in close agreement with previous values (Zhang et al., 2018) for BisGMA and BisGMA$_{60}$ME$_{40}$ resins cured using similar methods. Interestingly, Bf-D$_{60}$ME$_{40}$ displayed the same glass transition temperature as neat Bf-D. It is unclear why neat the Bf-D and iso-Bf-D resins showed such disparate behavior, but it may be linked to the differences in the end group configurations.

Table 11. DMA results for cured resins. (Paper IV)

Resin	E' (GPa)[1]	T_g (ºC)[2]
ME	2.58	149
BisGMA	3.07	199
F-D	3.91	179
Bf-D	3.88	178
iso-Bf-D	3.43	179
$BisGMA_{60}ME_{40}$	3.48	197
$F-D_{60}ME_{40}$	2.49	209
$Bf-D_{60}ME_{40}$	2.79	177
$iso-Bf-D_{60}ME_{40}$	2.73	203

[1] Storage modulus at 25 ºC. [2] Peak value of tan δ.

From the shapes of the DMA traces, it can be surmised that the addition of ME as a diluent increases the cross-linking density, which results in a flatter E' curve shape (Fig. 36a and 37a). Expectedly, it also appears to lead to a more heterogeneous structure, which can be seen from the broader and less sharp shape of the tan δ peaks (Fig. 36b and 37b). Nevertheless, neat F-D, Bf-D, and iso-Bf-D provided the highest E' values in the series, even compared to BisGMA. Based on their excellent thermomechanical properties, the three furan-derived epoxy methacrylates appear to be potential renewable alternatives for BisGMA.
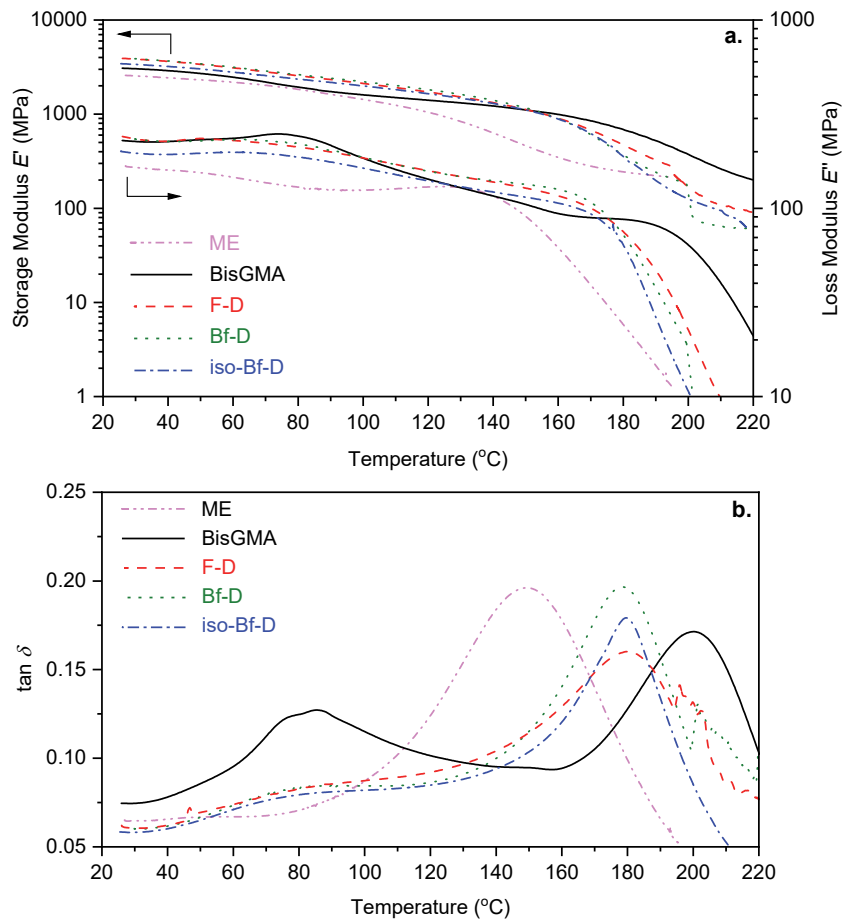
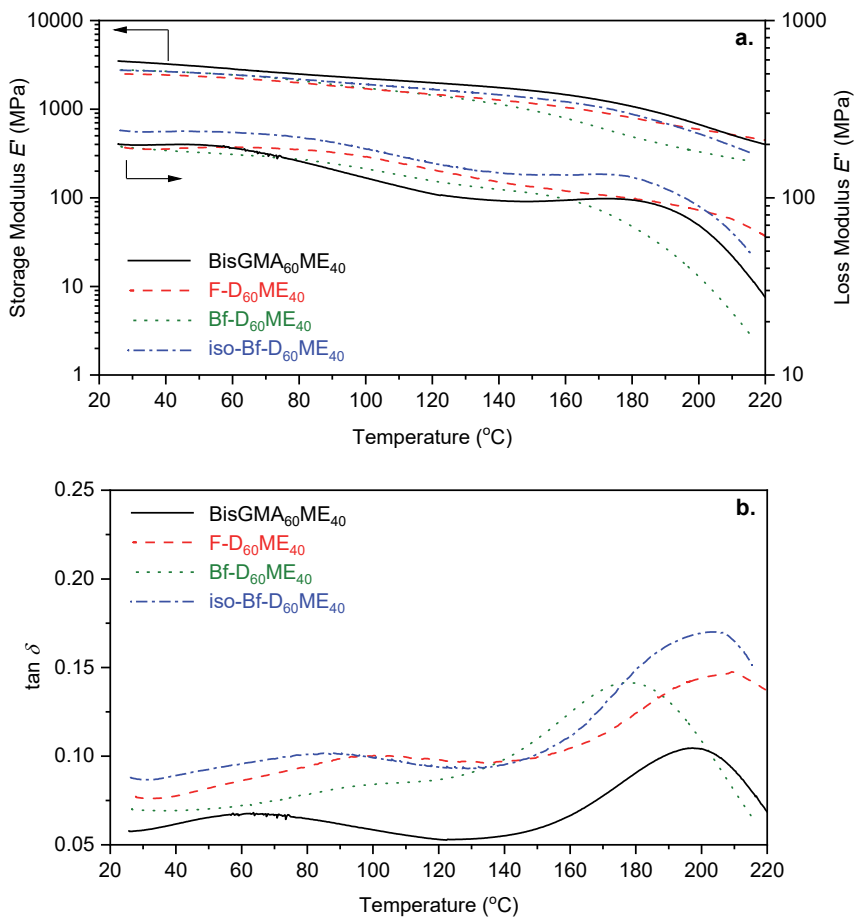**Fig. 36.** DMA traces of single component resins: E' and E'' (a), and tan δ (b). (Paper IV)

Fig. 37. DMA traces of ME-diluted resins: *E'* and *E''* (a), and tan *δ* (b). (Paper IV)

5   Summary

Furfural and 5-hydroxymethylfurfural are likely to be prominent platform chemicals in the future because of their facile preparation from biomass and an abundance of derivatives. They may prove especially important as raw materials for polymers considering the need for renewable alternatives to common aromatic high-performance materials such as poly(ethylene terephthalate). 2,5-Furandicarboxylic acid is already considered one of the most promising "new" biochemicals, with few other furans generating such broad interest. This interest is almost solely because of the interesting properties displayed by poly(ethylene furanoate), a biobased polyester prepared using FDCA. PEF has been shown to have excellent properties as a material, even surpassing many currently used materials, including PET, which gives hope that new biobased materials can also provide additional value in applications.

Following the objective of finding novel uses for furfural as a feedstock, several 2,2'-bifuran–based compounds and materials were studied in this work. In Paper I, the synthesis of the "base-compound", 5,5'-bisfurfural, was studied. Additionally, some syntheses of furfural-derived thiophene compounds were reported using the developed direct coupling method. In Paper II, an improved, extraneous solvent -free synthesis was developed to dimerize methyl 2-furoate, a derivative of furfural. In addition, the resulting 2,2'-bifuran monomer was used to prepare poly(ethylene bifuranoate) as an analog of PET and PEF. Compared to PET, the novel bifuran polyester was found to provide excellent oxygen barrier properties in addition to its enhanced capability of blocking the transmission of long-wavelength UV-light. The high glass transition temperature of PEBf is another promising feature, exceeding both PET and PEF in this aspect.

In Paper III, poly(butylene bifuranoate) was prepared as an analog to PBT and PBF, and for the first time, its detailed properties were characterized. PBBf was also copolymerized with PBF in various ratios. It was found that because of the incompatibility of furan and bifuran units, copolyesters with 10 mol% or more of comonomer tended to show signs indicative of slow crystallization such as absent melting events. However, compared to both PBBf and PBF, their copolyesters were shown to retain similar, excellent oxygen barrier properties. It was also noted that introducing the 2,2'-bifuran monomer into PBF resulted in noticeably increased UV-light absorbance. Furthermore, compared to PBF, the 2,2'-bifuran monomer provided an enhanced glass transition temperature, which varied monotonously with the bifuran content.

In Paper IV, both BFDCA and FDCA were used as precursors for novel epoxy methacrylates, prepared via the intermediate epoxies. The liquid epoxy methacrylates were cured both neat and with methacrylated eugenol as the diluent, by using a radical initiator. The thermally cured resins were then compared against similar BisGMA-based materials. Notably, the measured thermomechanical properties of the novel resins were either similar with, or close to the BisGMA-based references. The thermal degradation of the resins generally took place at lower temperatures compared to the BisGMA resins; however, methacrylated eugenol improved the thermal stability in addition to lowering the viscosity of the uncured resin.

The results obtained here demonstrate that by utilizing conceptually simple monomers derived from biomass-based compounds, high-performance materials can be prepared. It was also shown that these materials could provide performance advantages in some areas because of their unique chemical structures. Notably, furfural is an affordable and well-known aromatic building-block, which is the key starting compound for the 2,2'-bifuran materials studied in this work. They were shown to be a novel way to valorize furfural, itself produced from waste materials, into more valuable products. BFDCA especially can be identified as a promising monomer or comonomer for further studies in renewable polyesters.

5.1   Outlook on further research

In this work, the 2,2'-bifuran structure was accessed via a Pd-catalyzed coupling reaction. While a relatively low catalyst loading of 1 mol% was ultimately used, expensive and rare transition metals such as Pd can be considered undesirable from a sustainability perspective. For this reason, developing the coupling reaction further by using a recyclable Pd-catalyst, e.g., a heterogeneous supported catalyst, could significantly improve the attractiveness of 2,2'-bifurans as monomers. Furthermore, the direct coupling protocol's requirement for the halogenated coupling partner can be recognized as a cost-increasing characteristic. As such, the oxidative coupling of electron-poor furans should be studied. Combined with a recyclable catalyst, such a dehydrogenative coupling reaction could potentially allow low-cost, environmentally-friendly access to the proposed materials.

The bifuran polyesters presented in Papers II and III were comparable in their thermal stability to FDCA-based polyesters. However, during synthesis and melt-processing, the bifuran polyesters always obtained significant color. Presumably, this color was related to some thermal degradation process that gave visible light–

absorbing products. For this reason, the optimal synthesis conditions should be investigated in more detail, e.g., the influence of different transesterification catalysts and stabilizing agents (antioxidants) on 2,2'-bifuran polyesters still needs to be explored in detail.

Because of the considerable interest in biodegradable plastics, 2,2'-bifuran–based polyesters should be an interesting subject of biodegradability studies. While aromatic 2,2'-bifuran–based polyesters such as PEBf and PBBf are unlikely to be biodegradable, the high glass transition temperature and barrier enhancements provided by the 2,2'-bifuran units make BFDCA an interesting target for copolymerization with biodegradable aliphatic polyesters.

References

Antal, J. M., Mok, W. S. L., & Richards, G. N. (1990). Mechanism of formation of 5-(hydroxymethyl)-2-furaldehyde from D-fructose and sucrose. *Carbohydrate Research*, *199*, 91–109. doi.org/10.1016/0008-6215(90)84096-D

Araujo, C. F., Nolasco, M. M., Ribeiro-Claro, P. J. A., Rudić, S., Silvestre, A. J. D., Vaz, P. D., & Sousa, A. F. (2018). Inside PEF: Chain Conformation and Dynamics in Crystalline and Amorphous Domains. *Macromolecules*, *51*, 3515–3526. doi.org/10.1021/acs.macromol.8b00192

Asikainen, M, Thomas, D., & Harlin, A. (2016). Method of producing furan carboxylates from aldaric acids by using solid heterogeneous catalysts. International patent application WO2016166421A1 20161020.

Asrar, J. (1990). Synthesis and Properties of 4,4'-Biphenyldicarboxylic Acid and 2,6-Naphthalenedicarboxylic Acid. *Journal of Polymer Science Part A: Polymer Chemistry*, *37*, 3139−3146. doi.org/10.1002/(SICI)1099-0518(19990815)37:16<3139::AID-POLA11>3.0.CO;2-X

Banella, M. B., Bonucci, J., Vannini, M., Marchese, P., Lorenzetti, C., & Celli, A. (2019). Insights into the Synthesis of Poly(ethylene 2,5-Furandicarboxylate) from 2,5-Furandicarboxylic Acid: Steps toward Environmental and Food Safety Excellence in Packaging Applications. *Industrial & Engineering Chemistry Research*, *58*, 8955–8962. doi.org/10.1021/acs.iecr.9b00661

Belgacem, M. N., & Gandini, A. (2008). Monomers, polymers and composites from renewable resources, 1st edition. Elsevier. doi.org/10.1016/B978-0-08-045316-3.X0001-4

Billmeyer, F. (1949). Methods for estimating intrinsic viscosity. *Journal of Polymer Science*, *4*, 83−86. doi.org/10.1002/pol.1949.120040107

Bloom, J. W. G. & Wheeler, S. E. (2014). Benchmark Torsional Potentials of Building Blocks for Conjugated Materials: Bifuran, Bithiophene, and Biselenophene. *Journal of Chemical Theory and Computation*, *10*, 3647−3655. doi.org/10.1021/ct5004725

Burger, G. J. & Wills, A. D. (2000). Synthesis of 5,5'-diformyl-2-2'-difuran and its derivatives and apparatus therefor. International patent application WO2000015623A1 20000323.

Burgess, S. K., Karvan, O., Johnson, J. R., Kriegel, R. M., & Koros, W. J. (2014a). Oxygen sorption and transport in amorphous poly(ethylene furanoate). *Polymer*, *55*, 4748–4756. doi.org/10.1016/j.polymer.2014.07.041

Burgess, S. K., Kriegel, R. M., & Koros, W. J. (2015). Carbon Dioxide Sorption and Transport in Amorphous Poly(ethylene furanoate). *Macromolecules*, *48*, 2184–2193. doi.org/10.1021/acs.macromol.5b00333

Burgess, S. K., Leisen, J. E., Kraftschik, B. E., Mubarak, C. R., Kriegel, R. M., & Koros, W. J. (2014b). Chain Mobility, Thermal, and Mechanical Properties of Poly(ethylene furanoate) Compared to Poly(ethylene terephthalate). *Macromolecules*, *47*, 1383–1391. doi.org/10.1021/ma5000199

Caes, B. R., Teixeira, R. E., Knapp, K. G., & Raines, R. T. (2015). Biomass to Furanics: Renewable Routes to Chemicals and Fuels. *ACS Sustainable Chemistry & Engineering*, *3*, 2591–2605. doi.org/10.1021/acssuschemeng.5b00473

Cao, Y.-N., Tian, X.-C., Chen, X.-X., Yao, Y.-X., Gao, F., & Zhou, X.-L. (2017). Rapid Ligand-Free Base-Accelerated Copper-Catalyzed Homocoupling Reaction of Arylboronic Acids. *Synlett*, *28*, 601−606. doi.org/10.1055/s-0036-1588361

Chamas, A., Moon, H., Zheng, J., Qiu, Y., Tabassum, T., Jang, J. H., . . . Suh, S. (2020). Degradation Rates of Plastics in the Environment. *ACS Sustainable Chemistry & Engineering*, *8*, 3494–3511. doi.org/10.1021/acssuschemeng.9b06635

Chen, X., Chen, S., Xu, Z., Zhang, J., Miao, M., & Zhang, D. (2020). Degradable and recyclable bio-based thermoset epoxy resins. *Green Chemistry*, *22*, 4187–4198. doi.org/10.1039/D0GC01250E

Cheng, Z., Everhart, J. L., Tsilomelekis, G., Nikolakis, V., Saha, B., & Vlachos, D. G. (2018). Structural analysis of humins formed in the Brønsted acid catalyzed dehydration of fructose. *Green Chemistry*, *20*, 997–1006. doi.org/10.1039/C7GC03054A

Cho, J. K., Lee, J.-S., Jeong, J., Kim, B., Kim, B., Kim, S., . . . Lee, S.-H. (2013). Synthesis of carbohydrate biomass-based furanic compounds bearing epoxide end group(s) and evaluation of their feasibility as adhesives. *Journal of Adhesion Science and Technology*, *27*, 2127–2138. doi.org/10.1080/01694243.2012.697700

Choe, E. W. & Flint, J. A. (1993). Copolyesters for high-modulus fibers. International patent application WO9302122A1 19930204.

Choudhary, H., Nishimura, S., & Ebitani, K. (2013). Metal-free oxidative synthesis of succinic acid from biomass-derived furan compounds using a solid acid catalyst with hydrogen peroxide. *Applied Catalysis A: General*, *458*, 55−62. doi.org/10.1016/j.apcata.2013.03.033

Comer, C. M., Aurand, G. A., & Jessop, J. L. P. (2007). Photocatalytic synthesis of difuran derivatives for use as biorenewable heat-resistant monomers. *American Chemical Society, Polymer Preprints, Division of Polymer Chemistry*, *48*, 877–878.

Corma, C., Iborra, S., & Velty, A. (2007). Chemical Routes for the Transformation of Biomass into Chemicals. *Chem. Rev.*, *107*, 2411–2502. doi.org/10.1021/cr050989d

Crawford, R. J. (1998). Plastics engineering, 3rd edition. Oxford: Butterworth-Heinemann. doi.org/10.1016/B978-0-7506-3764-0.X5000-6

Cresp, T. M. & Sargent, M. V. (1973). Synthesis of Unsaturated Sulphur Compounds Containing Seventeen- and Twenty-one-membered Rings. *Journal of the Chemical Society, Perkin Transactions 1*, 1786−1790. doi.org/10.1039/P19730001786

Cureton, L. T., Napadensky, E., Annunziato, C., & La Scala, J. J. (2017). The effect of furan molecular units on the glass transition and thermal degradation temperatures of polyamides. *Journal of Applied Polymer Science*, *134*, 45514. doi.org/10.1002/app.45514

Das, U., Crousse, B., Kesavan, V., Bonnet-Delpon, D., & Bégué, J.-P. (2000). Facile Ring Opening of Oxiranes with Aromatic Amines in Fluoro Alcohols. *Journal of Organic Chemistry*, *65*, 6749–6751. doi.org/10.1021/jo000031c

Davidenko, N., Zaldívar, D., Peniche, C., Sastre, R., & San Román, J. (1996). Activity of the furfuryl ring in the free radical polymerization of acrylic monomers. *Journal of Polymer Science Part A: Polymer Chemistry*, *34*, 2759–2766. doi.org/10.1002/(SICI)1099-0518(19960930)34:13<2759::AID-POLA21>3.0.CO;2-A

Davy, K. W. M., Kalachandra, S., Pandain, M. S., & Braden, M. (1998). Relationship between composite matrix molecular structure and properties. *Biomaterials*, *19*, 2007–2014. doi.org/10.1016/S0142-9612(98)00047-7

Deng, J., Liu, X., Li, C., Jiang, Y., & Zhu, J. (2015a). Synthesis and properties of a bio-based epoxy resin from 2,5-furandicarboxylic acid (FDCA). *RSC Advances*, *5*, 15930–15939. doi.org/10.1039/C5RA00242G

Deng, J., Yang, B., Chen, C., & Liang, J. (2015b). Renewable Eugenol-Based Polymeric Oil-Absorbent Microspheres: Preparation and Oil Absorption Ability. *ACS Sustainable Chemistry & Engineering*, *3*, 599–605. doi.org/10.1021/sc500724e

Dick, G. R., Frankhouser, A. D., Banerjee, A., & Kanan, M. W. (2017). A scalable carboxylation route to furan-2,5-dicarboxylic acid. *Green Chemistry, 19*, 2966–2972. doi.org/10.1039/C7GC01059A

Edling, E. H., Sun, H., Paschke, E., Schiraldi, D. A., Tanko, J. M., Paradzinsky, M., & Turner, R. S. (2020). High barrier biosourced polyester from dimethyl [2,2'-bifuran]-5,5'-dicarboxylate. *Polymer*, *191*, 122258. doi.org/10.1016/j.polymer.2020.122258

Fei, X., Wang, J., Zhu, J., Wang, X., & Liu, X. (2020). Biobased Poly(ethylene 2,5-furancoate): No Longer an Alternative, but an Irreplaceable Polyester in the Polymer Industry. *ACS Sustainable Chemistry & Engineering, 8*, 8471–8485. doi.org/10.1021/acssuschemeng.0c01862

Fortman, D. J., Brutman, J. P., De Hoe, G. X., Snyder, R. L., Dichtel, W. R., & Hillmyer, M. A. (2018). Approaches to Sustainable and Continually Recyclable Cross-Linked Polymers. *ACS Sustainable Chemistry & Engineering*, *6*, 11145–11159. doi.org/10.1021/acssuschemeng.8b02355

Fu, H. Y., Zhao, L., Bruneau, C., & Doucet, H. (2012). Palladium-Catalysed Direct Heteroarylations of Heteroaromatics Using Esters as Blocking Groups at C2 of Bromofuran and Bromothiophene Derivatives: A One-Step Access to Biheteroaryls. *Synlett*, *23*, 2077−2082. doi.org/10.1055/s-0031-1290453

Fujisawa, S. (1994). Nuclear Magnetic Resonance Spectra of Bis-GMA and Iso-bis-GMA. *Dental Materials Journal*, *13*, 251–255. doi.org/10.4012/dmj.13.251

Gandini, A. & Belgacem, M. N. (1997). Furans in polymer chemistry. *Progress in Polymer Science*, *22*, 1203–1379. doi.org/10.1016/S0079-6700(97)00004-X

Gandini, A. & Lacerda, T. M. (2015). From monomers to polymers from renewable resources: Recent advances. *Progress in Polymer Science*, *48*, 1–39. doi.org/10.1016/j.progpolymsci.2014.11.002

Gandini, A., Lacerda, T. M., Carvalho, A. J. F., & Trovatti, E. (2016). Progress of Polymers from Renewable Resources: Furans, Vegetable Oils, and Polysaccharides. *Chemical Reviews*, *116*, 1637–1669. doi.org/10.1021/acs.chemrev.5b00264

Gandini, A., Silvestre, A. J. D., Neto, C. P., Sousa, A. F., & Gomes, M. (2009). The furan counterpart of poly(ethylene terephthalate): An alternative material based on renewable resources. *Journal of Polymer Science Part A: Polymer Chemistry*, *47*, 295–298. doi.org/10.1002/pola.23130

Geyer, R., Jambeck, J. R., & Law, K. L. (2017). Production, use, and fate of all plastics ever made. *Science Advances*, *3*, e1700782. doi.org/10.1126/sciadv.1700782

Gidron, O. & Bendikov, M. (2014). α-Oligofurans: An Emerging Class of Conjugated Oligomers for Organic Electronics. *Angewandte Chemie International Edition*, *53*, 2546–2555. doi.org/10.1002/anie.201308216

Gidron, O., Dadvand, A., Sun, E. W.-H., Chung, I., Shimon, L. J. W., Bendikov, M., & Perepichka, D. F. (2013a). Oligofuran-containing molecules for organic electronics. *Journal of Materials Chemistry C*, *1*, 4358–4367. doi.org/10.1039/C3TC00079F

Gidron, O., Varsano, N., Shimon, L. J. W., Leitus, G., & Bendikov, M. (2013b). Study of a bifuran vs. bithiophene unit for the rational design of π-conjugated systems. What have we learned? *Chemical Communications*, *49*, 6256−6258. doi.org/10.1039/C3CC41795F

Goncharov, L. B., Grekov, A. P., Chumikova, G. N., & Rudakov, E. S. (1985). Synthesis and properties of poly(acylhydrazones). *Ukrainskii Khimicheskii Zhurnal (Russian Edition)*, *51*, 99–101.

Gowda, R. R. & Chakraborty, D. (2011). Ceric Ammonium Nitrate Catalyzed Oxidation of Aldehydes and Alcohols. *Chinese Journal of Chemistry*, *29*, 2379−2384. doi.org/10.1002/cjoc.201180406

Grigg, R., Knight, J. A., & Sargent, M. V. (1966). Studies in Furan Chemistry. Part IV. 2,2'-Bifurans. *Journal of the Chemical Society [Section] C: Organic*, *0*, 976−981. doi.org/10.1039/J39660000976

Gruter, G.-J. M., Sipos, L., & Dam, M. A. (2012). Accelerating Research into Bio-Based FDCA-Polyesters by Using Small Scale Parallel Film Reactors. *Combinatorial Chemistry & High Throughput Screening*, *15*, 180–188. doi.org/10.2174/138620712798868374

Guidotti, G., Soccio, M., García-Gutiérrez, M.-C., Gutiérrez-Fernández, E., Ezquerra, T. A., Siracusa, V., . . . Lotti, N. (2019). Evidence of a 2D-Ordered Structure in Biobased Poly(pentamethylene furanoate) Responsible for Its Outstanding Barrier and Mechanical Properties. *ACS Sustainable Chemistry & Engineering*, *7*, 17863–17871. doi.org/10.1021/acssuschemeng.9b04407

Guidotti, G., Soccio, M., García-Gutiérrez, M. C., Ezquerra, T., Siracusa, V., Gutiérrez-Fernández, E., . . . Lotti, N. (2020). Fully Biobased Superpolymers of 2,5-Furandicarboxylic Acid with Different Functional Properties: From Rigid to Flexible, High Performant Packaging Materials. *ACS Sustainable Chemistry & Engineering*, *8*, 9558–9568. doi.org/10.1021/acssuschemeng.0c02840

Guidotti, G., Soccio, M., Lotti, N., Gazzano, M., Siracusa, V., & Munari, A. (2018). Poly(propylene 2,5-thiophenedicarboxylate) vs. Poly(propylene 2,5-furandicarboxylate): Two Examples of High Gas Barrier Bio-Based Polyesters. *Polymers*, *10*, 785. doi.org/10.3390/polym10070785

94

Hahladakis, J. N. & Iacovidou, E. (2019). An overview of the challenges and trade-offs in closing the loop of post-consumer plastic waste (PCPW): Focus on recycling. *Journal of Hazardous Materials*, *380*, 120887. doi.org/10.1016/j.jhazmat.2019.120887

Hayashi, S., Narita, A., Wasano, T., Tachibana, Y., & Kasuya, K. (2019). Synthesis and cross-linking behavior of biobased polyesters composed of bi(furfuryl alcohol). *European Polymer Journal*, *121*, 109333. doi.org/10.1016/j.eurpolymj.2019.109333

Holland, B. J. & Hay, J. N. (2002). The thermal degradation of PET and analogous polyesters measured by thermal analysis−Fourier transform infrared spectroscopy. *Polymer*, *43*, 1835–1847. doi.org/10.1016/S0032-3861(01)00775-3

Hong, S., Min, K.-D., Nam, B.-U., & Park, O. O. (2016). High molecular weight bio furan-based co-polyesters for food packaging applications: synthesis, characterization and solid-state polymerization. *Green Chemistry*, *18*, 5142−5150. doi.org/10.1039/C6GC01060A

Hu, F., La Scala, J. J., Sadler, J. M., & Palmese, G. R. (2014). Synthesis and Characterization of Thermosetting Furan-Based Epoxy Systems. *Macromolecules*, *47*, 3332–3342. doi.org/10.1021/ma500687t

Hu, H., Zhang, R., Sousa, A., Long, Y., Ying, W. B., Wang, J., & Zhu, J. (2018). Bio-based poly(butylene 2,5-furandicarboxylate)-b-poly(ethylene glycol) copolymers with adjustable degradation rate and mechanical properties: Synthesis and characterization. *European Polymer Journal*, *106*, 42–52. doi.org/10.1016/j.eurpolymj.2018.07.007

Huang, X., Chen, D., He, H., Li, J., Huang, J., & Li, B. (2017). Crystal structure and luminescent properties of novel coordination polymers constructed with bifurandicarboxylic acid. *Acta Crystallographica, Section B: Structural Science, Crystal Engineering and Materials*, *73*, 715−721. doi.org/10.1107/S2052520617003870

Iacovidou, E., Velenturf, A. P. M., & Purnell, P. (2019). Quality of resources: A typology for supporting transitions towards resource efficiency using the single-use plastic bottle as an example. *Science of the Total Environment*, *647*, 441–448. doi.org/10.1016/j.scitotenv.2018.07.344

Istasse, T. & Richel, A. (2020). Mechanistic aspects of saccharide dehydration to furan derivatives for reaction media design. *RSC Advances*, *10*, 23720–23742. doi.org/10.1039/D0RA03892J

Jiang, M., Liu, Q., Zhang, Q., Ye, C., & Zhou, G. (2012). A Series of Furan-Aromatic Polyesters Synthesized via Direct Esterification Method Based on Renewable Resources. *Journal of Polymer Science Part A: Polymer Chemistry*, *50*, 1026–1036. doi.org/10.1002/pola.25859

Jeong, J., Kim, B., Shin, S., Kim, B., Lee, J.-S., Lee, S.-H., & Cho, J. K. (2013). Synthesis and photo-polymerization of bio-based furanic compounds functionalized by 2-hydroxypropyl methacrylate group(s). *Journal of Applied Polymer Science*, *127*, 2483–2489. doi.org/10.1002/app.37959

Kandasamy, S., Samudrala, S. P., & Bhattacharya, S. (2019). The route towards sustainable production of ethylene glycol from a renewable resource, biodiesel waste: a review. *Catalysis Science & Technology*, *9*, 567–577. doi.org/10.1039/C8CY02035C

Kim, J. M., Lee, I., Park, J. Y., Hwang, K. T., Bae, H., & Park, H. J. (2018). Applicability of biaxially oriented poly(trimethylene terephthalate) films using bio-based 1,3-propanediol in retort pouches. *Journal of Applied Polymer Science*, *135*, 46251. doi.org/10.1002/app.46251

Kloxin, C. J., Scott, T. F., Adzima, B. J., & Bowman, C. N. (2010). Covalent Adaptable Networks (CANs): A Unique Paradigm in Cross-Linked Polymers. *Macromolecules*, *43*, 2643–2653. doi.org/10.1021/ma902596s

Knoop, R. J. I., Vogelzang, W., van Haveren, J., & van Es, D. S. (2013). High Molecular Weight Poly(ethylene-2,5-furanoate); Critical Aspects in Synthesis and Mechanical Property Determination. *Journal of Polymer Science Part A: Polymer Chemistry*, *51*, 4191–4199. doi.org/10.1002/pola.26833

Kovash, C. S., Pavlacky, E., Selvakumar, S., Sibi, M. P., & Webster, D. C. (2014). Thermoset Coatings from Epoxidized Sucrose Soyate and Blocked, Bio-Based Dicarboxylic Acids. *ChemSusChem*, *7*, 2289–2294. doi.org/10.1002/cssc.201402091

Kuster, B. F. M. & van der Steen, H. J. C. (1977). Preparation of 5-Hydroxymethylfurfural Part I. Dehydration of Fructose in a Continuous Stirred Tank Reactor. *Starch/Staerke*, *29*, 99–103. doi.org/10.1002/star.19770290306

Lafrance, M. & Fagnou, K. (2006). Palladium-Catalyzed Benzene Arylation: Incorporation of Catalytic Pivalic Acid as a Proton Shuttle and a Key Element in Catalyst Design. *Journal of the American Chemical Society*, *128*, 16496–16497. doi.org/10.1021/ja067144j

Laita, H., Boufi, S., & Gandini, A. (1997). The application of the Diels-Alder reaction to polymers bearing furan moieties. 1. Reactions with maleimides. *European Polymer Journal*, *33*, 1203–1211. doi.org/10.1016/S0014-3057(97)00009-8

Lange, J. & Wyser, Y. (2003). Recent Innovations in Barrier Technologies for Plastic Packaging – a Review. *Packaging Technology and Science*, *16*, 149–158. doi.org/10.1002/pts.621

Larsen, D. B., Sønderbæk-Jørgensen, R., Duus, J. Ø., & Daugaard, A. E. (2018). Investigation of curing rates of bio-based thiol-ene films from diallyl 2,5-furandicaboxylate. *European Polymer Journal*, *102*, 1–8. doi.org/10.1016/j.eurpolymj.2018.03.005

Li, N.-N., Zhang, Y.-L., Mao, S., Gao, Y.-R., Guo, D.-D., & Wang, Y.-Q. (2014). Palladium-Catalyzed C–H Homocoupling of Furans and Thiophenes Using Oxygen as the Oxidant. *Organic Letters*, *16*, 2732–2735. doi.org/10.1021/ol501019y

Li, X., Jia, P. & Wang, T. (2016). Furfural: A Promising Platform Compound for Sustainable Production of C4 and C5 Chemicals. *ACS Catalysis*, *6*, 7621–7640. doi.org/10.1021/acscatal.6b01838

Lichtenthaler, F. W. & Peters, S. (2004). Carbohydrates as green raw materials for the chemical industry. *Comptes Rendus Chimie*, *7*, 65–90. doi.org/10.1016/j.crci.2004.02.002

Liu, H., Mondschein, R. J., Chen, T., Long, T. E., & Turner, R. S. (2017). Terephthalate-co-bibenzoate polyesters. International patent application WO2017112031A1 20170629.

Liu, S., Amada, Y., Tamura, M., Nakagawa, Y., & Tomishige, K. (2014). One-pot selective conversion of furfural into 1,5-pentanediol over a Pd-added Ir–ReO$_x$/SiO$_2$ bifunctional catalyst. *Green Chemistry*, *16*, 617−626. doi.org/10.1039/C3GC41335G

Liu, Y., Zhao, J., Peng, Y., Luo, J., Cao, L., & Liu, X. (2020). Comparative Study on the Properties of Epoxy Derived from Aromatic and Heteroaromatic Compounds: The Role of Hydrogen Bonding. *Industrial & Engineering Chemistry Research*, *59*, 1914–1924. doi.org/10.1021/acs.iecr.9b05904

Mamman, A. S., Lee, J.-M., Kim, Y.-C., Hwang, I. T., Park, N.-J., Hwang, Y. K., . . . Hwang, J.-S. (2008). Furfural: Hemicellulose/xylose-derived biochemical. *Biofuels, Bioproducts and Biorefining*, *2*, 438–454. doi.org/10.1002/bbb.95

Manninen, V. M., Heiskanen, J. P., Pankov, D., Kastinen, T., Hukka, T. I., Hormi, O. E. O., & Lemmetyinen, H. J. (2014). The effect of diketopyrrolopyrrole (DPP) group inclusion in p-cyanophenyl end-capped oligothiophene used as a dopant in P3HT:PCBM BHJ solar cells. *Photochemical and Photobiological Sciences*, *13*, 1456–1468. doi.org/10.1039/C4PP00207E

Marotta, A., Ambrogi, V., Cerrutic, P., & Mija, A. (2018). Green approaches in the synthesis of furan based diepoxy monomers. *RSC Advances*, *8*, 16330–16335. doi.org/10.1039/C8RA02739K

Martínez de Ilarduya, A. & Muñoz-Guerra, S. (2014). Chemical Structure and Microstructure of Poly(alkylene terephthalate)s, their Copolyesters, and their Blends as Studied by NMR. *Macromolecular Chemistry and Physics*, *215*, 2138–2160. doi.org/10.1002/macp.201400239

Matos, M., Sousa, A. F., Fonseca, A. C., Freire, C. S. R., Coelho, J. F. J., & Silvestre, A. J. D. (2014). A New Generation of Furanic Copolyesters with Enhanced Degradability: Poly(ethylene 2,5-furandicarboxylate)-*co*-poly(lactic acid) Copolyesters. *Macromolecular Chemistry and Physics*, *215*, 2175−2184. doi.org/10.1002/macp.201400175

McClure, M. S., Glover, B., McSorley, E., Millar, A., Osterhout, M. H., & Roschangar, F. (2001). Regioselective Palladium-Catalyzed Arylation of 2-Furaldehyde. *Organic Letters*, *3*, 1677–1680. doi.org/10.1021/ol0158866

McKeen, L. W. (2012). Film Properties of Plastics and Elastomers, 3rd edition. Waltham: William Andrew. doi.org/10.1016/C2011-0-05606-5

McKeen, L. W. (2017). Permeability Properties of Plastics and Elastomers, 4th edition. Oxford: William Andrew.

Meng, J., Zeng, Y., Chen, P., Zhang, J., Yao, C., Fang, Z., & Guo, K. (2019a). New ultrastiff bio-furan epoxy networks with high T$_g$: Facile synthesis to excellent properties. *European Polymer Journal*, *121*, 109292. doi.org/10.1016/j.eurpolymj.2019.109292

Meng, J., Zeng, Y., Chen, P., Zhang, J., Yao, C., Fang, Z., . . . Guo, K. (2019b). Flame Retardancy and Mechanical Properties of Bio-Based Furan Epoxy Resins with High Crosslink Density. *Macromolecular Materials and Engineering*, *305*, 1900587. doi.org/10.1002/mame.201900587

Miao, J.-T., Yuan, L., Guan, Q., Liang, G., & Gu, A. (2017). Biobased Heat Resistant Epoxy Resin with Extremely High Biomass Content from 2,5-Furandicarboxylic Acid and Eugenol. *ACS Sustainable Chemistry & Engineering*, *5*, 7003–7011. doi.org/10.1021/acssuschemeng.7b01222

Mika, L. T., Cséfalvay, E., & Németh, Á. (2018). Catalytic Conversion of Carbohydrates to Initial Platform Chemicals: Chemistry and Sustainability. *Chemical Reviews*, *118*, 505–613. doi.org/10.1021/acs.chemrev.7b00395

Miller, D. J., Peereboom, L., Wegener, E., & Gattinger, M. (2017). Formation of 2,5-furan dicarboxylic acid from aldaric acids. United States patent application US20170144982A1 20170525.

Miyagawa, N., Ogura, T., Okano, K., Matsumoto, T., Nishino, T., & Mori, A. (2017). Preparation of Furan Dimer-based Biopolyester Showing High Melting Points. *Chemistry Letters*, *46*, 1535–1538. doi.org/10.1246/cl.170647

Moreau, C., Durand, R., Razigade, S., Duhamet, J., Faugeras, P., Rivalier, P., . . . Avignon, G. (1996). Dehydration of fructose to 5-hydroxymethylfurfural over H-mordenites. *Applied Catalysis A: General*, *145*, 211–224. doi.org/10.1016/0926-860X(96)00136-6

Mulay, S. V., Bogoslavsky, B., Galanti, I., Galun, E., & Gidron, O. (2018). Bifuran-imide: a stable furan building unit for organic electronics. *Journal of Materials Chemistry C*, *6*, 11951–11955. doi.org/10.1039/C8TC02908C

Nameer, S., Larsen, D. B., Duus, J. Ø., Daugaard, A. E., & Johansson, M. (2018). Biobased Cationically Polymerizable Epoxy Thermosets from Furan and Fatty Acid Derivatives. *ACS Sustainable Chemistry & Engineering*, *6*, 9442–9450. doi.org/10.1021/acssuschemeng.8b01817

Nishiyama, K., Takata, T., & Endo, T. (1996). Curing of epoxy resins based on diglycidyl 2,6-naphthalenedicarboxylate and properties of cured products. *Nettowaku Porima*, *17*, 7–12. doi.org/10.11364/networkpolymer1996.17.7

Okkerse, C. & van Bekkum, H. (1999). From fossil to green. *Green Chemistry*, *1*, 107–114. doi.org/10.1039/A809539F

Osipov, A. M., Metlova, L. P., Baranova, N. V., & Rudakov, E. S. (1978). New derivatives of difuryl: 2,2'-difuryl-5,5'-dicarbinol and 2,2'-difuryl-5,5'-dicarboxylic acid. *Ukrainskii Khimicheskii Zhurnal (Russian Edition)*, *44*, 398−399.

Pacheco, J. J. & Davis, M. E. (2014). Synthesis of terephthalic acid via Diels-Alder reactions with ethylene and oxidized variants of 5-hydroxymethylfurfural. *PNAS (Proceedings of the National Academy of Sciences of the United States of America)*, *111*, 8363–8367. doi.org/10.1073/pnas.1408345111

Pang, J., Zheng, M., Sun, R., Wang, A., Wang, X., & Zhang, T. (2016). Synthesis of ethylene glycol and terephthalic acid from biomass for producing PET. *Green Chemistry*, *18*, 342–359. doi.org/10.1039/C5GC01771H

Papadopoulos, L., Magaziotis, A., Nerantzaki, M., Terzopoulou, Z., Papageorgiou, G. Z., & Bikiaris, D. N. (2018). Synthesis and characterization of novel poly(ethylene furanoate-co-adipate) random copolyesters with enhanced biodegradability. *Polymer Degradation and Stability*, *156*, 32–42. doi.org/10.1016/j.polymdegradstab.2018.08.002

Papamokos, G., Dimitriadis, T., Bikiaris, D. N., Papageorgiou, G. Z., & Floudas, G. (2019). Chain Conformation, Molecular Dynamics, and Thermal Properties of Poly(*n*-methylene 2,5-furanoates) as a Function of Methylene Unit Sequence Length. *Macromolecules*, *52*, 6533–6546. doi.org/10.1021/acs.macromol.9b01320

Partenheimer, W. & Grushin, V. V. (2001). Synthesis of 2,5-Diformylfuran and Furan-2,5-Dicarboxylic Acid by Catalytic Air-Oxidation of 5-Hydroxymethylfurfural. Unexpectedly Selective Aerobic Oxidation of Benzyl Alcohol to Benzaldehyde with Metal/Bromide Catalysts. *Advanced Synthesis & Catalysis*, *343*, 102–111. doi.org/10.1002/1615-4169(20010129)343:1<102::AID-ADSC102>3.0.CO;2-Q

Pedersen, M. J., Jurys, A., & Pedersen, C. M. (2020). Scalable synthesis of hydroxymethyl alkylfuranoates as stable 2,5-furandicarboxylic acid precursors. *Green Chemistry*, *22*, 2399–2402. doi.org/10.1039/D0GC00770F

Peutzfeldt, A. (1997). Resin composites in dentistry: the monomer systems. *European Journal of Oral Sciences*, *105*, 97–116. doi.org/10.1111/j.1600-0722.1997.tb00188.x

Poulopoulou, N., Kasmi, N., Bikiaris, D. N., Papageorgiou, D. G., Floudas, G., & Papageorgiou, G. Z. (2018). Sustainable Polymers from Renewable Resources: Polymer Blends of Furan-Based Polyesters. *Macromolecular Materials and Engineering*, *303*, 1800153. doi.org/10.1002/mame.201800153

Raheem, A. B., Noor, Z. Z., Hassan, A., Hamid, M. K. A., Samsudin, S. A., & Sabeen, A. H. (2019). Current developments in chemical recycling of post-consumer polyethylene terephthalate wastes for new materials production: A review. *Journal of Cleaner Production*, *225*, 1052–1064. doi.org/10.1016/j.jclepro.2019.04.019

Rojo, L., Vazquez, B., Parra, J., Bravo, A. L., Deb, S., & Roman, J. S. (2006). From natural products to polymeric derivatives of "Eugenol": A new approach for preparation of dental composites and orthopedic bone cements. *Biomacromolecules*, *7*, 2751–2761. doi.org/10.1021/bm0603241

Román-Leshkov, Y., Barrett, C. J., Liu, Z. Y., & Dumesic, J. A. (2007). Production of dimethylfuran for liquid fuels from biomass-derived carbohydrates. *Nature*, *447*, 982–985. doi.org/10.1038/nature05923

Sanderson, R. D., Schneider, D. F., & Schreuder, I. (1995). Synthesis of difuran diesters from furfural, and their evaluation as plasticizers for poly(vinyl chloride). *Journal of Applied Polymer Science*, *55*, 1837–1846. doi.org/10.1002/app.1995.070551314

Seo, K. J., Kim, M. J., Jeong, J., Lee, Y. C., Noh, S. T., & Chung, Y. (2011). Polymerization and characterization of polyesters using furan monomers from biomass. *Polymer (Korea)*, *35*, 526–530.

Shah, T. H., Bhatty, J. I., Gamlen, G. A., & Dollimore, D. (1984). Aspects of the chemistry of poly(ethylene terephthalate): 5. Polymerization of bis(hydroxyethyl)terephthalate by various metallic catalysts. *Polymer*, *25*, 1333–1336. doi.org/10.1016/0032-3861(84)90386-0

Shen, G., Zhang, S., Lei, Y., Shi, J., Xia, Y., Mei, G., . . . Yin, G. (2019). Catalytic carbonylation of renewable furfural derived 5-bromofurfural to 5-formyl-2-furancarboxylic acid in oil/aqueous bi-phase system. *Molecular Catalysis*, *463*, 94–98. doi.org/10.1016/j.mcat.2018.11.021

Sippola, R. J., Hadipour, A., Kastinen, T., Vivo, P., Hukka, T. I., Aernouts, T., & Heiskanen, J. P. (2018). Carbazole-based small molecule electron donors: Syntheses, characterization, and material properties. *Dyes and Pigments*, *150*, 79–88. doi.org/10.1016/j.dyepig.2017.11.014

Siracusa, V. & Blanco, I. (2020). Bio-Polyethylene (Bio-PE), Bio-Polypropylene (Bio-PP) and Bio-Poly(ethylene terephthalate) (Bio-PET): Recent Developments in Bio-Based Polymers Analogous to Petroleum-Derived Ones for Packaging and Engineering Applications. *Polymers*, *12*, 1641. doi.org/10.3390/polym12081641

Sousa, A. F., Vilela, C., Fonseca, A. C., Matos, M., Freire, C. S. R., Gruter, G.-J. M., . . . Silvestre, A. J. D. (2015). Biobased polyesters and other polymers from 2,5-furandicarboxylic acid: a tribute to furan excellency. *Polymer Chemistry*, *6*, 5961–5983. doi.org/10.1039/C5PY00686D

Stamatov, S. D. & Stawinski, J. (2005). Regioselective opening of an oxirane system with trifluoroacetic anhydride. A general method for the synthesis of 2-monoacyl- and 1,3-symmetrical triacylglycerols. *Tetrahedron*, *61*, 3659–3669. doi.org/10.1016/j.tet.2005.02.034

Straathof, A. J. J. & Bampouli, A. (2017). Potential of commodity chemicals to become bio-based according to maximum yields and petrochemical prices. *Biofuels, Bioproducts and Biorefining*, *11*, 798–810. doi.org/10.1002/bbb.1786

Tachibana, Y., Hayashi, S., & Kasuya, K. (2018). Biobased Poly(Schiff-Base) Composed of Bifurfural. *ACS Omega*, *3*, 5336–5345. doi.org/10.1021/acsomega.8b00466

Tachibana, Y., Kimura, S., & Kasuya, K. (2015). Synthesis and Verification of Biobased Terephthalic Acid from Furfural. *Scientific Reports*, *5*, 8249. doi.org/10.1038/srep08249

Taljaard, B. & Burger, G. J. (2002a). Synthesis of 5,5'-Diformyl-2,2'-difuran from 2-Furfural by Photochemical Aryl Coupling. *Advanced Synthesis & Catalysis*, *344*, 1111–1114. doi.org/10.1002/1615-4169(200212)344:10<1111::AID-ADSC1111>3.0.CO;2-0

Taljaard, B. & Burger, G. J. (2002b). Palladium-Catalysed Dimerisation of Furfural. *South African Journal of Chemistry*, *55*, 56–66.

Terzopoulou, Z., Karakatsianopoulou, E., Kasmi, N., Majdoub, M., Papageorgiou, G. Z., & Bikiaris, D. N. (2017). Effect of catalyst type on recyclability and decomposition mechanism of poly(ethylene furanoate) biobased polyester. *Journal of Analytical and Applied Pyrolysis*, *126*, 357–370. doi.org/10.1016/j.jaap.2017.05.010

Thiyagarajan, S., Pukin, A., van Haveren, J., Lutz, M., & van Es, D. S. (2013). Concurrent formation of furan-2,5- and furan-2,4-dicarboxylic acid: unexpected aspects of the Henkel reaction. *RSC Advances*, *3*, 15678–15686. doi.org/10.1039/C3RA42457J

Thiyagarajan, S., Vogelzang, W., Knoop, R. J. I., Frissen, A. E., van Haveren, J., & van Es, D. S. (2014). Biobased furandicarboxylic acids (FDCAs): effects of isomeric substitution on polyester synthesis and properties. *Green Chemistry*, *16*, 1957–1966. doi.org/10.1039/C3GC42184H

Tomás, R. A. F., Bordado, J. C. M., & Gomes, J. F. P. (2013). *p*-Xylene Oxidation to Terephthalic Acid: A Literature Review Oriented toward Process Optimization and Development. *Chemical Reviews*, *113*, 7421–7469. doi.org/10.1021/cr300298j

Tsanaktsis, V., Papageorgiou, G. Z., & Bikiaris, D. N. (2015a). A facile method to synthesize high-molecular-weight biobased polyesters from 2,5-furandicarboxylic acid and long-chain diols. *Journal of Polymer Science Part A: Polymer Chemistry*, *53*, 2617–2632. doi.org/10.1002/pola.27730

Tsanaktsis, V., Vouvoudi, E., Papageorgiou, G. Z., Papageorgiou, D. G., Chrissafis, K., & Bikiaris, D. N. (2015b). Thermal degradation kinetics and decomposition mechanism of polyesters based on 2,5-furandicarboxylic acid and low molecular weight aliphatic diols. *Journal of Analytical and Applied Pyrolysis*, *112*, 369–378. doi.org/10.1016/j.jaap.2014.12.016

van Berkel, J. G., Guigo, N., Kolstad, J. J., & Sbirrazzuoli, N. (2018). Biaxial Orientation of Poly(ethylene 2,5-furandicarboxylate): An Explorative Study. *Macromolecular Materials and Engineering*, *303*, 1700507. doi.org/10.1002/mame.201700507

Van Landuyt, K. L., Snauwaert, J., De Munck, J., Peumans, M., Yoshida, Y., Poitevin, A., . . . Van Meerbeek, B. (2007). Systematic review of the chemical composition of contemporary dental adhesives. *Biomaterials*, *28*, 3757–3785. doi.org/10.1016/j.biomaterials.2007.04.044

van Putten, R.-J., van der Waal, J. C., de Jong, E. Rasrendra, C. B., Heeres, H. J., & de Vries, J. G. (2013). Hydroxymethylfurfural, A Versatile Platform Chemical Made from Renewable Resources. *Chemical Reviews*, *113*, 1499–1597. doi.org/10.1021/cr300182k

van Vugt-Lussenburg, B. M. A., van Es, D. S., Naderman, M., le Notre, J., van der Klis, F., Brouwer, A., & van der Burg, B. (2020). Endocrine activities of phthalate alternatives; assessing the safety profile of furan dicarboxylic acid esters using a panel of human cell based reporter gene assays. *Green Chemistry*, *22*, 1873−1883. doi.org/10.1039/C9GC04348A

Vannini, M., Marchese, P., Celli, A., & Lorenzetti, C. (2015). Fully biobased poly(propylene 2,5-furandicarboxylate) for packaging applications: excellent barrier properties as a function of crystallinity. *Green Chemistry*, *17*, 4162–4166. doi.org/10.1039/C5GC00991J

Vassilev, S. V., Baxter, D., Andersen, L. K., & Vassileva, C. G. (2010). An overview of the chemical composition of biomass. *Fuel*, *89*, 913–933. doi.org/10.1016/j.fuel.2009.10.022

Wang, J., Liu, X., Jia, Z., Liu, Y., Sun, L., & Zhu, J. (2017a). Synthesis of bio-based poly(ethylene 2,5-furandicarboxylate) copolyesters: Higher glass transition temperature, better transparency, and good barrier properties. *Journal of Polymer Science Part A: Polymer Chemistry*, *55*, 3298–3307. doi.org/10.1002/pola.28706

Wang, J., Liu, X., Zhang, Y., Liu, F., & Zhu, J. (2016). Modification of poly(ethylene 2,5-furandicarboxylate) with 1,4-cyclohexanedimethylene: Influence of composition on mechanical and barrier properties. *Polymer*, *103*, 1–8. doi.org/10.1016/j.polymer.2016.09.030

Wang, J., Liu, X., Zhu, J., & Jiang, Y. (2017b). Copolyesters Based on 2,5-Furandicarboxylic Acid (FDCA): Effect of 2,2,4,4-Tetramethyl-1,3-Cyclobutanediol Units on Their Properties. *Polymers*, *9*, 305. doi.org/10.3390/polym9090305

Wang, S. & Brisse, F. (1998). Alternating Conjugated and Nonconjugated Polymer. 1. Crystal Structures and Polymorphism of Poly(hexamethylene 2,2'-bithiophene-5,5'-dicarboxylate), P6BT. *Macromolecules*, *31*, 2265–2277. doi.org/10.1021/ma9717350

Weber, F. & Brückner, R. (2015). Asymmetric Dihydroxylation of Esters and Amides of Methacrylic, Tiglic, and Angelic Acid: No Exception to the Sharpless Mnemonic! *European Journal of Organic Chemistry*, *11*, 2428–2449. doi.org/10.1002/ejoc.201403622

Werpy, T. & Petersen, G. (2004). Top Value Added Chemicals from Biomass: Volume I -- Results of Screening for Potential Candidates from Sugars and Synthesis Gas. United States: N. p. doi:10.2172/15008859

Wiesner, I. (1967). Reaction of epichlorohydrin with 2,2-bis(4-hydroxyphenyl)propane. Chromatographic separation and identification of some intermediates. *Collect. Czech. Chemical Communications*, *32*, 448–453.

Wilsens, C. H. R. M., Wullems, N. J. M., Gubbels, E., Yao, Y., Rastogi, S., & Noordover, B. J. (2015). Synthesis, kinetics, and characterization of bio-based thermosets obtained through polymerization of a 2,5-furandicarboxylic acid-based bis(2-oxazoline) with sebacic acid. *Polymer Chemistry*, *6*, 2707–2716. doi.org/10.1039/C4PY01609B

Witt, U., Müller, R.-J., & Deckwer, W.-D. (1996). Studies on sequence distribution of aliphatic/aromatic copolyesters by high-resolution ^{13}C nuclear magnetic resonance spectroscopy for evaluation of biodegradability. *Macromolecular Chemistry and Physics*, *197*, 1525−1535. doi.org/10.1002/macp.1996.021970428

Wojcieszak, R. & Itabaiana, I. (2020). Engineering the future: Perspectives in the 2,5-furandicarboxylic acid synthesis. *Catalysis Today*, *354*, 211–217. doi.org/10.1016/j.cattod.2019.05.071

Wu, B., Xu, Y., Bu, Z., Wu, L., Li, B.-G., & Dubois, P. (2014). Biobased poly(butylene 2,5-furandicarboxylate) and poly(butylene adipate-co-butylene 2,5-furandicarboxylate)s: From synthesis using highly purified 2,5-furandicarboxylic acid to thermo-mechanical properties. *Polymer*, *55*, 3648−3655. doi.org/10.1016/j.polymer.2014.06.052

Yin, B., Yu, B. & Xie, Y. (2020). Bifuranyl carboxylic ester environment-friendly plasticizer for thermoplastic resin. Chinese patent application CN110776668A 20200211.

Yu, Z., Zhou, J., Cao, F., Wen, B., Zhu, X., & Wei, P. (2013). Chemosynthesis and Characterization of Fully Biomass-Based Copolymers of Ethylene Glycol, 2,5-Furandicarboxylic Acid, and Succinic Acid. *Journal of Applied Polymer Science, 130*, 1415–1420. doi.org/10.1002/APP.39344

Yuan, H., Liu, H., Du, J., Liu, K., Wang, T., & Liu, L. (2020). Biocatalytic production of 2,5-furandicarboxylic acid: recent advances and future perspectives. *Applied Microbiology and Biotechnology*, *104*, 527–543. doi.org/10.1007/s00253-019-10272-9

Zeitsch, K. J. (2000). The chemistry and technology of furfural and its many by-products, 1st edition. Sugar Series. Amsterdam: Elsevier.

Zhang, J. & Weitz, E. (2012). An in Situ NMR Study of the Mechanism for the Catalytic Conversion of Fructose to 5-Hydroxymethylfurfural and then to Levulinic Acid Using [13]C Labeled D-Fructose. *ACS Catalysis*, *2*, 1211–1218. doi.org/10.1021/cs300045r

Zhang, S., Lan, J., Chen, Z., Yin, G., & Li, G. (2017). Catalytic Synthesis of 2,5-Furandicarboxylic Acid from Furoic Acid: Transformation from C5 Platform to C6 Derivatives in Biomass Utilizations. *ACS Sustainable Chemistry & Engineering*, *5*, 9360–9369. doi.org/10.1021/acssuschemeng.7b02396

Zhang, Y., Li, Y., Thakur, V. K., Gao, Z., Gu, J., & Kessler, M. R. (2018). High-performance thermosets with tailored properties derived from methacrylated eugenol and epoxy-based vinyl ester. *Polymer International*, *67*, 544–549. doi.org/10.1002/pi.5542

Zhang, Z. & Huber, G. W. (2018). Catalytic oxidation of carbohydrates into organic acids and furan chemicals. *Chemical Society Reviews*, *47*, 1351–1390. doi.org/10.1039/C7CS00213K

Zhou, C.-H., Xia, X., Lin, C.-X., Tong, D.-S., & Beltramini, J. (2011). Catalytic conversion of lignocellulosic biomass to fine chemicals and fuels. *Chemical Society Reviews*, *40*, 5588–5617. doi.org/10.1039/C1CS15124J

Zhu, J., Cai, J., Xie, W., Chen, P.-H., Gazzano, M., Scandola, M., & Gross, R. (2013). A. Poly(butylene 2,5-furan dicarboxylate), a Biobased Alternative to PBT: Synthesis, Physical Properties, and Crystal Structure. *Macromolecules*, *46*, 796−804. doi.org/10.1021/ma3023298

Zhu, S., Li, X., & Xiao, G. (2018). Bio-Based Resin for Preparation of Toner with High Mechanism Properties and Thermal Properties and Its Preparation Method. Chinese patent application CN107840923A 20180327.

Original publications

List of original publications:

I   Kainulainen, T. P. & Heiskanen, J. P. (2016). Palladium catalyzed direct coupling of 5-bromo-2-furaldehyde with furfural and thiophene derivatives. *Tetrahedron Letters*, *57*(45), 5012–5016. doi.org/10.1016/j.tetlet.2016.09.097

II   Kainulainen, T. P., Sirviö, J. A., Sethi, J., Hukka, T. I., & Heiskanen, J. P. (2018). UV-Blocking Synthetic Biopolymer from Biomass-Based Bifuran Diester and Ethylene Glycol. *Macromolecules*, *51*(5), 1822–1829. doi.org/10.1021/acs.macromol.7b02457

III Kainulainen, T. P., Hukka, T. I., Özeren, H. D., Sirviö, J. A., Hedenqvist, M. S., & Heiskanen, J. P. (2020). Utilizing Furfural-Based Bifuran Diester as Monomer and Comonomer for High-Performance Bioplastics: Properties of Poly(butylene furanoate), Poly(butylene bifuranoate), and Their Copolyesters. *Biomacromolecules*, *21*(2), 743–752. doi.org/10.1021/acs.biomac.9b01447

IV   Kainulainen, T. P., Erkkilä, P., Hukka, T. I., Sirviö, J. A., & Heiskanen, J. P. (2020). Application of Furan-Based Dicarboxylic Acids in Bio-Derived Dimethacrylate Resins. *ACS Applied Polymer Materials*, *2*(8), 3215–3225. doi.org/10.1021/acsapm.0c00367

Paper I is reprinted with permission from Elsevier. Papers II, III, and IV are reprinted under CC-BY 4.0 license. Original publications are not included in the electronic version of the dissertation.

734. Mohanani, Rahul Prem (2019) Requirements fixation: the effect of specification formality on design creativity

735. Salman, Iflaah (2019) The effects of confirmation bias and time pressure in software testing

736. Hosseini, Seyedrebvar (2019) Data selection for cross-project defect prediction

737. Karvonen, Juhani (2019) Demography and dynamics of a partial migrant close to the northern range margin

738. Rohunen, Anna (2019) Advancing information privacy concerns evaluation in personal data intensive services

739. Haghighatkhah, Alireza (2020) Test case prioritization using build history and test distances : an approach for improving automotive regression testing in continuous integration environments

740. Santos Parrilla, Adrian (2020) Analyzing families of experiments in software engineering

741. Kynkäänniemi, Sanna-Mari (2020) The relationship between the reindeer (*Rangifer tarandus tarandus*) and the ectoparasitic deer ked (*Lipoptena cervi*) : reindeer welfare aspects

742. Grundstrom, Casandra (2020) Health data as an enabler of digital transformation : a single holistic case study of connected insurance

743. Honka, Johanna (2020) Evolutionary and conservation genetics of European domestic and wild geese

744. Alasaarela, Mervi (2020) Tietojärjestelmän käytön vaikutus laatuun ja tuottavuuteen sairaalaorganisaatiossa palveluhenkilöstön kokemana

745. Korhonen, Tanja (2020) Tools and methods to support the key phases of serious game development in the health sector

746. Alahuhta, Kirsi (2020) Consequences of incomplete demographic information on ecological modelling of plant populations with hidden life-history stages

747. Tyrmi, Jaakko (2020) Genomics and bioinformatics of local adaptation : Studies on two non-model plants and a software for bioinformatics workflow management

748. Lavrinienko, Anton (2020) The effects of exposure to radionuclide contamination on microbiota of wild mammals

ACTA UNIVERSITATIS OULUENSIS

SERIES EDITORS

A
SCIENTIAE RERUM NATURALIUM
University Lecturer Tuomo Glumoff

B
HUMANIORA
University Lecturer Santeri Palviainen

C
TECHNICA
Postdoctoral researcher Jani Peräntie

D
MEDICA
University Lecturer Anne Tuomisto

E
SCIENTIAE RERUM SOCIALIUM
University Lecturer Veli-Matti Ulvinen

F
SCRIPTA ACADEMICA
Planning Director Pertti Tikkanen

G
OECONOMICA
Professor Jari Juga

H
ARCHITECTONICA
University Lecturer Anu Soikkeli

EDITOR IN CHIEF
University Lecturer Santeri Palviainen

PUBLICATIONS EDITOR
Publications Editor Kirsti Nurkkala

UNIVERSITY OF OULU